8-2010

Predicting Long-Term Well Performance from Short-Term Well Tests in the Piedmont

David Hisz
Clemson University, dhisz@clemson.edu

PREDICTING LONG-TERM WELL PERFORMANCE FROM SHORT-TERM WELL TESTS IN THE PIEDMONT

A Thesis
Presented to
the Graduate School of
Clemson University

In Partial Fulfillment
of the Requirements for the Degree
Master of Science
Hydrogeology

---

by
David B. Hisz
August 2010

Accepted by:
Dr. Lawrence C. Murdoch, Committee Chair
Dr. Ronald W. Falta
Dr. Stephen Moysey

ABSTRACT

A reliable estimate of the physically sustainable discharge of a well is a fundamental aspect affecting management of water resources, but there are surprisingly few analyses describing on how to make such an estimate. Current available methods include either an empirical or a quantitative approach. The empirical method is based on holding the head or flow rate constant in order to maintain a target drawdown for as long as possible. The second method involves conducting a constant rate test to calculate the properties of the aquifer, *T* and *S*, and extrapolate the drawdown using a type curve (i.e. Theis analysis).

To improve well performance prediction, we have been using the effects of streams on short-term hydraulic well tests to predict long-term performance during pumping. An analysis was developed to calculate the long-term steady state specific capacity of a well using early-time information from a constant-rate test. The analysis first considers a homogeneous confined aquifer with a well fully penetrating the aquifer. A more detailed analysis considers a variable strength of interaction between a stream and a well extends the versatility of this method to a wide range of conditions.

The analysis is evaluated numerically to explore effects from typical Piedmont geometries not included in the analysis. Evaluating the analytical solution with numerical models allowed the characterization of different Piedmont geometries to determine the effectiveness of the analysis. Numerical models were allowed to reach steady state conditions, and the analysis was compared to the numerical results.

The analysis was then evaluated with two field examples from well tests in the Piedmont of South Carolina. The results show that the analysis successfully predicts the long term performance of wells within a few percent of the actual observed steady state specific capacities.

DEDICATION

For my parents.

ACKNOWLEDGMENTS

I would like to thank my advisor, Larry Murdoch, for his patience throughout this research project. My committee members, Ron Falta and Stephen Moysey, for offering helpful suggestions on short notice, and Greg Kinsmen for providing the long-term data set from the GEGT site for evaluation.

TABLE OF CONTENTS

Page

Table of Contents (Continued)

Page

LIST OF TABLES

LIST OF FIGURES

List of Figures (Continued)

Figure Page

List of Figures (Continued)

Figure Page

List of Figures (Continued)

Figure Page

LIST OF SYMBOLS

b ……Aquifer thickness

b' ……Saprolite thickness

E_1 ……Exponential Integral

E_{Sc} ……Percent relative error

g ……Stream function from Hunt (1999)

h ……Hydraulic head

h_o ……Hydraulic head in stream

k ……Hydraulic Conductivity

kPa ……Kilopascal

k_{rx} ……Fractured rock hydraulic conductivity

k_s ……Well skin hydraulic conductivity

k_{sap} ……Saprolite hydraulic conductivity

L ……Distance to stream

L_{eff} ……Effective Distance to stream

LAR ……Lower aquifer rock well

q_s ……Flux from stream to aquifer

Q …… Volumetric flow rate

Q_w …… Volumetric flow rate of well

r_d ……Dimensionless radius

r_s ……Radius of drawdown

r_w ……Well radius

R ……Flux due to fluid sources

s ……Drawdown

s_a ……Actual drawdown

s_d ……Dimensionless drawdown

s_e ……Expected drawdown

$s_{d0.8}$ ……Dimensionless drawdown at break in slope

List of Smbols (Continued)

s_{dss} ……Dimensionless steady state drawdown

s_k ……Skin factor

s_{ss} ……Steady state drawdown

S ……Storativity

S_c ……Specific Capacity

$S_{c0.8}$ ……Specific Capacity at break in slope

S_{cbs} ……Specific capacity at break in slope

S_{css} ……Steady-state specific capacity

$S_{css}real$ ……Actual Steady-state specific capacity

S_{FRM} ……Formation storativity

S_{rx} ……Fractured rock storativity

S_s ……Specific storage

S_{sap} ……Saprolite storativity

t ……Time

t_b ……Time for boundary interaction Streltsova (1988)

t_d ……Dimensionless time

$t_{d0.8}$ ……Dimensionless time when drawdown changes by 80% of maximum

t_0 ……Time at the x-intercept

$t_{0.8}$ ……Time when drawdown changes by 80% of maximum slope

$t_{0.8}calc$ ……Time to stream interaction

$t_{0.8}obs$ ……Observed break in slope time

t_{sap} ……time for end of saprolite effect

t_w ……time actual drawdown observed

T ……Transmissivity

T_{rx} ……Fractured rock Transmissivity

w ……Stream width

x ……Spatial coordinate

List of Symbols (Continued)

x_d ……Dimensionless spatial coordinate in the x direction

x_{dw} ……Dimensionless well radius

y ……Spatial coordinate

y_d ……Dimensionless spatial coordinate in the y direction

z ……Vertical direction

Δs ……change in drawdown slope

∇^2 ……Laplace operator

β ……Stream stream term

δ ……Dirac delta function

λ ……Streambed leakage term

π ……pi (3.14159)

ω ……Correction term

INTRODUCTION

Effective management of water supplies requires a reliable assessment of well performance. The maximum sustainable volumetric discharge is a primary measure of well performance, and several methods are used to estimate this value. One approach is strictly empirical. A well is pumped at constant rate until the drawdown stabilizes at a constant level. The observed volumetric rate during this test might be an acceptable estimate of well performance if the stabilized drawdown is roughly equal to the maximum drawdown, which commonly is limited by the location of the pump in the well (Driscoll, 1986). In many cases, the stabilized drawdown may be considerably less than the maximum value, so the well could produce at a larger rate than that observed during the test. In this situation, the common procedure is to extrapolate the observed rate using the observed steady state specific capacity (ratio of volumetric rate to drawdown; Todd, 1959; Walton, 1968). The maximum volumetric rate is then determined as the product of the steady state specific capacity and the maximum allowable drawdown based on the configuration of the pump or other design aspects of the well (Rosco Moss 1990).

The merit of the empirical approach is that it is straightforward to conduct and analyze. A common problem is that the duration of pumping that is practical to use in the field is too short for the well to reach steady state conditions. As a result, well tests are typically terminated during the transient response, and the observed specific capacity exceeds the steady state specific capacity because the drawdown will continue to increase. The volumetric discharge determined in this scenario will over-estimate the actual discharge under steady conditions.

The empirical approach may cause problems if the well is put into service and its performance falls short of expectations. The use of this technique is widespread and many large databases of well performance are populated with estimates obtained in this manner. A potential result is that the performance of entire regional aquifer systems may be over-estimated.

Hydrologists have recognized the shortcomings of the empirical approach and they have moved to replaced it with more quantitative methods involving well tests that analyze transient behavior. Pumping the well until steady state is achieved is not required in this case. A typical strategy is to conduct a constant-rate pumping test, measure drawdown, and then use parameter estimation methods with an appropriate well function to estimate aquifer properties (Kruseman and de Ridder, 1991). Those properties are then used with theoretical models of the aquifer to anticipate the long-term performance of the well. This general strategy is the mainstay of guidelines developed by the USEPA (Osborne 1993) and adopted by many states in the form of regulations to characterize well performance.

One shortcoming of this approach is that little guidance is available on how to develop a theoretical model for projecting well performance forward in time. In the absence of such guidance, many practioners probably predict well performance with the same well functions used to analyze short-term well test. The most common of these are the Theis or Jacob solutions to the drawdown in the vicinity of a well in an infinite aquifer (Theis, 1941; Hantush and Jacob, 1955), which are able to fit data from many short-term constant-rate tests remarkably well. These solutions predict that drawdown

increases as a function of the natural log of time, so the specific capacity decreases as the inverse of log time.

Many wells are known to reach steady state, and indeed, this is required if the empirical approach to characterizing well performance is to provide meaningful results. Projecting the transient behavior of the well by extrapolating an inverse semi-log straight line will underestimate performance if the well goes to steady state. The importance of this effect will depend on local hydrogeologic conditions because aquifers that are unconfined, relatively shallow, and overlain by abundant surface water will host wells that go to steady state more quickly than aquifers that are buried deeply beneath confining layers.

The two readily available methods (empirical and semi-log linear extrapolation) have basic faults that may cause them to either over- or under-estimate well performance. This means that performance estimates derived from well tests may have errors that result from flaws in how the test was analyzed. This suggests that the information used to anticipate the role of individual wells in water supplies may be unreliable. Many other analytical well functions have been published and wells can also be analyzed using numerical models, so there are myriad alternatives to simply extrapolating an inverse semi-log straight line. Calibrating a numerical model, however, is beyond the scope of many projects where estimates of well performance are needed. And, although analytical well functions are available to represent many aquifer scenarios, little information exists in how to use them for estimating well performance—their purpose in the scientific literature has been almost exclusively to estimate aquifer parameters.

Estimating the sustainable discharge of a well is a common need wherever aquifers are tapped as water supplies, so it is ironic that 75 years after Theis published his landmark paper about analyzing transient well tests there remains limited scientific guidance on how to make this estimate. One complicating factor is that establishing "sustainability" requires addressing a long list of processes. Physical attributes of the well and aquifer will result in a maximum volumetric discharge that the well can produce over a long period of pumping (Theis, 1935, 1940). This rate may not be sustainable, however, because it could deplete surface water flow and damage aquatic ecosystems, result in subsidence that damages surface structures, cause seawater intrusion that degrades water quality, diminish the performance of neighboring wells, or cause other problems. Moreover, changes in recharge accompanying alterations in land use, precipitation patterns, or other factors could also impact sustainable discharge of a well (Alley et al 1999; Kalf et al 2005). .

Even though the list of factors affecting well sustainability is a long one, they all build on the performance defined by the basic physical attributes of the well and aquifer. The physically sustainable discharge is what is sought by the empirical and semi-log straight line extrapolation approaches (Brown et al. 1963), and it is the starting point for more comprehensive evaluations. Despite the importance of the physically sustainable discharge, the currently available methods for estimating this quantity are biased toward either over- or under-estimation, so improvements in these methods would be useful contributions to the management of ground water supplies. .

OBJECTIVE

The objective of this research is to develop and evaluate short-term, transient well tests as methods to predict the long-term performance of wells. In particular, the objective is to predict the physically sustainable discharge of wells in a hydrogeologic setting typical of the Piedmont providence in the eastern U.S.

APPROACH

The approach used for this investigation is to first develop a conceptual model that represents the essential details of a well completed an aquifer system typical of the Piedmont province. The conceptual model will be used to derive the boundary conditions for analytical expressions describing well performance in an idealized setting resembling the Piedmont. That analysis will be the basis for a proposed method for estimating long-term well performance. The proposed method will be evaluated and refined by comparing it first to the results of numerical simulations of well tests, and then later to results of field experiments.

THESIS ORGANIZATION

Chapter One starts with an overview describing the evolution of the "safe yield" concept with respect to aquifer development with insights into development of the sustainable yield concept applied to ground water wells. Current guidelines for conducting aquifer tests in states within the Piedmont providence will be reviewed. Typical hydrogeologic features, aquifer properties, important boundary conditions and

geometries typical found in the Piedmont terrain will be used to create a hydrogeologic conceptual model at the close of Chapter One.

Chapter Two describes the theoretical analyses used to predict the long-term performance of a well. Two approaches are given to represent a stream as 1) a single layer with a fully penetrating constant-head boundary, and 2) a three layer system with a partially penetrating stream separated from the aquifer by a saprolite layer.

A numerical evaluation of the method for estimating long-term well performance is presented in Chapter Three to evaluate typical Piedmont aquifer properties. A baseline example is developed for the Piedmont, and simulated pumping tests are conducted. The results from the numerical tests are compared to the theoretical for evaluation the analyses.

Chapter Four concerns field application of the method for predicting well performance. An approach for estimating well performance is presented. The approach is then tested using synthetic drawdown data as an example. The method is then applied to two field examples to evaluate long-term performance from short-term well tests

The results are summarized in Chapter Five.

CHAPTER 1

BACKGROUND

A reliable estimate of well yield is critical for the long-term operation of a well. Over-estimating the yield of a well will increase the probability of decreased performance, aquifer damage around the vicinity of the wellbore, well equipment failure, loss of water supply, and a risk exists of depleting the water resource itself (Driscoll, 1986). Well performance is often described as a specific capacity (Rorabaugh, 1953; Bennett and Patten, 1960, Walton, 1968, Summers, 1972).

$$S_c = \frac{Q}{s} \tag{1.1}$$

where Q is volumetric discharge and s is the drawdown. Well performance will increase with discharge and decrease with drawdown, so S_c is often calculated to monitor performance (Figure 1.1).

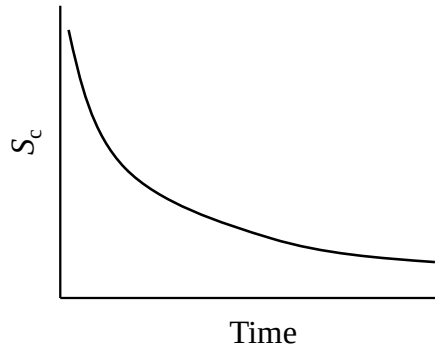

Figure 1.1. Schematic of specific capacity as a function of time

Under steady state conditions, the drawdown and the discharge are constant, so the specific capacity will also be constant. The volumetric discharge under these conditions is often referred to as a "safe yield", (Rosco Moss Co., 1990). The "safe yield" concept has been debated for nearly a century (Lee, 1915; Meizer, 1923; Theis, 1940; Todd, 1959; Walton; 1970; Bouwer, 1978; Bredehoeft, 1982; and Sophocleous, 2000) as the development of ground water has continued to increase.

Demand for irrigation and the availability of groundwater increased in the late 19th century as improvements of irrigation methods and decreasing pumping costs were developed, resulting in a need to characterize the rate of water moving into and out of underground water reservoirs.

Lee (1915) first described the term "safe yield" as a rate of water that can be removed annually and permanently without dangerous depletion of the aquifer storage reserve. Although Lee is unclear how "dangerous" depletion should be determined, his definition became the starting point for considering safe yield at the basin scale. Determination of the annual safe yield of an aquifer was first characterized as the average rate of recharge to a basin, excluding the rate of water returned to the basin from infiltration (i.e. from irrigation) (Lee, 1915). The term "basin" is used to mean an area filled with alluvial material, commonly in valleys (Lee, 1915; Conkling, 1945; and Todd, 1950), although I will use the term basin interchangeable with ground water reservoir. This insight from Lee lead to empirical studies focused on defining both groundwater inflows and outflows from basins.

Lee recognized that over pumping would drain water from surface water bodies, and correlated discharge to surface water bodies to the natural recharge into the basin. Safe yield became the rate of recharge required to maintain discharge rates to surface water bodies (Lee, 1915).

Observations made by Lee (1915) and Meinzer (1920, 1923) lead to the development of a water balance to characterize water entering and leaving a basin (Meinzer, 1920; Todd, 1950).

Theis (1940) first incorporated the water balance approach by modifying safe yield to a perennial safe yield based on induced recharge into the system and discharge out of the system as the rate of water that could be utilized. Ultimately, pumping rates or perennial safe yield must equal a fraction of the discharge rate to streams to minimize "undesirable" effects on the basin aquifer. This implies that abstraction may be localized within a larger system (Kalf and Woolley 2005), thus suggesting that basin-wide recharge may over-estimate a safe yield.

Conkling (1946) defines safe yield as a rate of water averaged over a period of 1 year, which is less than the annual rate of recharge and does not excessively lower the water table. Safe yield would be affected when the water table dropped beyond pumping capabilities, or when excessive drawdown degraded water quality. This approach is based on the rate of recharge to the system, which suggests over pumping can change water quality by intrusion; such as salt water entering the aquifer. If the annual extraction rate from an aquifer did not exceed the average recharge rate, lower the water table beyond current pumping costs, or create changes in water quality from the intrusion

of undesirable water into the aquifer then a well was operating under safe yield conditions (Conkling 1946). Therefore, a well is operating at a safe yield annually if no undesired effects are created (Todd 1959).

Groundwater pumping stresses the balance between inflows and outflows within the aquifer. For a groundwater system to be balanced during pumping adjustments to either recharge into or discharge out of the aquifer must occur, or the amount of water released from storage will increase (Theis, 1935, Conkling, 1945, Freeze, 1971, Sophocleous, 2000). As groundwater storage levels decrease due to pumping, a new balance between inflows and outflows must be determined at lower storage levels (Sophocleous, 2000).

Bredehoeft et al. (1982, 1997) described an example of the equilibrium of an island under natural conditions and showed how changes to the system changed with time based on the volume of water removed. Under predevelopment conditions, precipitation first falls onto the island and a water table forms. After the water table is developed, recharge to the aquifer is balanced by discharge to ocean, lake or pond body.

Sustainable development occurs when the volume of water that is captured from a pumping well equals the volume of water discharging out of the system (Bredehoeft 2002). Bredehoeft's description of an island, suggests that however important recharge is to sustainability of a system, that value is not constant, and only the amount of discharge occurring can be removed by pumping before changes to storage start occurring. These insights are indicative of the change from considering "safe" to "sustainable" yield within the groundwater community.

Sophocleous (1998, 2000) expands on Bredehoeft groundwater discharge being the key for sustainable development by including surface water depletion or induced recharge with changes in groundwater storage cased by over-pumping. Comparison of stream systems in Kansas were used to show affects of natural recharge compared to stream depletion. As natural recharge changes, stream depletion may increase. Therefore, sustainable yield should be less than a safe yield based on natural recharge to the system (Kalf 2005; Alley and Leake 2004). The ability to measure and observe these undesirable effects became the focus to determine if a withdrawal rate was safe.

The safe yield of an aquifer has been described as the amount of recharge into the aquifer (Lee, 1915; Meinzer, 1915, 1920; and Todd, 1950). The belief that if only the rate of water entering the system as recharge is removed then the system has no changed to the volume of water in storage. Once the volume of water in storage changes as a result of pumping, the sustainable development value of the system must all so change.

Alley and Leake (2004) expanded the effects of stream depletion by investigating yield with respect to the well capture zone. As pumping rates increase, so too must the capture zone which can lead to unsustainable capture zones. A well with an unsustainable capture zone over long-term development may result in the depletion of surface water bodies.

WELL PERFORMANCE

Determination of a well's performance, both for short and long-term use, is a common problem for water supply managers. Current methods for predicting a well performance include combinations of empirical, analytical, and numerical analysis. The

method often used varies depending on the circumstances and use of a well. This section will describe commonly used well testing methods used for determining the properties of an aquifer. Following the description of well tests, a review of state regulations will be discussed to illustrate the methods required by state agencies for determining well performance.

Constant-rate (constant-discharge) pumping tests is the preferred method for determining the performance of a well as it provides small to large-scale estimates of hydraulic parameters, and responses that can be analyzed using diagnostic methods (Kruseman and de Ridder, 1990). A constant-rate test consists of pumping a well for a period of time, commonly 24 to 72 hours, while the volume of water removed from the aquifer is held constant throughout the entire test (Driscoll 1986). Water levels are measured in the pumping well during the test to determine the amount of drawdown, the change in head from pre-pumping conditions, caused by the pumping rate. The objective of a constant rate is to pump a well to obtain hydraulic properties of the aquifer as the well reaches or behaves under near-equilibrium conditions, i.e. negligible changes in water levels with time (Roscoe Moss 1990). These tests normally show semi- or quasi steady-state conditions, as true equilibrium may never be obtain during the test duration (Kruseman and de Ridder 2000).

Government Regulations

Regulations describing field and analytical methods for estimating well performance have been established by most states. This section reviews the methods for

determining the performance of a well required by states located within the Piedmont terrain in the eastern U.S. There are industry-wide standards used for conducting constant-rate tests, however, the methods required for analyzing test data vary between states.

Selected EPA Suggested Guidelines for Conducting an Aquifer Test

The USEPA developed guidelines (Osborne, 1993) for well pumping tests that have become a standard reference for well testing design, operation, and data analysis. Many state agencies have adopted and refined the methods in this report for their aquifer testing regulations.

Pretest Procedure

Prior to starting a well test, it is necessary to establish a baseline trend in water levels in all wells for at least a week Baseline trends will indicate increasing or decreasing water levels, and drawdown during the test must be corrected to account for the pre-pumping trends (Osborne 1993).

Although not required, it is recommended to record barometric pressure changes along with the baseline water levels and continue through the testing period. This data can be used to correct for effects of barometric changes during the test (Osborne 1993).

Rate Control

The pumping rate should be controlled and not allowed to vary more than 5 percent. The EPA suggests that a 10 percent variation in discharge can result in a 100 percent variation in the estimation of aquifer transmissivity based on previous sensitivity

analysis of pumping test data (Osborne 1993). Discharge rates should be confirmed as often as possible or at least 4 times per day.

Duration of Test

There is not a set duration an aquifer should be pumped since the objective of the test, aquifer type, location of boundaries, and data collection needs may vary from site to site. The test should continue long enough for the data collected to adequately define the shape of a type curve for reliable calculation of aquifer parameters. Some tests may require pumping until drawdown stabilizes (the rate of change in water levels becomes small), especially when local boundaries are of interest (Osborne 1993). It is recommended that pumping be continued for as long as possible and at least for 24 hours.

Analysis of Test Results

The method of analysis used will depend on local aquifer conditions and the parameters to be estimated. Data should be plotted on a semi-log or log-log plot and fit with a type curve to determine *T* and *S*, and perhaps other properties.

State Agency Regulations

Unglaciated fractured rock aquifers occur in South Carolina, North Carolina, Georgia, Alabama, Virginia, and Maryland, and these states have developed regulations for testing wells in this hydrogeologic setting. Aquifer test and analysis guidelines for each state are based on the suggested EPA guidelines describe in the previous section (Table 1.1).

Georgia The Georgia Environmental Protection Division (GEPD) sets the guidelines for conducting an aquifer test. A constant-rate pumping test must be conducted for at least 24 hours. Once the drawdown has stabilized, the test must be continued for 4 hours. (GEPD., 2000). Georgia EPD has no description on how the performance of a well is determined, only that a well must be pumped at the specified production rate for at least 24 hours. Analysis of the test data must then follow standard methods employed by the United States Geological Survey, or any other method accepted by the hydrogeology community. (GEPD., 2000).

South Carolina The South Carolina Department of Health and Environmental Control (SC DHEC) requires that a pumping test being performed for a public water supply well for at least 24 hours (SC DHEC, 2006). The rate used during the test is recorded as the maximum capacity of the well. SC DHEC stipulates that the drawdown and well yield at the end of the test be used to calculate specific capacity. The recommended analysis is the same as EPA guidelines. SC DHEC does not require stabilization of drawdown.

North Carolina North Carolina Department of Environmental Protection (NCDEP) requires that a pumping test be conducted and analyzed based on a recognized and appropriate method that is valid for site conditions. For example, field data from boring logs, geologic mapping, and location of streams or other surface water should be consistent with the analysis used to analyze the well test. NCDEP will not accept an analysis based on a best fit result and conclusions made on a best fit alone, they suggest using information on methods of pumping tests found in references such as Kruseman and deRitter (1990) (NCDEP, 2007).

Virginia Virginia Department of Environmental Quality (V DEQ) guidelines follow the EPA guidelines with a minor change in flow rate documentation and stabilization. A well should be tested for at least 24 hours at the expected operational rate. DEQ does not require additional pumping after stabilization. Flow rate documentation during aquifer testing is required. Flow rates need to be recorded every hour for the duration of the test period. If the rate varies by more than 5 percent or insufficient flow rate recordings are submitted the test results could be rejected (DEQ 2007). V DEQ recommends that the evaluation of aquifer test data use the Theis or Hantush type curves. Detailed instructions are offered for different assumptions on each curve by V DEQ.

Alabama Alabama Department of Environmental Management A(DEM) follows EPA quidelines for aquifer testings; however they have expanded the language to include capacity of well. The duration of the test should be sufficient for water levels to stabilize (+/- 0.1 feet) at the design capacity or production rate, for at least 12 hours.

Under the capacity test guidelines, ADEM requires a well to be pumped for an additional 24 hrs after the drawdown has stabilized. Following the 24 hr period, the rate needs to be increased by 150% and pumped for another 6 hours after stabilization of drawdown at the new rate. Following the 6 hour period, the pumping can be terminated. If stabilization fails at 150% of the designed capacity, a written request for approval must be submitted (ADEM Admin. Code r. 335-7-5-.09).

Maryland Maryland Department of the Environment (MDE) uses the EPA guidelines for aquifer testing. Test durations vary based on hydrologic setting but usually 24 hours is the minimum. In fractured rock settings, testing is usually 72 hours (personal

communication with MDE). MDE utilizes an internal watershed model to approve pumping rates after aquifer properties are submitted from aquifer testing (personal communication with MDE).

Out of the 6 states reviewed, Alabama has the strictest procedures for determining the yield of a well. The requirement for a well to stabilize at 150% of the designed production rate is intended to prevent the aquifer from be over stressed. South Carolina and Maryland allow more leeway during testing as long as the designed flow rates are used during the aquifer test. All states require a minimum of 24 hours of pumping in order to determine aquifer properties. The terms "safe yield" or "sustainable pumping rate" is not used in any state aquifer testing or analysis guidelines. The capacity test requirement within ADEM is the closest to defining a sustained rate.

State	Agency	Minimum Pumping Duration	Stabilization of drawdown	Suggested Analysis	Other Notes/ Requirements
Maryland	MDE	24 hrs	none	Theis or other	State Model
Virginia	DEQ	24 hrs	none	Theis/Hantush	Flow rate variability +/- 5%
North Carolina	NCDEP	24 hrs	none	Theis or other	Analysis must be based on site conditions
South Carolina	DHEC	24 hrs	none	Theis or other	Q = proposed production rate
Georgia	GEPD	24 hrs	4 hrs	Theis or other	Q = proposed production rate
Alabama	DEM	12 hrs	24 hrs	Theis or other	after 24 stabilization, increase Q by 150%, and restabilize for 6 hrs

Note: Stabilization refers to a change in water lever of 0.1 ft/12 hrs

Table 1.1. Aquifer Test and Analysis regulations for six states from the Piedmont Province.

Piedmont Hydrogeology

This section describes the development and current hydrogeological features important to Piedmont terrain in the southeastern United States. Understanding the spatial variability in hydrogeological features used in current conceptual models is important during the interpretation of hydraulic well tests.

Location

The Piedmont Physiographic Province extends from Alabama to Pennsylvania and into New Jersey (Figure 1.2), and is bounded to the southeast by the Atlantic Coastal Plain and to the northwest by the Blue Ridge Mountains. The Piedmont Province is often classified in conjunction with the Blue Ridge Region as the Blue Ridge and Piedmont Aquifer System (BRPAS); one of the largest igneous and metamorphic aquifer systems in the United states. BRPAS contains hundreds of local aquifers composed of fractured igneous and metamorphic rock units (Swain et al., 2004).

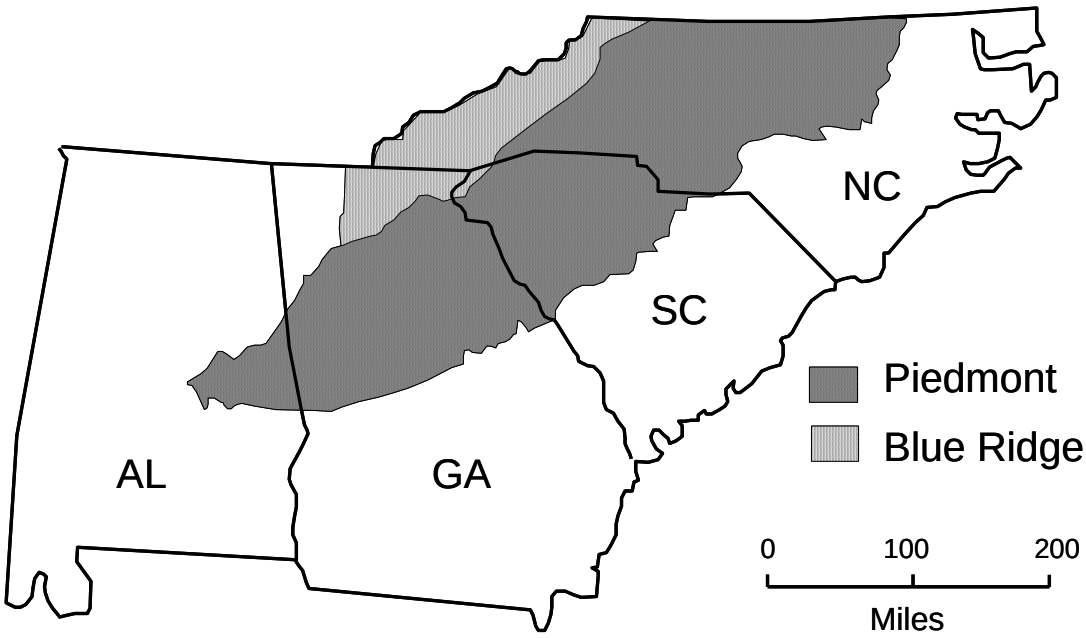

Figure 1.2. Location of Piedmont Terrain in the Southeastern United States (modified from Swain et al. 2004)

Geology

The Piedmont terrain is the result of at least three major tectonic events from the Proterozoic to Mesozoic. The North American and African plates separated and diverged during the Grenville Orogeny, one billion years ago, setting the stage for the formation of the Piedmont and Armorica Island Arc systems during the late PreCambrian (Stern and others, 1979). Plate motion changed and the North American and African plates converged in the late Proterozoic. The Piedmont Island Arc system first made contact with the North American continent in the early Cambrain (550 to 570 million years ago). It was thrust onto the North American Craton during the Taconic Orogeny (Hatcher, 1974). A convergent margin persisted and the Avalonian Arc was sutured onto the North

American plate during the Acadian Orogeny in the Devonian (350 – 400 m.y.a). Thrust faults and folds, and high grade metamorphism occurred during the Taconic and Acadian Orogenies (Stern and others, 1979).

The Piedmont Province is divided into two regions; western and eastern, which are separated by the central Piedmont suture (Hatcher, 1991).The Inner Piedmont Terrane represents the western section. The Inner Piedmont is bounded to the west by the Brevard Fault Zone and to the east by the Central Suture, within the Carolinas. Rock types are contained in numerous blocks of thrust sheets comprised mainly of schist, gneiss, and amphibolites. Some ultra-mafics and intrusive granitoids (Horton and McConnell, 1991) are also present. The Avalon Terrane, the eastern section, is bounded to the west by the Central Suture and to the east by the Atlantic Costal Plain, which are divided into groups of differing metamorphic belts.

Hydrogeologic Conceptual Model

The currently recognized hydrogeologic conceptual model consider the Piedmont Province to be underlain by a two-layer system composed of regolith and underlying fractured bedrock (Heath, 1989; LeGrand, 1988) (Figure 1.3). The regolith consists of bioturbated soil and saprolite. The contact between the regolith and fractured rock commonly is gradational, and in some cases a transition zone of weathered rock is recognized between these two units.

Saprolite, the dominant feature of the regolith, is a clay-rich material resulting from in-place weathering of bedrock. Textual features from the original bedrock, such as fractures and bedding planes, are preserved in the (Heath , 1989; Daniels, 2002). The

transition zone represents the grading of unconsolidated material into bedrock. Porosity values decrease with depth in the transition zone (LeGrand, 1967; Rutledge, 1996; Heath, 1989; Daniels, 2002). Higher permeability values are found in the transition zone. Particle sizes range from clays to large boulders of un-weathered bedrock.

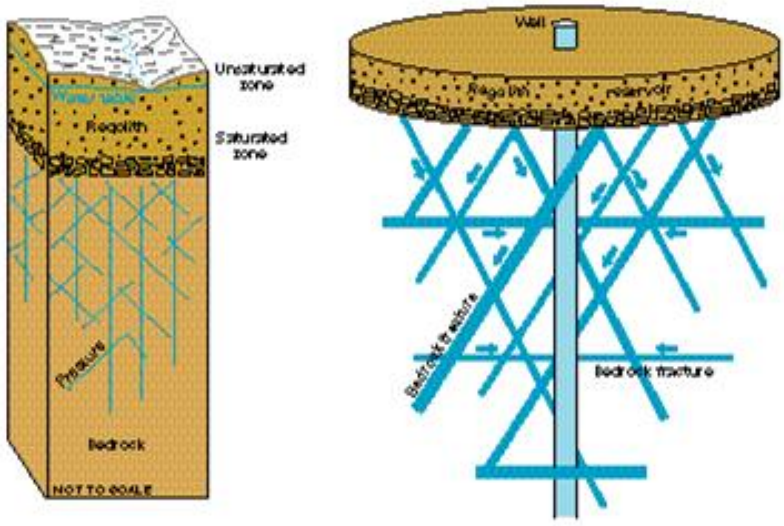

Figure 1.3. Conceptual hydrogeology model of the Piedmont Province (Heath, 1989)

Porosity ranges from 35 to 55 percent throughout the regolith, which is considered to be a storage reservoir for the underlying bedrock (Heath, 1990; Daniels, 2002; LeGrand, 2004; Williams, 2001). Groundwater flow moves through the regolith and into fractures in the underlying bedrock, while another component of flow moves

through the regolith and parallel to the bedrock surface towards discharge areas such as streams and springs (Figure 1.4).

Crystalline rock and saprolite systems are characterized as unconfined aquifers. Water enters as recharge and flows through the unsaturated zone until reaching the water table of the saturated zone of the regolith. Groundwater then flows to areas of discharge such as streams, lakes, seeps, and springs. Igneous and metamorphic rocks comprise the bedrock and have low porosity and permeability values. Vertical and horizontal fracture systems are the secondary sources of permeability in the bedrock (LeGrand, 1967).

Piedmont Well Yield

Several studies (Stafford, 1983; Snipes, 1984, Daniel, 1992, Swain et al., 2004) have described typical yields Piedmont wells. Daniel (1992) found average flow rates ranged from 50 to 110 m^3/day (9 to 20 gpm) by reviewing 3787 wells throughout the Piedmont terrain, with an average yield of 80 m^3/day (Daniels, 1992). Well depth and diameter was defined as a controlling factor for a wells yield, as deeper and larger diameter wells tend to have increased wellbore storage, allowing for increased drawdown during pumping.

Snipes (1983) and Stafford et al (1984) related well yields in the Piedmont to the presences of fracture zones. Wells with greater yields were most often associated near fracture traces, or linements. Snipes (1894) presented well distance to fracture traces correlated to increased yield.

Swain et al (2004) related the available well yield data from wells in the Piedmont terrain to the rock formation each well was completed within. On average, the largest

yields were found with wells drilled in Gneiss – Schist, which ranged upwards of 300 m^3/day. Wells drilled in phyllite and gabbro produced the lower yields ranging from 20 to 50 m^3/day (Table 1.2).

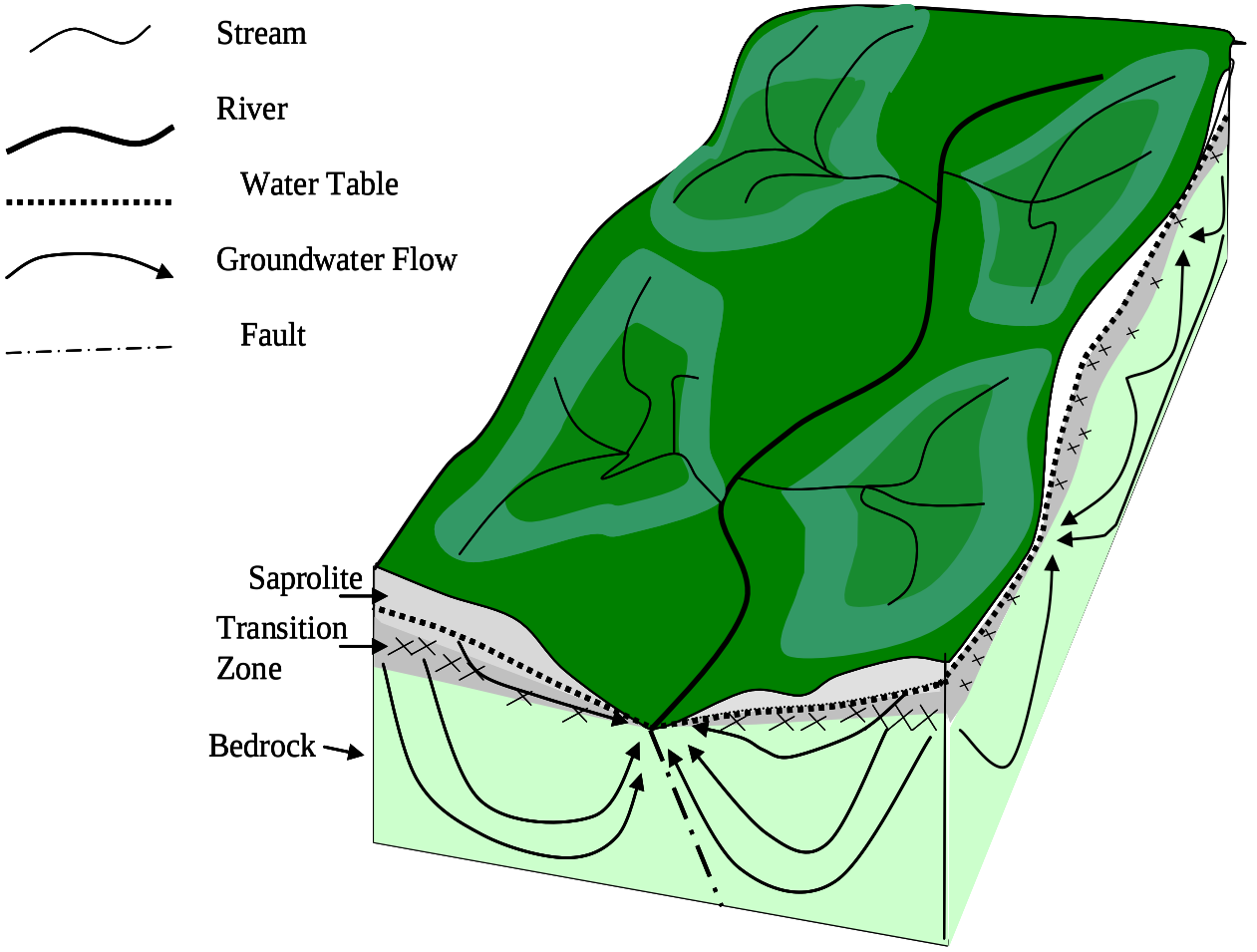

Figure 1.4. Modified existing conceptual model showing flow paths through out system

Rock Type	Average Transmissivity m^2/d	Well Yield m^3/d
Phyllite-Gabbro	3.7	27 - 55
Gneiss-Schist	10.2	55 - 327
Shale Sandstone	32.5	190 - 1200

Table 1.2. Well yields and transmissivity values from wells in the Piedmont, modified from Swain and others 2004.

Statistical analyses by Swain et al (2004) show yields of wells completed in metamorphic rocks are higher than yields of wells completed in igneous formations.

Revised Conceptual Model

Wells in the Piedmont are known to go to steady state because they are pumped for long periods without systematic increases in drawdown. The two-layer hydrogeologic conceptual model (Heath, 1989) attributes well performance in the Piedmont to the removal of water stored in the saprolite. While this process is certainly important, it precludes the possibility that wells go to steady state.

It appears that the hydrogeologic conceptual model for wells in the Piedmont should be modified to allow for conditions that include both transient removal of water from storage and steady state conditions. In general, steady state conditions will only occur when water can be derived from a source other than removal from storage. Surface

water is the only viable option for such a source in the Piedmont. Stream spacing in the Piedmont is roughly 1 km (Bott 2006), so wells will typically be within 500 m of a stream.

The revised conceptual hydrogeologic model for the Piedmont considers fractured rock overlain by saprolite with a stream along the top of the saprolite (Fig. 1.5). The fractured rock is characterized by moderate *K* and small *S*, whereas the saprolite is characterized by moderate *K* and moderate to high *S* (Table 1.3). The resistance to flow between the fractured aquifer and the overlying saprolite ranges from high to low, depending on the depth of the transmissive fractures in the rock and the hydraulic properties of the rock between the saprolite and the transmissive fractures.

	L (m)	w (m)	b' (m)	T (m^2/d)	S_{sap}	S_{rx}
Minimum	1	1	1	1	1.E-04	1.E-06
Maximum	500	30	30	30	0.3	1.E-03

Table 1.3. Typical Piedmont property ranges (Heath, 1990; Daniels, 2002; LeGrand, 2004; Williams, 2001).

Pumping a well in this hydrogeologic setting will initially remove water from storage in the fractured rock. This will be followed by a period of removal of water from storage in the saprolite. Eventually, drawdown caused by the well will interact with the stream and this will cause the system to go to steady state.

The stream-well interaction is what causes steady conditions. In an idealized case where recharge is negligible, steady state occurs when the flow out of the stream matches the pumping rate. However, recharge in most natural systems will cause mounding of the initial water level, with the ambient ground water system characterized by a divide between two streams (Fig. 1.6). Pumping produces drawdown that is superimposed on this system, creating two divides in cross section (Fig. 1.6). Water between the divides is captured by the well, whereas water outside of the divides continues to flow to the streams. It is important to recognize that steady recharge will influence the location of the capture zone, but it has no effect on the hydraulic transient caused by the well. As a result, recharge has no influence on when the well goes to steady state, nor does it affect the magnitude and distribution of drawdown that occurs at that time. We propose that this behavior is typical of wells operating in the Piedmont.

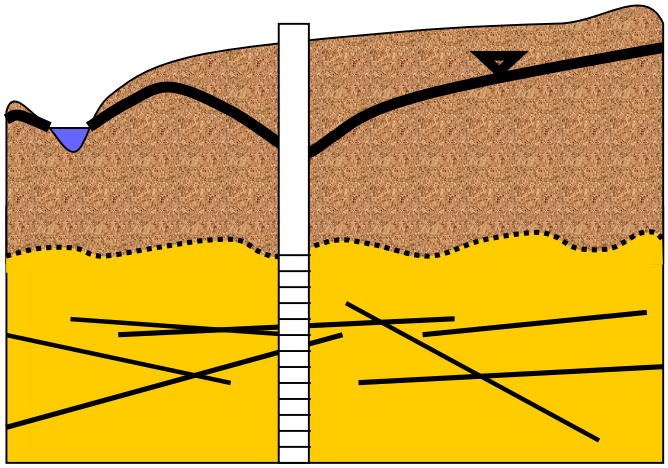

Figure 1.5. Conceptual model of the Piedmont including a stream atop the saprolite layer.

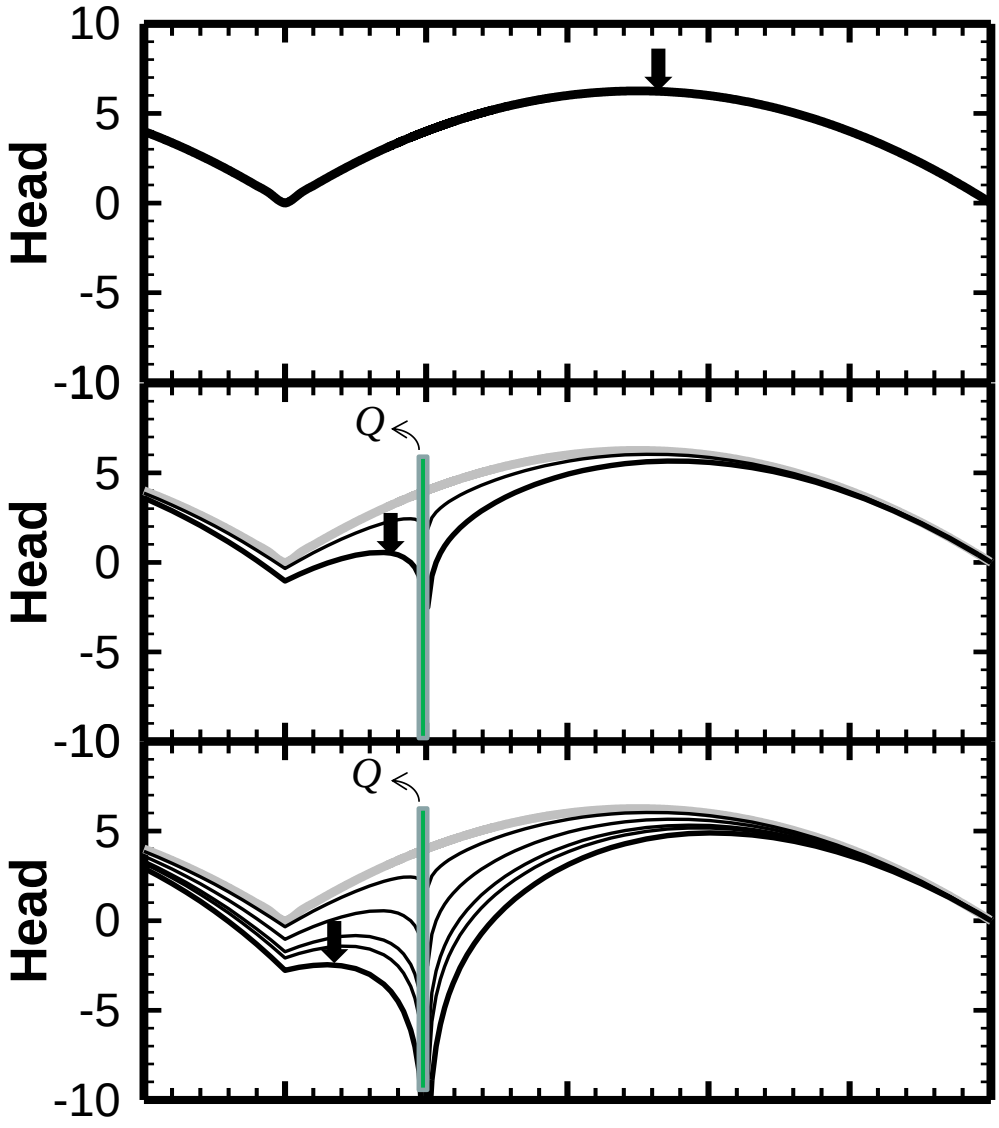

Figure 1.6. Hydraulic head profiles at different times in a aquifer with a well pumping between a stream and recharge zone. Black arrow represents a ground water divide between a pumping well and stream.

CHAPTER 2

DESCRIPTION OF THE ANALYSIS

There appear to be two methods currently in use for estimating the physically sustainable yield, or the specific capacity of a well. One is an empirical method that simply observes the well performance during a short test and assumes it will remain unchanged in the long term. The other method uses a short-term test to determine aquifer parameters, and then applies these parameters to analyses that predict long-term performance. The second method provides a scientifically tenable approach to estimating well performance, but there are few publications describing or evaluating this technique.

The purpose of the following chapter is to outline analyses that are intended to estimate well performance in hydrogeologic conditions typical of the Piedmont. There are myriad factors that could affect well performance and a few of them include:

1. Interference from nearby wells
2. Interaction with surface water
3. Interaction with saprolite
4. Well skin
5. Transient recharge
6. Large drawdown changes saturated thickness, dewaters fractures
7. Unknown heterogeneities
8. Aquifer terminates or is compartmentalized

A complete analysis of well performance would include all of these, and perhaps other, factors. It would be possible to include many factors affecting well performance in a numerical analysis, which would certainly have the potential to provide an accurate prediction. A detailed numerical simulation could require considerable skill to set up and considerable effort to calibrate, and while this level of effort would be warranted for some applications, it would likely be too costly for many cases.

An alternative is to consider the factors that are most important and use an analytical solution to develop a closed form solution. Some factors must be ignored in this approach, so it is important to identify and include those that are have the most control on performance. It is also important to verify that the factors that have been omitted either have a limited effect on the results, and that it is possible to recognize and account for their effect.

We will assume that the well that is being used is relatively isolated and unaffected by drawdown from neighboring wells. Of course, there are many cases where the performance of wells in close proximity is important to understand, but this problem will be deferred for later after the problem involving a single well has been evaluated. We will be interested in evaluating cases where wells go to steady state because this behavior is observed in the Piedmont. In order for steady state to occur, there must be a source of water other than removal from storage. Streams are common in the Piedmont, with the stream density (average spacing between streams) roughly 1 km. This implies that most wells will be within 500m of a stream. We propose that wells in the Piedmont that go to steady state do so by interacting with streams. In some cases, the wells may

recover water from the streams, but the more likely scenario is that the well captures water that has recharged the aquifer and is destined to discharge to the stream (Bredehoeft 1997, 2002).

It will be important to include a stream in the analysis, but steady recharge will be ignored because it has no effect on the magnitude and distribution of drawdown. Steady recharge will affect flow paths and the well capture zone, but the focus of this analysis will be drawdown. Recharge can be included to the analysis developed here using superposition.

Well skin plays an important role in well performance (Earlougher 1977) and it is fairly straightforward to characterize in the field. It is also fairly straightforward to include in theoretical analyses, so it will included in the theoretical approach used here. Saprolite is recognized as a key component affecting well performance in the Piedmont (LeGrand, 1967, 1988, 2004; Heath, 1989; Rutledge, 1996; Daniel, 1992, 2002; Swain, 2004), and we will include it in our evaluation. The approach we will use it to avoid explicitly recognizing saprolite in the analysis (although it can be included in the form of effective parameters). However, several analyses will be presented that evaluate the roles of contrasts in both K and S between the rock aquifer and the overlying saprolite.

Some wells used for water supply may be highly stressed by large drawdowns, particularly in times of drought. Large drawdowns can dewater fractures in open boreholes, and this will introduce non-linear responses that are difficult to anticipate. We recognize that this effect does occur and can be important, and that direct extrapolation of results of the linear problem assuming small drawdown may be provide inadequate

estimates of performance when large drawdowns occur. This effect probably will be included in later work, but here we will assume that drawdowns are small.

Heterogeneities can certainly play a big role in well performance, and the magnitude of their effect will depend on their size and relative distribution of properties. Heterogenieties with characteristic dimensions that are small compared to the region affected by drawdown probably can be represented for problems involving pressures using effective average properties of K and S (in contrast to problems involving transport where small scale heterogeneities may be important). As a result, the properties used in the analysis will be assumed to be average values.

Large-scale heterogeneities may have significant effects on well performance that cannot be represented by averaging. An excellent example of this is a rock aquifer that consists of finite regions of interconnected fractures bounded by regions where fracture connectivity is low. This effectively partitions the aquifer into compartments. Well performance can abruptly decrease when drawdown interacts with compartmental boundaries. This important effect will be addressed briefly, but a thorough treatment will be deferred.

CONFIGURATION

The analysis will assume that the well fully penetrates a homogeneous aquifer of infinite extent, which is overlain by a sink representing a stream (Fig. 2.1). The stream is separated from the well by a distance L, and from the aquifer by a thickness, b'. The thickness of the aquifer is b.

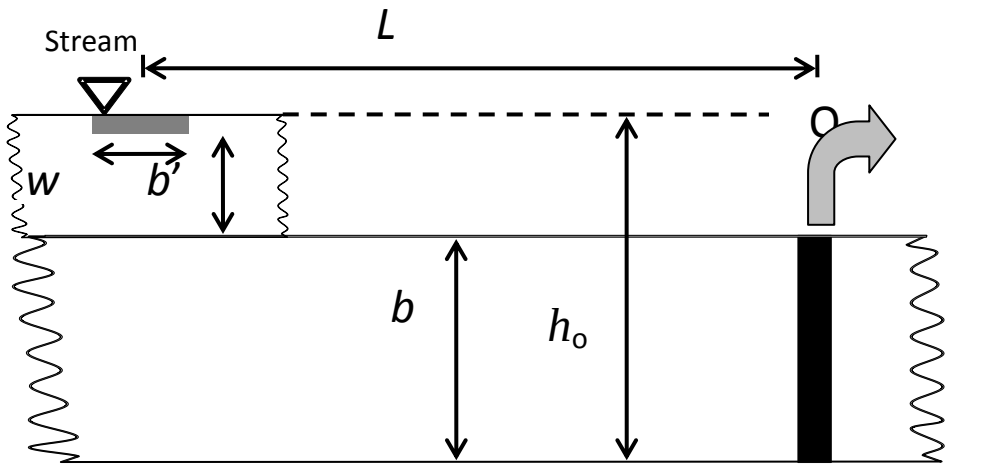

Figure 2.1. Cross-section of geometry used in the analysis.

THEORETICAL ANALYSIS

The problem will be analyzed by assuming the well fully penetrates the aquifer and the saturated thickness is large compared to the drawdown. Vertical flow is ignored. This allows the use of the linearized form of the differential equation describing head in an aquifer

$$T\nabla^2 h = S\frac{\partial h}{\partial t} - R \tag{2.1}$$

where derivatives in the vertical, *z*, direction are zero, *T* is transmissivity, *S* is storativity, and *R* is flux due to fluid sources. The origin of coordinates is at the stream and a well is at $x = L$, $y = 0$. The pumping rate of the well is Q_w. The stream overlies the aquifer and the flux from the stream to the aquifer is

$$q_s = \frac{K_{sap}}{b'}(h_o - h) \tag{2.2}$$

where K_{sap} and b' are respectively the hydraulic conductivity and thickness of the material between the top of the aquifer and the stream (Fig. 2.1). h_o is the head in the stream. The source term is (Hunt 1999)

$$R = \frac{K_{sap}}{b'}(h_o - h)\delta(x) - Q_w\delta(x-L)\delta(y) \tag{2.3}$$

where δ is the Dirac delta function. The initial condition is

$$h(x, y, 0) = 0 \tag{2.4}$$

The far-field boundary condition is

$$\lim_{(x^2+y^2)\to\infty} h(x, y, t) = 0 \tag{2.5}$$

For convenience, the analysis will be presented in terms of drawdown

$$s(x, y, t) = h(x, y, 0) - h(x, y, t) \tag{2.7}$$

The solution to this boundary value problem can be obtained using Laplace and Fourier transforms (Hunt, 1999).

$$s(x, y, t, \lambda) = \frac{Q_w}{4\pi T}\left\{E_1\left(\frac{(L-x)^2 + y^2}{4Tt/S}\right) - g(x, y, t, \lambda)\right\} \tag{2.8a}$$

$$g(x, y, t, \lambda) = \int_0^\infty e^{-\theta} E_1\left(\frac{(L + |x| + 2T\theta/\lambda)^2 + y^2}{4Tt/S}\right) d\theta \tag{2.8b}$$

The function $g(x, y, t, \lambda)$ accounts for the effects of the stream, where λ is streambed leakage.

The dimensionless drawdown is

$$s_d(x_d, y_d, t_d, \beta) = \left\{ E_1\left(\frac{\left(1 - x_d\right)^2 + {y_d}^2}{t_d} \right) - G(x_\partial, y_d, t_d, \beta) \right\} \tag{2.9a}$$

where

$$G(x_d, y_d, t_d, \beta) = \int_0^\infty e^{-\theta} E_1 \left(\frac{\left(1 + \left|x_d\right| + \frac{2\theta}{\beta}\right)^2 + {y_d}^2}{t_d} \right) d\theta \tag{2.9b}$$

accounts for the effects of the stream, and

$$t_d = \frac{4tT}{L^2 S} \tag{2.9c}$$

$$s_d = \frac{s 4\pi T}{Q_w} \tag{2.9d}$$

$$\begin{aligned} x_d &= x / L \\ y_d &= y / L \end{aligned} \tag{2.9e}$$

$$\beta = \frac{L k_{sap} w}{T b'} \tag{2.9f}$$

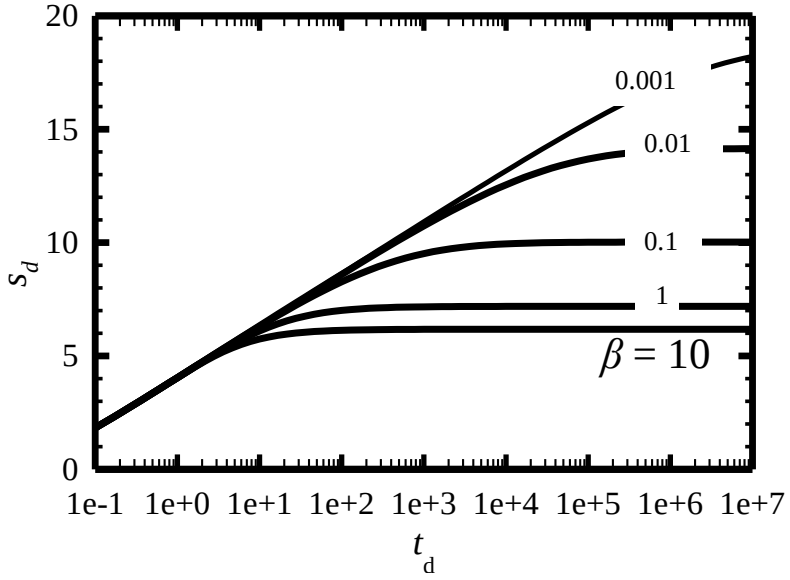

Figure 2.2. Dimensionless drawdown as a function of dimensionless time for different values of β.

The parameter β characterizes the interaction between the stream and the aquifer. When β is large, G is equivalent to an image well function (Hunt 1999; Butler 2001) at x_d = -1, which causes the stream to behave as a constant head boundary of the aquifer (Fig. 2.2). Decreasing the value of β implies a decrease in the influence of the stream on the drawdown, and it increases the drawdown and the time required to reach steady state. It is noteworthy, however, that the presence of the stream always causes to well to go to steady state regardless of the value of β .

STEADY STATE BEHAVIOR

The long-term behavior of the well will approach steady state conditions. Using the natural log approximation for E_1 (Jefferys 2004) gives

$$s_d(x_d,0,t_d,\beta)=\left\{\ln\left(\frac{t_d}{1.78\left(1-x_d\right)^2}\right)-\int_0^{\infty}e^{-\theta}\ln\left(\frac{t_d}{1.78\left(1+\left|x_d\right|+\frac{2\theta}{\beta}\right)^2}\right)d\theta\right\} \qquad (2.10)$$

which gives

$$\int_0^{\infty}e^{-\theta}\ln\left(\frac{t_d}{1.78\left(1+\left|x_d\right|+\frac{2\theta}{\beta}\right)^2}\right)d\theta=\ln\left(\frac{t_d}{1.78(1+x_d)^2}\right)-2e^{\frac{\beta}{2}(1+x)}E_1\left(\frac{\beta}{2}(1+x_d)\right) \qquad (2.11)$$

So the steady state drawdown profile perpendicular to the stream and intersecting the well is

$$s_{d\,ss}(x_d,0,\beta)=\ln\left(\frac{\left(1+x_d\right)^2}{\left(1-x_d\right)^2}\right)+2e^{\frac{\beta}{2}(1+x_d)}E_1\left(\frac{\beta}{2}(1+x_d)\right) \qquad (2.12)$$

The drawdown at the well can be obtained using $x_{\mathrm{dw}} = 1 + r_{\mathrm{d}}$. Assuming the distance to the stream is much larger than the well radius, $x_{dw}\approx 1$. It follows that the dimensionless steady state drawdown at the well is

$$s_{dss}(r_{dw},\beta)=\ln\left(\frac{4}{r_{dw}{}^2}\right)+2e^{\beta}E_1\left(\beta\right)+2s_k \qquad (2.13a)$$

where $r_{dw} = r_w/L$ in keeping with the scaling in 2.9. The skin factor, s_k, is introduced to account for head losses in the vicinity of the well, and it is assumed (Earlougher, 1977)

$$s_k = \left(\frac{K}{K_s} - 1\right)\ln\left(\frac{r_s}{r_w}\right) = \frac{2\pi T}{Q}\left(s_a - s_e\right) \tag{2.13b}$$

where s_a and s_e are the actual and expected drawdowns, respectively. Following (1.1), the specific capacity of the well at steady state is

$$S_{css} = \frac{Q_w}{s_{ss}} \tag{2.14}$$

where s_{ss} is the steady state drawdown, so from 2.9d

$$S_{css} = \frac{2\pi T}{\ln\left(\frac{2L}{r_w}\right) + e^{\beta}E_1\left(\beta\right) + s_k} \tag{2.15a}$$

which can be expressed alternatively as

$$S_{css} = \frac{2\pi T}{\ln\left(\frac{2L}{r_w}\right)}\left(\frac{1}{1+\omega}\right) \tag{2.15b}$$

where the second term is a correction that accounts for contributions from β and s_k as

$$\omega = \frac{e^{\beta} E_1(\beta) + s_k}{\ln\left(\frac{2L}{r_w}\right)} \qquad (2.15c)$$

INTERPRETING SHORT-TERM TESTS

The long-term behavior of a well in an idealized aquifer depends on *T*, *S*, *L*, β , and s_k. There are several ways that this analysis (2.15) can be applied, depending on the available data and assumptions that are appropriate. All of the methods assume that *T*, *S*, and s_k can be determined from the short-term well test using standard methods. The most ideal application occurs when at least one monitoring well is available to facilitate estimating *S*, and s_k.

Using the **full analysis** (eq. 2.15) requires estimates of *L* and β. *L* can be measured by surveying, or from reliable maps. The data required to determine β (eq. 2.9f) can be obtained from drilling and localized in-situ measurements. It may be possible to estimate β with sufficient accuracy for some applications when direct measurements are unavailable.

In some cases it may be appropriate to assume the stream cuts through the aquifer and β is large. Perhaps the stream is known to cut the aquifer, or perhaps no information is available for calculating β so 2.9f cannot be solved. The term involving β in (2.15) probably can be safely ignored when $\beta > 10$. In this case, the stream behaves as a constant head boundary and the image well solution (Muskat, 1935; Hantush and Jacob, 1955; Hantush,1965; Ferris, 1959) can be used to approximate well performance. The

drawdown for this case will approach a semi-log straight line soon after the start of pumping, and then the slope of the curve will decrease when the effects of drawdown reach the boundary. Eventually the curve will flatten completely and the drawdown will remain constant (Fig. 2.3).

When β is large, the steady state specific capacity (eq. 2.15) becomes

$$S_{css} = \frac{2\pi T}{\ln\left(\frac{2L}{r_w}\right) + s_k} \tag{2.16}$$

There are at least 3 methods that can be used for implementing the simplification in eq. 2.16.

Simplification Method 1

Measure *L* using surveying techniques or from a map, and substitute into 2.16.

Simplification Method 2

The distance between the well and a stream may be unknown, or there may be several streams or lakes of different sizes in the vicinity of the well that make direct measurement of *L* ambiguous. In this case, it may be feasible to use the drawdown curve to estimate an effective value of *L*.

The slope of the drawdown curve decreases from a constant value when the drawdown interacts with the stream. The slope changes gradually at first and the initial change can be subtle and difficult to locate precisely. In most plots, it is quite clear that the slope has changed when it is 0.8 of the maximum slope. This time, $t_{0.8}$, can be

identified approximately by manually fitting a straight line and selecting the time when the slope deviates from the line. Alternatively, this time can be identified unambiguously by plotting the normalized first derivative.

The time when the semi-log slope changes to 0.8 of the maximum slope can be determined using (2.9) for large β as

$$s_s(x_d, y_d, t_d) = E_1\left(\frac{((1-x_d)^2 + y_d{}^2)}{t_d}\right) - E_1\left(\frac{(1+x_d)^2 + y_d{}^2)}{t_d}\right) \tag{2.17}$$

which is the image well solution (Muskat, 1935; Hantush and Jacob, 1955; Hantush,1965; Ferris, 1959). The slope on a semi-log plot is

$$\frac{ds}{d(\ln(t_d))} = \frac{ds}{dt_d}\frac{dt_d}{d\ln(t_d)} = \frac{ds}{dt_d}t_d \tag{2.18}$$

Setting $y_d = 0$, $x_d = 1 + r_d$ in 2.17 to get the drawdown at the well, and substituting 2.17 into 2.18 gives the response at the well

$$\frac{dP_d}{d(\ln(t_d))} = e^{-\frac{r_{wd}{}^2}{t_d}} - e^{-\frac{(r_{wd}-2)^2}{t_d}} \tag{2.19}$$

where $r_d = r_w/L$. Assuming the well radius is small compared to the distance between the stream and the well gives $r_w << L$, or $r_{wd} \rightarrow 0$, so the semi-log slope of the drawdown at the well is

$$\frac{dP_d}{d(\ln(t_d))} = 1 - e^{-\frac{4}{t_d}} \tag{2.20}$$

The semi-log slope is equal to 0.8 at $t_{d0.8}$, so from 2.20

$$t_{d0.8} = 2.48 \tag{2.21}$$

It follows from 2.9c that the time when the semi-log slope has changed by 0.8 is

$$t_{0.8} = 0.6213\frac{SL^2}{T} \tag{2.22}$$

Solving 2.22 for the distance to the stream

$$L = \sqrt{\frac{1.61\ Tt_{0.8}}{S}} \tag{2.23}$$

and substituting into 2.16

$$S_{css} = \frac{2\pi T}{\ln\left(\frac{2.54}{r_w}\sqrt{\frac{Tt_{0.8}}{S}}\right) + s_k} \tag{2.24}$$

Note that an alternate use for the analysis outlined above is to compare $t_{0.8}$ determined from field data to the results from 2.22 where L is measured in the field. Where $t_{0.8}$ measured from a plot of field data is significantly less than the results from

2.22, then it may be that the change in slope in the field data is due to something other than interaction with a stream.

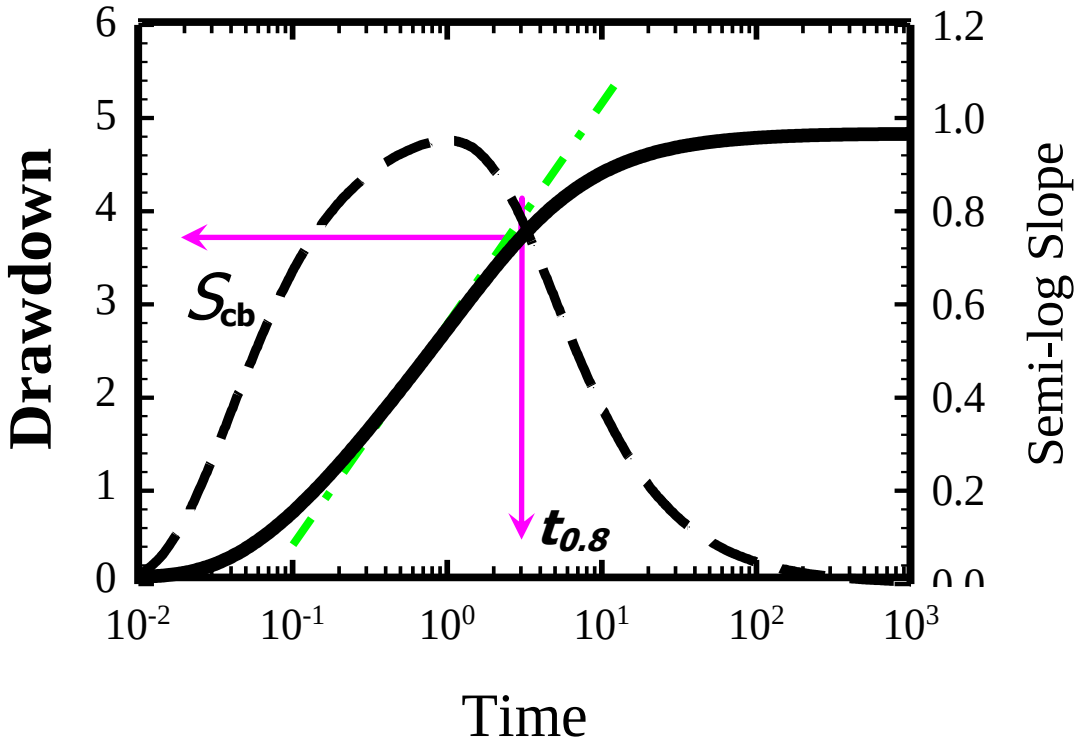

Figure 2.3. Drawdown as a function of time (thick black line), and semi-log slope of drawdown (dashed) . $t_{0.8}$ is identified using a line fit to the semi-log linear portion of the drawdown curve (green dashed and dotted line). $t_{0.8}$ also identified using the derivative plot (pink arrows) .

Simplification Method 3

In cases where *L* is unknown and only a single well is available, it will be difficult to obtain a reliable value of *S* from the well test so Method 2 (eq. 2.24) may be unsuitable.

An alternative approach that also uses data at the time when the semi-log slope changes seems feasible. The drawdown prior to interaction with the stream is given by

$$s_d(r_{wd}, t_d) = \ln\left(\frac{t_d}{1.78 r_{wd}^{\ 2}}\right) \tag{2.25}$$

so at $t_d = 2.48$, the dimensionless time when boundary interaction becomes detectable, the drawdown is

$$s_d(r_{wd}, 2.48) = \ln\left(\frac{0.56}{r_{wd}^{\ 2}}\right) \tag{2.26}$$

The dimensionless drawdown at the well at steady state is eq. 2.13a

$$s_{dss}(r_{dw}) = \ln\left(\frac{4}{r_{dw}^{\ 2}}\right) \tag{2.27}$$

where β is large and s_k is ignored.

the difference between the drawdown at steady state and at $t_{0.8}$ is

$$s_{dss} - s_{d0.8} = \ln\left(\frac{4}{0.56}\right) = 1.966 \tag{2.28}$$

Using the definitions of dimensionless drawdown (eq. 2.9d) and specific capacity (eq. 2.14), and rearranging

$$S_{css} = \frac{TS_{c0.8}}{0.157S_{c0.8} + T} \tag{2.29}$$

where $S_{c0.8}$ is the specific capacity at the break in slope ($t = t_{0.8}$).

CHAPTER 3.0

NUMERICAL EVALUTION

Several methods are available for estimating long-term well performance, and in the previous chapter I presented one that is theoretically based and should be straightforward to apply. The method will be evaluated by comparing data describing the actual performance of wells under different conditions to the performance predicted by the proposed method. This will be done first by using numerical models to represent wells operating in hydrogeologic scenarios similar in the Piedmont. The parameters and geometries of the scenarios used to set up the models will then be used in the method for estimating well performance. The difference between the observed and predicted performances will be used to provide a quantitative assessment of the error resulting from the proposed method.

NUMERICAL ANALYSIS

The numerical simulations were conducted using MODFLOW (McDonald and Harbaugh, 1988) with the Groundwater Vista 4.0 version 4.19 interface (Rumbaugh, 1998). MODFLOW is a finite-difference groundwater flow model that solves the partial differential equation describing the three-dimensional movement of groundwater of constant density through porous material given as (McDonald and Harbaugh 1988):

$$S_s \frac{\partial h}{\partial t} = \frac{\partial}{\partial x}\left(K_{xx} \frac{\partial h}{\partial x} \right) + \frac{\partial}{\partial y}\left(K_{yy} \frac{\partial h}{\partial y} \right) + \frac{\partial}{\partial z}\left(K_{zz} \frac{\partial h}{\partial z} \right) \pm q_w \qquad (3.1)$$

where K_{xx}, K_{yy}, K_{zz} are hydraulic conductivity values (LT^{-1}) along the x, y, and z coordinates, h is the potentiometric head (L), q_w is a volumetric flux per unit volume representing sources and/or sinks of water (T^{-1}), S_s is the specific storage (L^{-1}), and t is time (T).

Geometry

The model consists of a rectangular region containing a vertical well and a stream represented as a region of constant-head. The region is divided into two zones of different properties representing saprolite of thickness, b', and the underlying fractured rock of thickness, b. The well is screened across the bottom zone. A stream is represented as a long, straight strip of constant head cells at a distance, L, from the pumping well along the top of the upper zone (Figure 3.1). The lateral dimensions of the rectangular region are large, and the region is assumed to be of infinite extent.

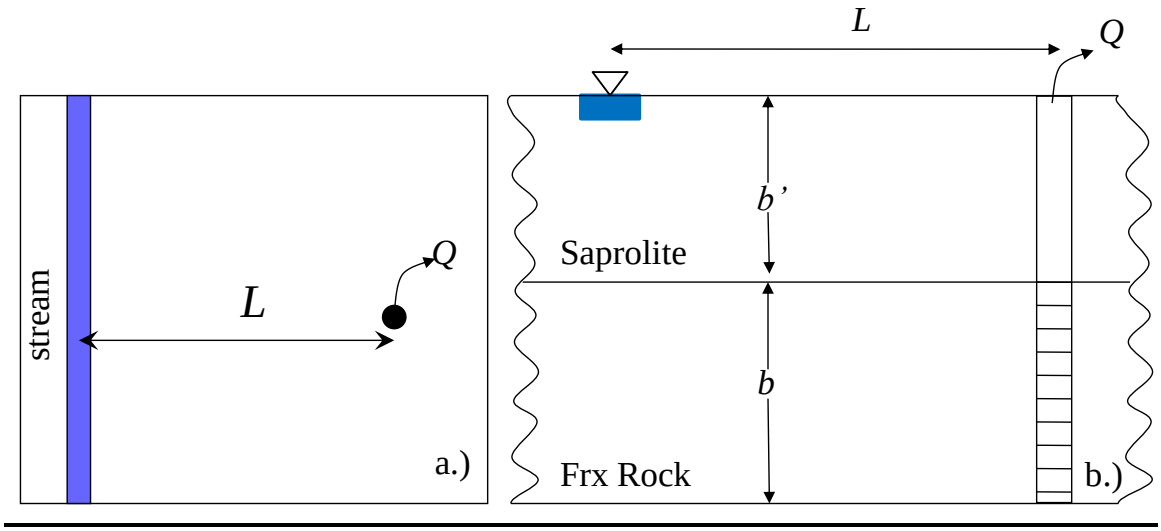

Figure 3.1. Conceptual geometry a.) plan view b.) side view of well screened in a layer separated from a partially penetrating stream by a layer representing a saprolite aquifer.

Boundary Conditions

The model is bounded on the sides and bottom by no-flow conditions. The top is no-flow except a single row of cells in the top layer is held at constant head to represent a stream. The width and location of the row representing the stream were varied to account for different geometries (Table 3.1). The distance between the well and the stream ranged from 10m < L < 500m . (Table 3.1).

The well is represented as a fully penetrating, vertical analytic element in the center of lower zone. The well is pumped at a constant rate of 0.03 m^3/min for all the simulations. The analytic element distributes the total volumetric rate evenly over all the

cells representing the well. Screen elevations are set to the top and bottom layers of the bottom zone.

Distance (m)	Column Number	Actual Model Distance (m)
L=10	80-85	8.64
L=30	81	31.79
L=50	78	55.93
L=100	73	105.91
L=250	58	255.98
L=500	33	505.91

Table 3.1. Location in column numbers and model distances from the pumping well to constant head strips used in the numerical simulations.

Parameters

Parameters consist of hydraulic conductivity of the rock and saprolite, K_{rx} and K_{sap}, and specific storages of S_{rx} and S_{sap}. which were set to S = 0.0001, and was held constant in the bottom aquifer, S_{rx}, and varied in the upper aquifer from S_{sap} = 0.0001 to 0.3. Hydraulic conductivity was assumed to be isotropic and both K and S were assumed to be uniform within each layer.

Grid Design

A grid was designed to solve the discretized form of eq. (3.1) with acceptable numerical performance using the geometry and boundary conditions of the problem. There were three objectives for designing a grid; (1) the size is large enough to prevent far-field boundary effects during pumping, (2) the mass balance error is less than 1%. (3) a stream can be represented at different distances from a pumping well; (3) the run time is modest (less than 10 minutes) to allow for multiple runs to be conducted in a reasonable time.

The grid contained 200 rows by 200 columns with 8 layers for a total of 320,000 cells. The well was located in row 100, column 100. The well is at the center of 10 x 10 square cells that are 0.5 m on a side (Fig. 3.2). The spacing of the column and rows was increased geometrically outward from the central region of uniform cells (Fig. 3.2). A 1.2 multiplier was used to increment the grid size (Anderson and Woessner, 1992), and this resulted in a total model domain 1.66×10^{7} m on a side. Local adjustments in the grid were made by changing the spacing of the columns to match a particular stream location and width.

Solver

The Strongly Implicit Package was used to solve the partial differential equation. This solver was chosen because it was able to successfully converge for most cases in less than 5 minutes. The stress period duration was set to 10,000,000 minutes with 100 time steps and a time step multiplier of 1.2. This allowed each model case to reach steady state conditions, with a convergence criteria of 0.001. Mass balance percent error ranged from 6.7×10^{-6}% to 1.3×10^{-6}.

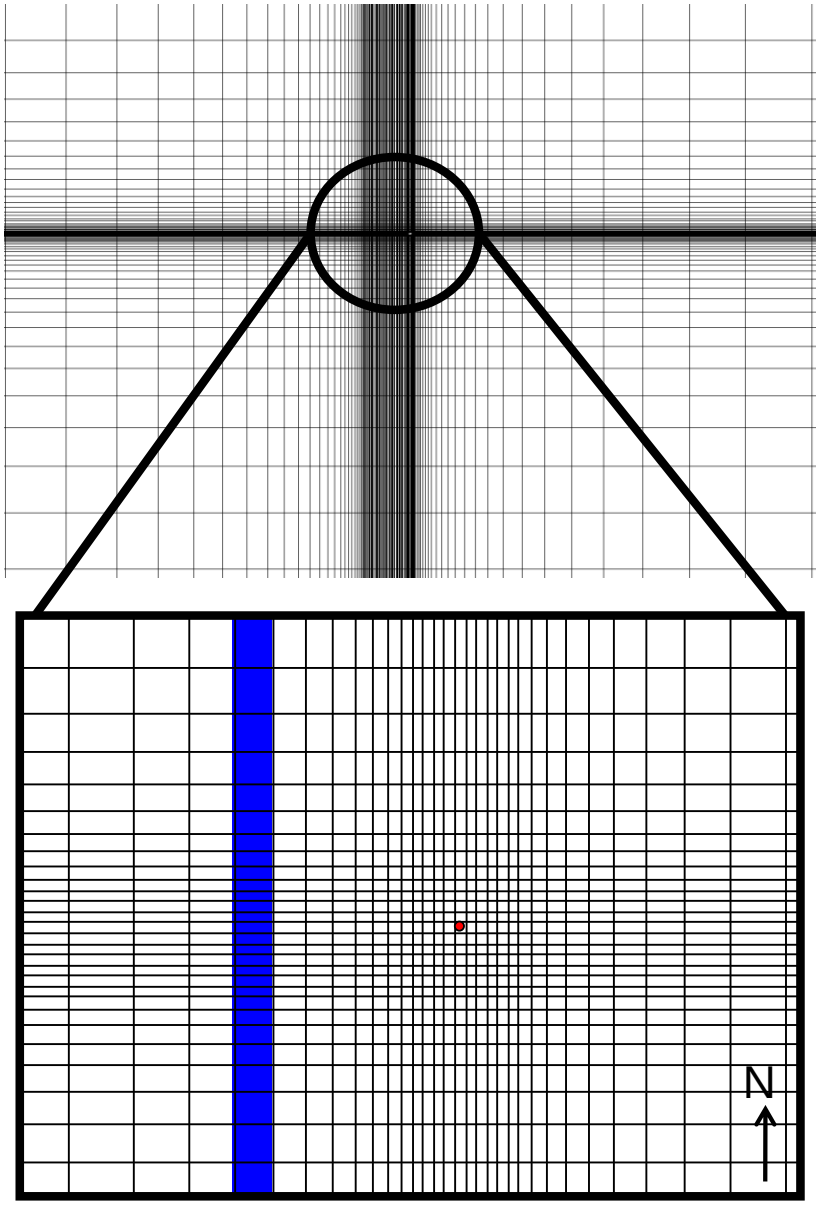

Figure 3.2. Map view of model grid showing location of the constant head boundary representing stream (blue) relative to the pumping well (red).

Geometry Cases

Idealized cases were developed in which dimensions were determined for conditions typical of the Piedmont (Figure 3.3). Stream width, *w*, ranges from 1 m to 10 m, representing first to second-order stream channels in the Piedmont (Sweeney 1992; Bott et al. 2006). The distance to the stream, *L*, ranges from 10 m to 500 m. The spacing of first-order streams in the Piedmont is approximately 1 km (Harman 1989; Bott 2006), so I assumed the greatest distance to a stream as 500m. Saprolite thickness, *b'*, ranges from 5 to 30 m based on thicknesses summarized by (LeGrand 1967; Kasper 1989; Seaton 2000). The rock aquifer thickness, *b*, was assumed to range from 5 to 70 m (LeGrand 1969; Heath 1989; Cressler 1996 and 2000).

A *baseline* case was formulated to represent average values, and *high* and *low* cases represented end members of the ranges (Table 3.2). The baseline case was further refined into include four sub-cases to provide additional resolution on the dimensions of the saprolite (Table 3.2).

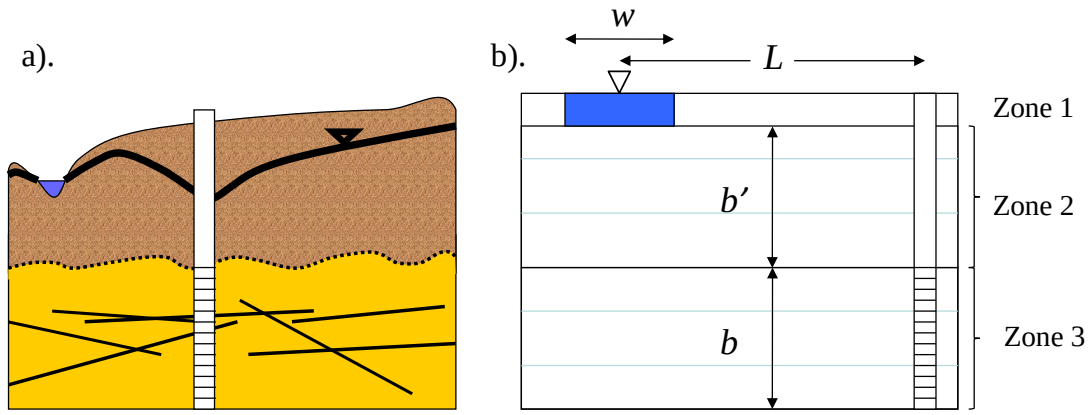

Figure 3.3. a.) Conceptual cross-section of the hydrogeology of the Piedmont and b.) Conceptual model represented as three zones in a numerical model with dimensions *w, L, b', b*.

Table 3.2. Dimensions of cases used to characterize range of geometries.

	Low	Baseline	High	Low Case 1	Low Case 2	Low Case 3	Low Case 4
w (m)	1	10	30	1	10	1	10
b'(m)	5	10	30	10	5	10	5
b (m)	5	30	70	30	5	5	30

Evaluation

The evaluation was conducted by running transient simulations until steady conditions were achieved, and then using the input values from the numerical model to estimate well performance using the method described in Chapter Two. Changes in drawdown diminished gradually in the numerical models and I assumed that steady state conditions were reached when the maximum change in head between time steps was equal to the convergence criteria (0.001m) for three consecutive time steps. In most cases, this occurred during simulation times of less than 10 years. Most simulations were run to 200 years to ensure that steady conditions were reached. Specific capacity at steady state, S_{css}, was determined by dividing the pumping rate by the drawdown at the end of the simulation.

Specific capacities estimated using the methods described in Chapter Two (eqs. 2.15 and 2.16) were based on the parameters and dimensions used in the numerical model. T and S were obtained from values assigned to the zone representing the rock aquifer. The stream strength term, β, was determined using the model inputs for K_{sap}, T_{rx}, b', L, and w.

The accuracy of the predicted S_{css} will be assessed using the percent relative error

$$E_{Sc} = \frac{\text{Predicted } S_{ssc} \text{ - Actual } S_{ssc}}{\text{Actual } S_{ssc}} * 100 \qquad (3.1)$$

The numerical model was used as a surrogate for field tests, so the results from the numerical model will be taken as "actual" values, whereas the results from eqs. 2.15 and 2.16 will be used as "predicted."

2D HOMOGENEOUS VALIDATION

A geometry mimicking the 2D solution was set up using w =10 m, b = 30m, L = 275 m, T = 28 m^2/d and S_s = 0.0001 m^{-1} (Figure 3.4). Cells in the upper layer were set to constant head where the stream occurs, and they were set to no-flow elsewhere. The saprolite thickness was set '=0 to ensure the model was 2-D. The simulation was run for 10 x 10^6 minutes (~19 years).

The observed specific capacity is S_{css} = 0.1106 m^2/min (Figure 3.5). The predicted value using eq. 2.16 is S_{css} = 0.1145 m^2/min, giving $E_{Sc.}$ = -0.279 %. This small error is probably due to truncation when eq. 3.1 is discretized.

This result demonstrates that eq. 2.16 can predict results nearly exactly when the geometries, parameters and boundary conditions used in the numerical model are the same as those used to derive the analytical expressions in Chapter Two. The following sections present results where geometries and parameters are used to represent field conditions that differ from conditions assumed in Chapter Two.

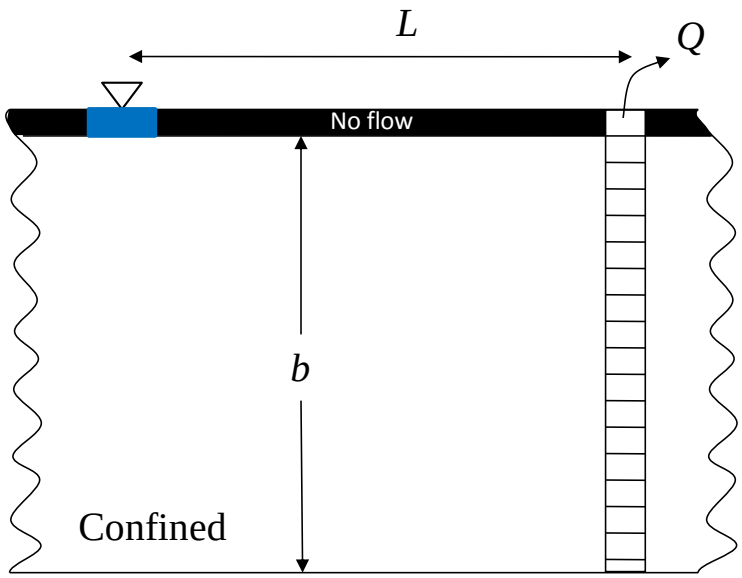

Figure 3.4. Model geometry for validation of numerical model.

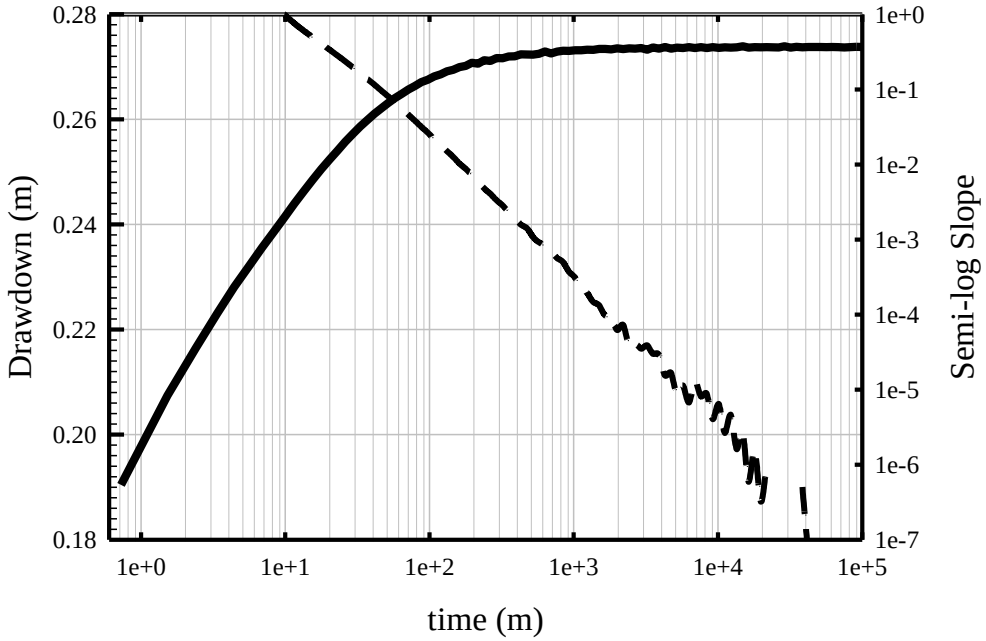

Figure 3.5. Drawdown (solid line) and semi-log slope (dash line) as functions of time for the 2D homogeneous baseline model.

BASELINE EVALUATION

The aquifer will now be represented in 3-D by expanding the vertical dimension and using the geometry in Figure 3.3a. The baseline model characterizing average Piedmont geometries (Table 3.1) will be used with rock properties of T = 26 m^2/d and S = 0.0001 m^{-1}. These data give β=0.4 using eq. 2.9f.

The drawdown slope stabilized and met the head change convergence criteria per time step at approximately 80 days. The observed specific capacity at the end of pumping is S_{ssc} = 0.002739 m^2/min (Figure 3.6). The result predicted by eq. (2.22) is S_{ssc} =0.002864 m^2/min. The error in the baseline numerical model is 4.55% (Figure 3.6).

This result shows that the full analysis slightly over-predicts S_{css} for the baseline case. This error occurs because the flow converges on the stream through relatively low K material in the 3-D numerical model, whereas the flow paths are straight and go through uniform material where they intersect the stream in the 2-D model. The convergence of flow lines in 3-D causes head loss that is not considered in 2-D, and the low K of the saprolite increases this effect. These effects cause the S_{css} in the 3-D model to be less than that predicted by the full analysis.

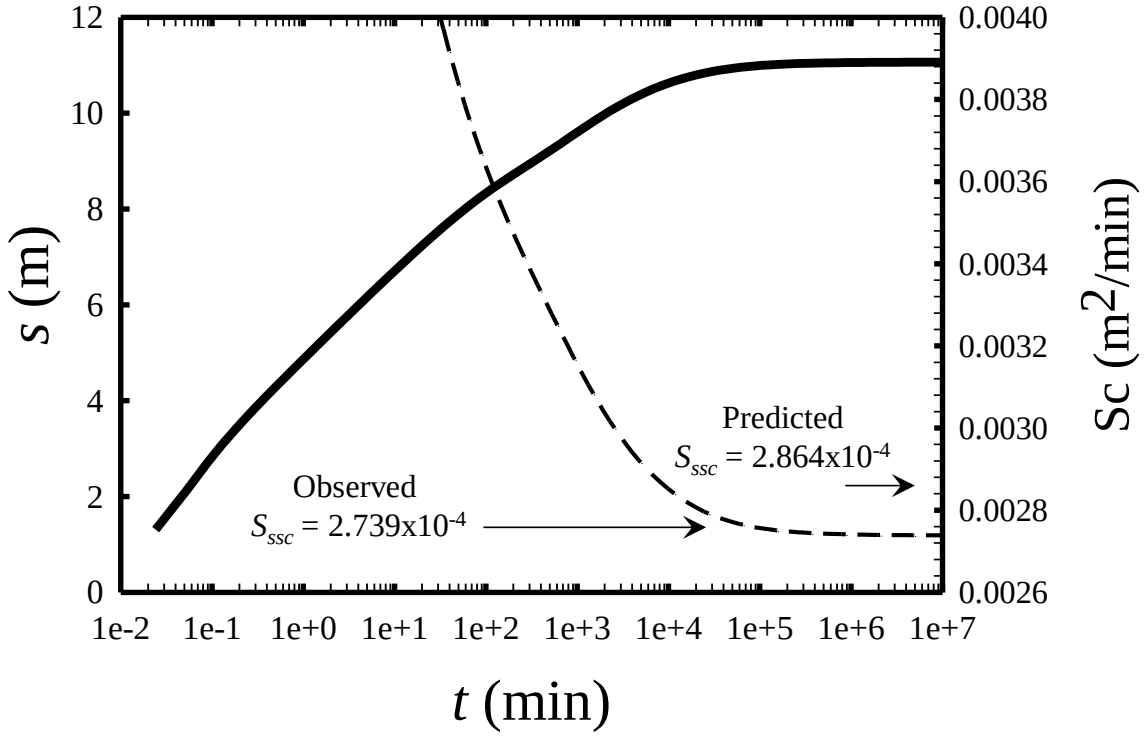

Figure 3.6. Drawdown (solid line) and Specific Capacity (dash line) as functions of time for the baseline model evaluation.

Effect of Contrasts in Hydraulic Conductivity

The proposed method for analyzing S_{css} (eq. 2.15 or 2.16) considers a homogeneous aquifer, but the hydraulic conductivity of the saprolite may differ from the underlying rock and this is expected to affect specific capacity. To evaluate this effect, the hydraulic conductivity of the saprolite, K_{sap}, was varied from 10^{-4} to 10^{-7} m/min while K_{rx} was held constant. The baseline geometry (Table 3.1) was used for the dimensions.

Variations in K_{sap} result in a relative error, E_{Sc}, ranging from -11.3 to 5.7 %. The relative error resembles a negative parabola with positive values for $0.005 < K_{sap}/K_{rx} < 0$

and negative values outside this range. The maximum error is 6.03 % when K_{sap} / K_{rx} = 0.081 and $E_{Sc} \approx 0$ for $K_{sap} / K_{rx} \approx 0.0053$ and 0.59.

The results show that the error inferred to be caused by converging flow in the 3-D case (open circle in Figure 3.7) is reduced when the K_{sap} either increases or decreases from the value used in the example above (shown in Figure 3.6). There are several interacting effects that influence the error. Increasing the hydraulic conductivtiy of the saprolite increases the effective T of the overall aquifer, but this increase is omitted from the eq. 2.16, which is based on the properties of the rock aquifer. This causes the predicted S_{css} to exceed the actual one when $K_{sap} / K_{rx} > 0.6$. Other effects also contribute, but they all appear to be relatively small because the error is less than 6% for a reasonable range of K_{sap}.

Effect of Partial Penetration of Stream

The effect of distance to the stream was evaluated by scaling L to r_w and evaluating cases in the range $10 < L/r_w < 2000$ for the different scenarios in Table 3.1 . The error in the predicted S_{css} ranges from 10^{-4} to 0.08 for the baseline case, and the errors in the other cases are somewhat greater or less than this range (Figure 3.8). The error in all six examples is insensitive to L/r_w where $L/r_w > 200$, but it becomes increasingly positive for $L/r_w < 200$. In general, the change in the error over the range $10 < L/r_w < 200$ is less than 0.1.

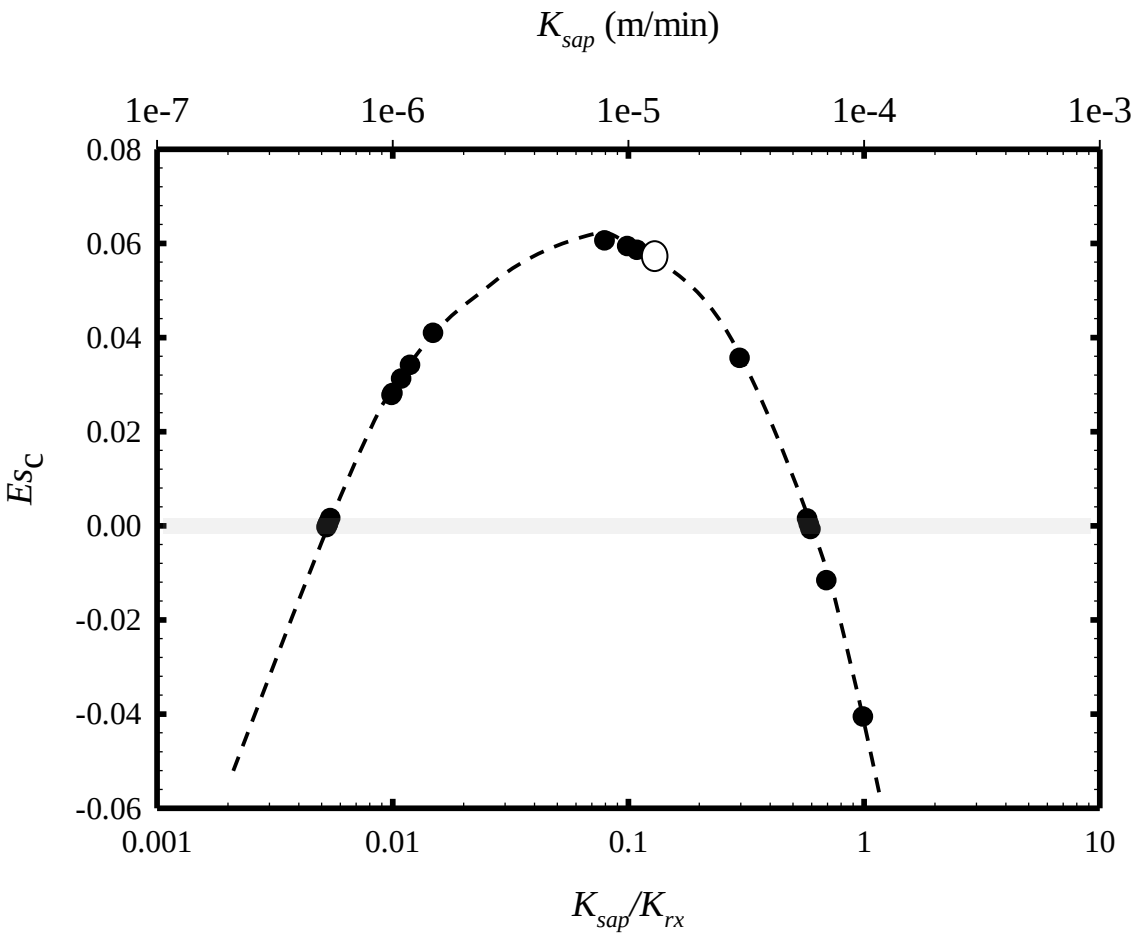

Figure 3.7. Relative error in specific capacity estimate as a function of the ratio K_{sap} / $K_{rx.}$ Simulation from baseline case in Figure 3.6 shown as open symbol.

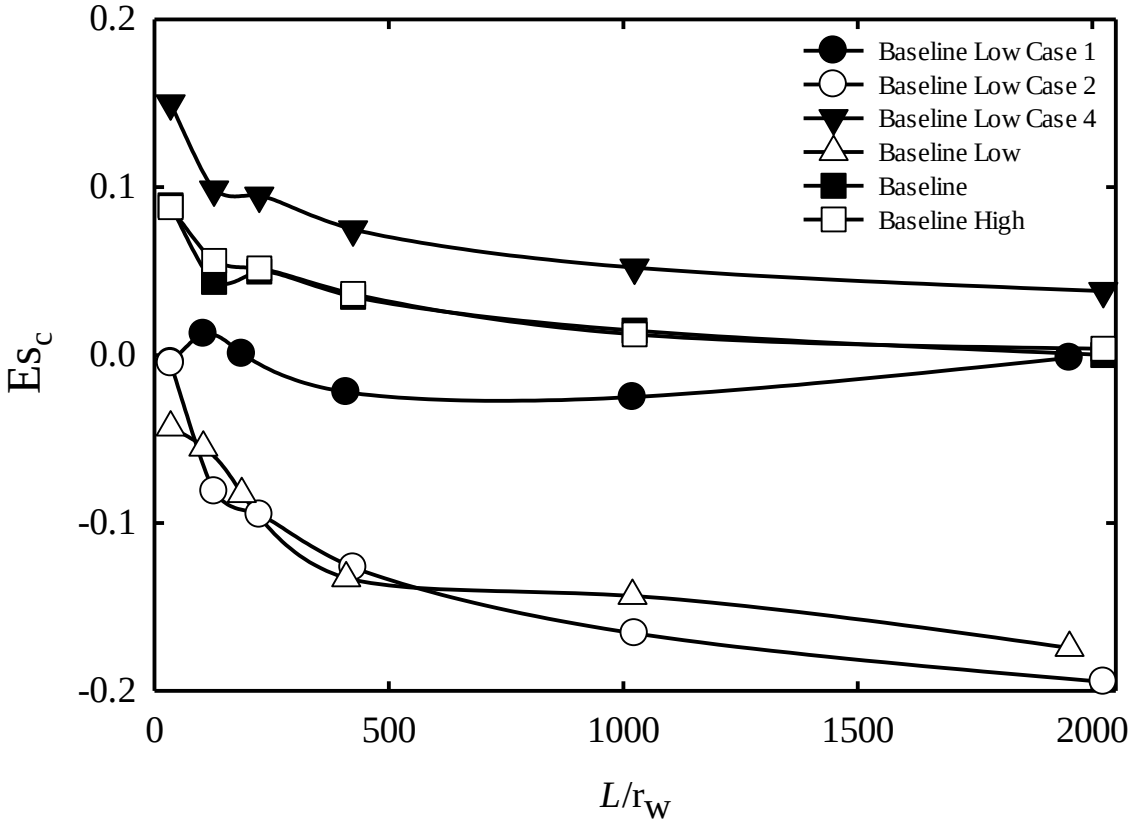

Figure 3.8. Relative error in specific capacity estimate as a function of L/r_w for different geometric configurations.

The increase in error with deceasing L/r_w appears to result from differences in the geometry of the flow lines between the 2-D and 3-D models. Convergence of flow lines causes head losses near the stream in the 3-D model to be greater than in the 2-D model. This effect increases with decreasing L, when L is less than several times the aquifer thickness. This effect occurs because changing L only affects the flow paths in the vicinity of the stream when the well is relatively close to the well (L~<3b).
Error caused by proximity to a stream appears to be limited to distances that are within a few aquifer thicknesses. Even in these cases, however, the error caused by proximity to the stream appears to be less than 10%.

Baseline Low Case 4 had the greatest error, ~15%, close to the stream. The geometry consists of a wide stream, w=10 m, with a thin saprolite layer, b'=1 m.

Both the *Baseline Low* and *Baseline Low Case 2* geometries have equal thickness of saprolite and rock aquifers, $b' = b$ = 5 m, representing a low end ofaquifer thicknesses in the Piedmont. At large, $L/r_w > 300$, the stream strength term, β, due to a thin saprolite thickness, b', dominates flow and may behave similar to a fully penetrating constant head boundary. As $L/r_w < 300$, the error decreases and approaches 0 as L/r_w approaches zero. An aquifer overlain by a thin saprolite will increase the error in predicted S_{scc} as $L/r_w > 300$.The magnitude of the error due to this effect appears to be less than 0.1.

Effect of stream strength term β on analysis

The different numerical examples were evaluated using both the full analysis (eq. 2.15) and the approximation (eq. 2.16). The error caused by the full analysis is always

less than that caused by the approximation (Fig 3.9). However, the differences in errors are small when $\beta > 1$. For example, the relative error is 0.05 using eq. 2.15 and it is 0.08 using eq 2.16 for the numerical case when $\beta = 1$, and the errors are less than this for cases when $\beta > 1$ (Fig. 3.9).

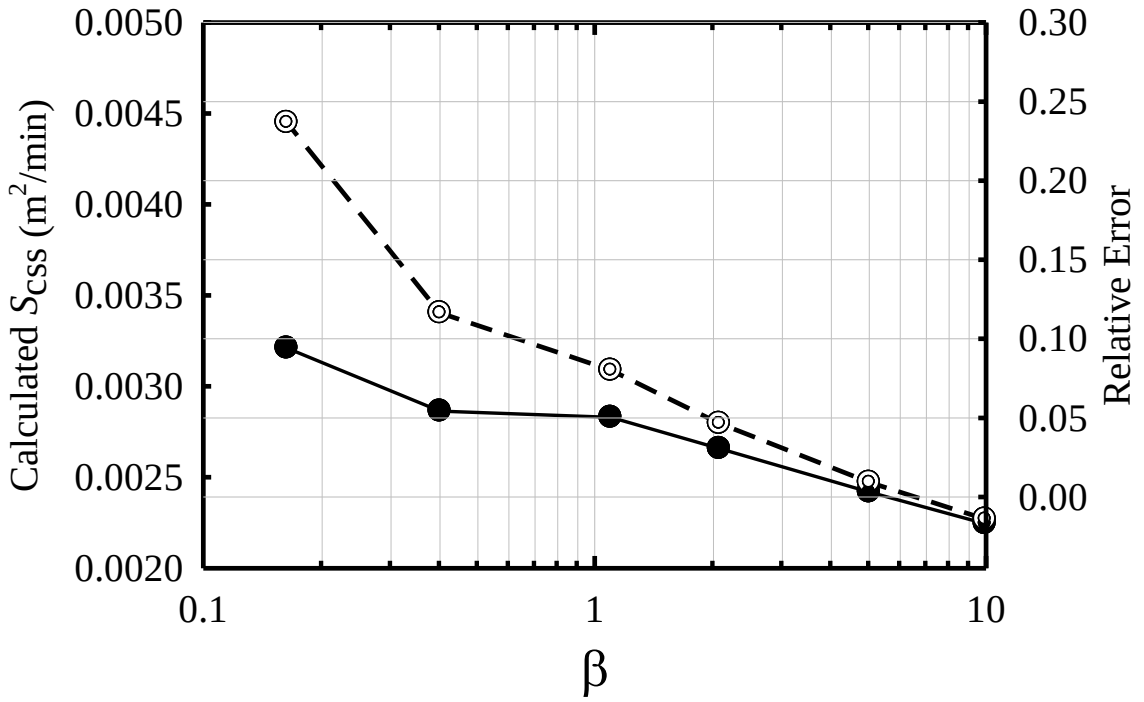

Figure 3.9. Calculated S_{css} and relative errors for full analysis (eq. 2.15) (black circle) and method 1 (eq. 2.16) (white circle) using data from numerical examples.

EFFECT OF SAPROLITE STORAGE

Water released from storage in the saprolite overlying the fractured rock aquifer in the Piedmont is not included in the analytical solution, but it will likely affect the type curve and well performance. Indeed, release of water from storage in the saprolite has been interpreted as a dominant factor affecting well performance in the Piedmont (LeGrand 1967). Storativity of the saprolite in the baseline model was varied from 10^{-4}

to 0.3 to evaluate this effect. This range spans the transition from compressibility to pore-drainage processes in the release of water from storage. Confined conditions were assumed to provide a simple transition from the baseline case.

Increasing the storativity of the saprolite has a major affect on the drawdown curve. The type of effect caused by storage in saprolite is illustrated by an example that includes the baseline case as outlined above, and the baseline case with S_{sap}=0.3. The two curves representing drawdown at the pumping well are nearly identical at early times, and both follow a semi-log straight line whose slope is inversely proportional to T of the rock aquifer. The curves diverge at roughly t = 100 min when the slope of the curve representing S_{sap}= 0.3 decreases, while the baseline curve maintains roughly constant slope on the semi-log plot (Fig. 3.10). The drawdown stabilizes with nearly a flat slope from approximately t = 800 to 8000 mins resulting in a quasi-steady state condition for S_{sap}= 0.3. The well could easily be interpreted as reaching steady state at this time, but the condition is only temporary. The drawdown slope steepens after t = 8000 and approaches a new semi-log straight line. Eventually, after approximately $2x10^6$ minutes (3.9 years) in Figure 3.9, the slope flattens and the two curves merge. Ultimately, both systems analyzed in Figure 3.9 go to steady state at the same drawdown, so their S_{css} values are identical and independent of the storage properties of the saprolite..

The analysis shown in Figure 3.9 was extended using additional values for of S_{sap}. The slope of the drawdown curve flattens at the same time in all three cases, but the length of time the slope remains stabilized decreases as S_{sap} decreases and approaches S_{sap} = S_{rx} (Figure 3.11).

Saprolite storage appears to temporarily flatten the drawdown curve in a style resembling a dual porosity response (Streltsova, 1988). The effect of saprolite has little influence on the ultimate S_{css}, but it could cause a significant temporary improvement in well performance, or it could be misinterpreted as a true steady state that causes the well performance to be over-estimated. This warrants a more detailed evaluation of the effect of saprolite on well performance.

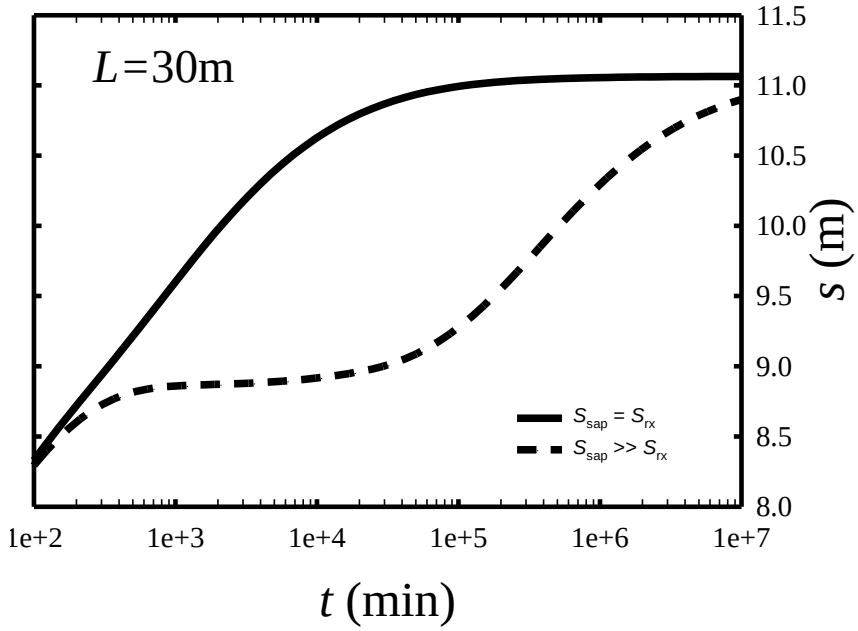

Figure 3.10. Drawdown as a function time for different saprolite storage values. Solid line S = 0.0001, Dash line *S*= 0.3

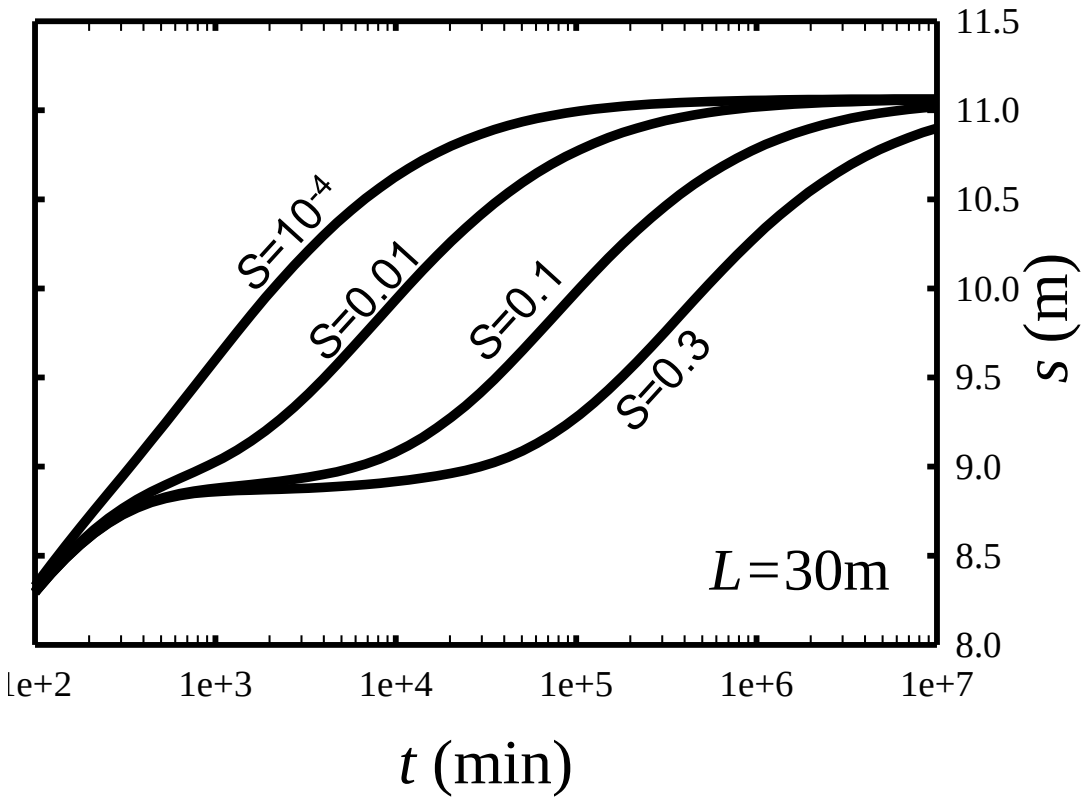

Figure 3.11. Drawdown with time in a partially penetrating well in an aquifer with overlying saprolite of varying specific yield. Model geometry from baseline case.

Effect of Distance to Stream

To evaluate the effect of L on the saprolite effect, the baseline configuration was run with S_{sap} ranging from 0.001 to 0.3 at different distances from the stream. The objective was to determine how changes in L affect the drawdown curve.

Drawdown in the fractured rock aquifer increases as L increases. For example, the steady-state drawdown, s_{ss}, increases from 10.36 m for L=10 m to s_{ss} = 13.5 m for L = 500. This seems to be a reasonable response because increasing L causes the extent of the cone of depression to increase prior to stream interaction (Figure 3.12).

Regardless of L, the time and duration of the perturbation caused by varying saprolite properties remained the same for each numerical configuration. It appears (Fig. 3.12) that the drawdown response caused by the saprolite is independent of L.

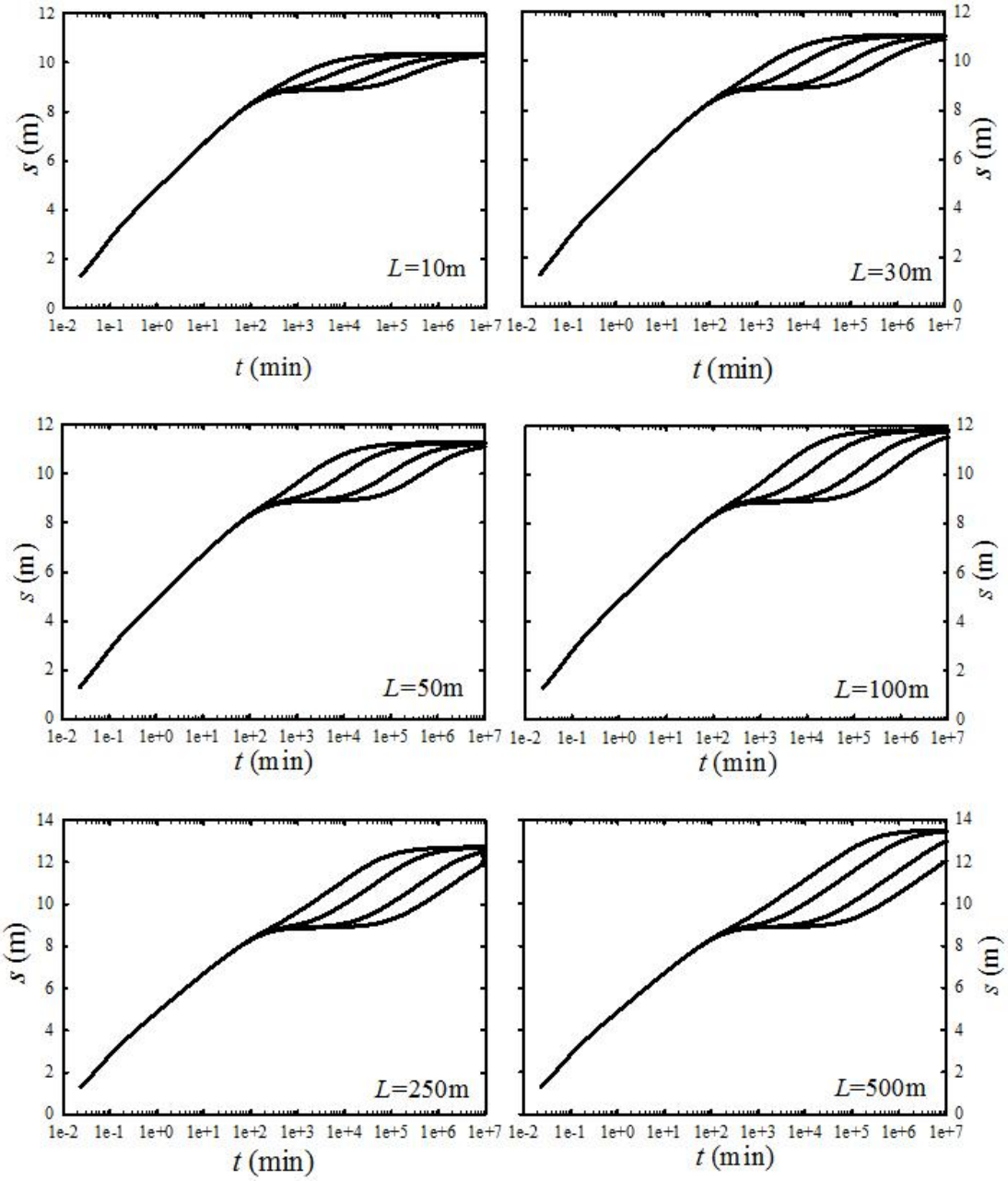

Figure 3.12. Drawdown as function of L and S_{sap} = 0.001 to 0.3 for the baseline case model at varying distances to stream.

Model	*K*sap	*K*rx	*T* rock	*Ssap*	*S*	*b'*	*b*	*L*	r_w
	(m/min)	*(m/min)*	*(m^2/min)*	*(1/m)*	*(1/m)*	*(m)*	*(m)*	*(m)*	*(m)*
10_500	5.90E-05	1.00E-04	3.00E-03	0.001	1.00E-03	10	30	500	0.25
10_500	5.90E-05	1.00E-04	3.00E-03	0.01	1.00E-03	10	30	500	0.25
10_500	5.90E-05	1.00E-04	3.00E-03	0.1	1.00E-03	10	30	500	0.25
10_500	5.90E-05	1.00E-04	3.00E-03	0.3	1.00E-03	10	30	500	0.25
10_250	5.90E-05	1.00E-04	3.00E-03	0.001	1.00E-03	10	30	500	0.25
10_250	5.90E-05	1.00E-04	3.00E-03	0.01	1.00E-03	10	30	500	0.25
10_250	5.90E-05	1.00E-04	3.00E-03	0.1	1.00E-03	10	30	500	0.25
10_250	5.90E-05	1.00E-04	3.00E-03	0.3	1.00E-03	10	30	500	0.25
10_100	5.90E-05	1.00E-04	3.00E-03	0.001	1.00E-03	10	30	500	0.25
10_100	5.90E-05	1.00E-04	3.00E-03	0.01	1.00E-03	10	30	500	0.25
10_100	5.90E-05	1.00E-04	3.00E-03	0.1	1.00E-03	10	30	500	0.25
10_100	5.90E-05	1.00E-04	3.00E-03	0.3	1.00E-03	10	30	500	0.25
10_50	5.90E-05	1.00E-04	3.00E-03	0.001	1.00E-03	10	30	500	0.25
10_50	5.90E-05	1.00E-04	3.00E-03	0.01	1.00E-03	10	30	500	0.25
10_50	5.90E-05	1.00E-04	3.00E-03	0.1	1.00E-03	10	30	500	0.25
10_50	5.90E-05	1.00E-04	3.00E-03	0.3	1.00E-03	10	30	500	0.25
10_30	5.90E-05	1.00E-04	3.00E-03	0.001	1.00E-03	10	30	500	0.25
10_30	5.90E-05	1.00E-04	3.00E-03	0.01	1.00E-03	10	30	500	0.25
10_30	5.90E-05	1.00E-04	3.00E-03	0.1	1.00E-03	10	30	500	0.25
10_30	5.90E-05	1.00E-04	3.00E-03	0.3	1.00E-03	10	30	500	0.25
10_10	5.90E-05	1.00E-04	3.00E-03	0.001	1.00E-03	10	30	500	0.25
10_10	5.90E-05	1.00E-04	3.00E-03	0.01	1.00E-03	10	30	500	0.25
10_10	5.90E-05	1.00E-04	3.00E-03	0.1	1.00E-03	10	30	500	0.25
10_10	5.90E-05	1.00E-04	3.00E-03	0.3	1.00E-03	10	30	500	0.25

Table 3.3. Baseline simulation parameters.

Model	L/r_w (unitless)	Lreal (m)	w (m)	L/r_w real (unitless)	b'/r_w (unitless)	b/r_w (unitless)	β (unitless)
10_500	2000	506	10	2024	40	120	9.95
10_500	2000	506	10	2024	40	120	9.95
10_500	2000	506	10	2024	40	120	9.95
10_500	2000	506	10	2024	40	120	9.95
10_250	2000	256	10	1024	40	120	5.03
10_250	2000	256	10	1024	40	120	5.03
10_250	2000	256	10	1024	40	120	5.03
10_250	2000	256	10	1024	40	120	5.03
10_100	2000	106	10	424	40	120	2.08
10_100	2000	106	10	424	40	120	2.08
10_100	2000	106	10	424	40	120	2.08
10_100	2000	106	10	424	40	120	2.08
10_50	2000	56	10	224	40	120	1.10
10_50	2000	56	10	224	40	120	1.10
10_50	2000	56	10	224	40	120	1.10
10_50	2000	56	10	224	40	120	1.10
10_30	2000	32	6.44	127	40	120	0.40
10_30	2000	32	6.44	127	40	120	0.40
10_30	2000	32	6.44	127	40	120	0.40
10_30	2000	32	6.44	127	40	120	0.40
10_10	2000	9	9.63	35	40	120	0.16
10_10	2000	9	9.63	35	40	120	0.16
10_10	2000	9	9.63	35	40	120	0.16
10_10	2000	9	9.63	35	40	120	0.16

Table 3.4. Baseline simulation parameters.

Duration of Saprolite Effect

The saprolite effect could be misinterpreted as steady-state conditions during all test, resulting in an over-estimation of specific capacity (Figure 3.11). The saprolite effect can be evaluated by making use of an analysis of a well producing from a two-layer system, where one layer is a productive aquifer containing the well and the other is a semi-permeable bed that releases water from storage. This analysis was described by Streltsova (1988), who assumes that drawdown in the aquifer is affected by release of water from storage in the semi-permeable bed, but the lateral flow in the semi-permeable bed is negligible. This allowed Streltsova (1988) to derive an analytical expression to the drawdown resulting from a well pumping in a system resembling Figure 3.12 where the stream has been omitted.

According to Streltsova (1988), drawdown in the aquifer at early time causes water to be released from storage in the saprolite, which remains at near ambient heads (the term "saprolite" is used to put the Steltsova's analysis in the context of this thesis because she used different terms to describe this layer). This is the beginning of the saprolite effect. However, the head in the saprolite drops as water is released from storage, and eventually the heads in the two layers equilibrate and they behave as one large layer with effective properties. The saprolite effect ends when the heads in the two layers equilibrate. This causes an increase in the rate of drawdown. According to Streltsova (1988), heads in the saprolite and aquifer equilibrate to within 1% of each other, and the saprolite effect ends at:

$$t_{sap} \approx 0.73 \frac{b' S_{sap}}{K_{sap}} \tag{3.2}$$

This time occurs in the transition period after the slope has decreased to its flattest point and before it steepens to the new semi-log slope (Fig. 3.14)

The time when the drawdown at the well is affected by an aquifer boundary begins to be affected by the stream for the system consisting of an aquifer overlain by saprolite can be determined from (2.22) as

$$t_{0.8} = 0.62 \frac{L^2 (S_s + S_{sap})}{(T_s + T_{sap})} \tag{3.3a}$$

where the T and S values are summed to create effective properties for the combination of rock and saprolite.

Streltsova (1988) presents a time when drawdown interacts with a boundary between aquifer materials of different K as

$$t_b = 1.78 \frac{L^2 (S_s + S_{sap})}{T} \tag{3.3b}$$

where the T is taken as an effective value. The two equations are identical except for their coefficient, which result from a difference in the method used to define $t_{0.8}$ and t_b. We define $t_{0.8}$ as the time when the semi-log slope decreases to 0.8 of the maximum value. Streltsova was interested in a problem involving a vertical boundary defining materials of two different aquifer properties, and in this case the drawdown curve forms a semi-log straight line at early times and after the drawdown interacts with the boundary

the curve changes and becomes log-linear with a different slope at later times. Straight lines fit through the two semi-log straight portions of the curve intersect at tb, according to Streltsova. This definition causes $t_b > t_{0.8}$, and explains the different between coefficients in 3.3a and 3.3b.

We will use eq. (3.3a) to estimate the time when effects of interaction between a well and a stream could first be detected (Fig. 3.18). It is noteworthy that eq. 3.3 is independent of the saprolite effect. In some cases these two effects may be superimposed, and comparing t_{sap} and t_b can provide a means for recognizing this combination.

It follows from eq. 3.2 and 3.3a that the t_{sap} and $t_{0.8}$ occur at the same time when

$$L_s \approx b' \sqrt{\frac{S_{sap}}{S_{sap}+S_{rx}} \frac{T_{sap}+T_{rx}}{T_{sap}}} \qquad (3.4)$$

which indicates that $t_{0.8}$ will occur before than t_{sap} when $L < L_s$, and $t_{0.8}$ will occur after than t_{sap} when $L > L_s$. In general the term under the square root sign in 3.4 will be greater than 1 and less than 10, so L_s is approximately equal to the thickness of the saprolite.

Typical t_{sap} values

The duration of the saprolite effect depends on the dimensions and properties of the saprolite and aquifer. Ranges of expected t_{sap} times were evaluated using values of b' = 1, 5, 10, 20, and 30 m, T'= 1, 5, 10, 20, and 30 m^2/d, and S_{sap} ranging from 10^{-4} to 0.3 (eq. 3.2). Values of t_{sap} were determined by randomly selecting a parameter value from each of the typical Piedmont parameter ranges to create a data set containing 1 million random samples. t_{sap} times were calculated from the random parameter data sets

The results show that t_{sap} is strongly influenced by S_{sap}. A probability of 83% for the random combinations of parameters indicate t_{sap} will occur in less than 1 week (Figure 3.15) and a probability of 70% for values of t_{sap} less than 3 days (Figure 3.16), even considering the largest value of S_{sap} (Figure 3.13). These findings suggest that many pumping tests of standard duration (24 to 72 hours) will be influenced by the saprolite effect and some of them may be long enough to see the end of the saprolite effect (Figure 3.16). The implication is that the appearance of an apparent steady state during many pumping tests is only a temporary effect resulting from the saprolite.

Typical t_b values

The time to stream interaction depends on the dimensions and properties of the saprolite and aquifer. Ranges of expected t_b times were evaluated using values of b' = 1, 5, 10, 20, and 30 m, T'= 1, 5, 10, 20, and 30 m^2/d, and S_{sap} ranging from 10^{-4} to 0.3 (eq. 3.3) Values of t_b were determined by randomly selecting a parameter value from each of the typical Piedmont parameter ranges to create a data set containing 1 million random samples. t_b times were calculated from the random parameter data sets

The results indicate that t_b has a probability of less than 10 for stream interaction to occur within a week of pumping (Figure 3.17). These results indicate S_{sap} and T are the controlling factors for a well to interact with a stream boundary. For t_b > several months, a large distance to the steam, S_{sap} > 0.1, and a T < 20 m^2/day are the ranges required for a large t_b. Another combination of parameters that gives large values of t_b is L and S. For example, a large distance to the stream, L > 200 m and a large storativity S_{sap} > 0.01, results in t_b > 100 days (Figure 3.14). The probability that stream interaction

will occur during a typical pumping tests is less than 5%, this further suggests that the appearent steady-state conditions observed during pumping may be caused by saprolite. To improve the identification of stream interaction during a pumping test, $t_{0.8}$ can be determined using eq. 3.3b

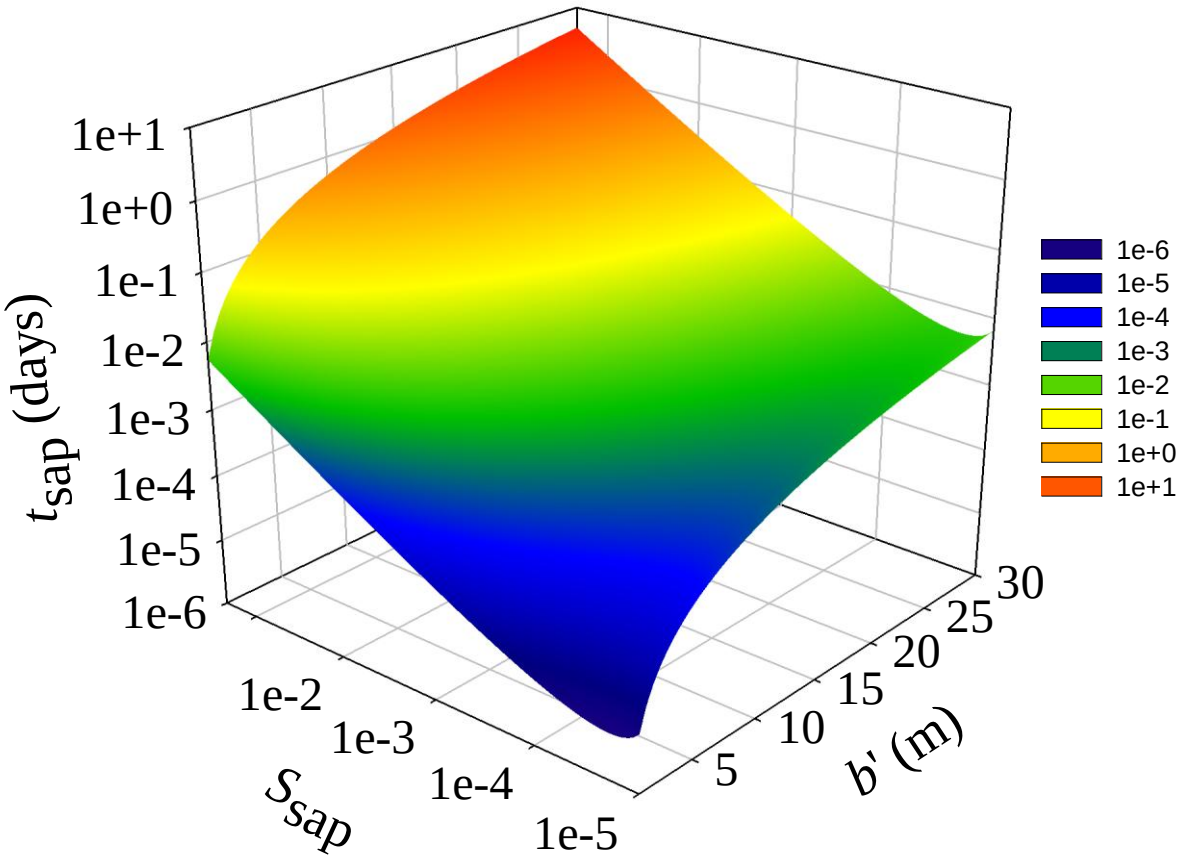

Figure 3.13. Surface plot of expected t_{sap} times using typical Piedmont saprolite and aquifer values as a function of saprolite storativity, S_{sap}, and saprolite thickness, b'.

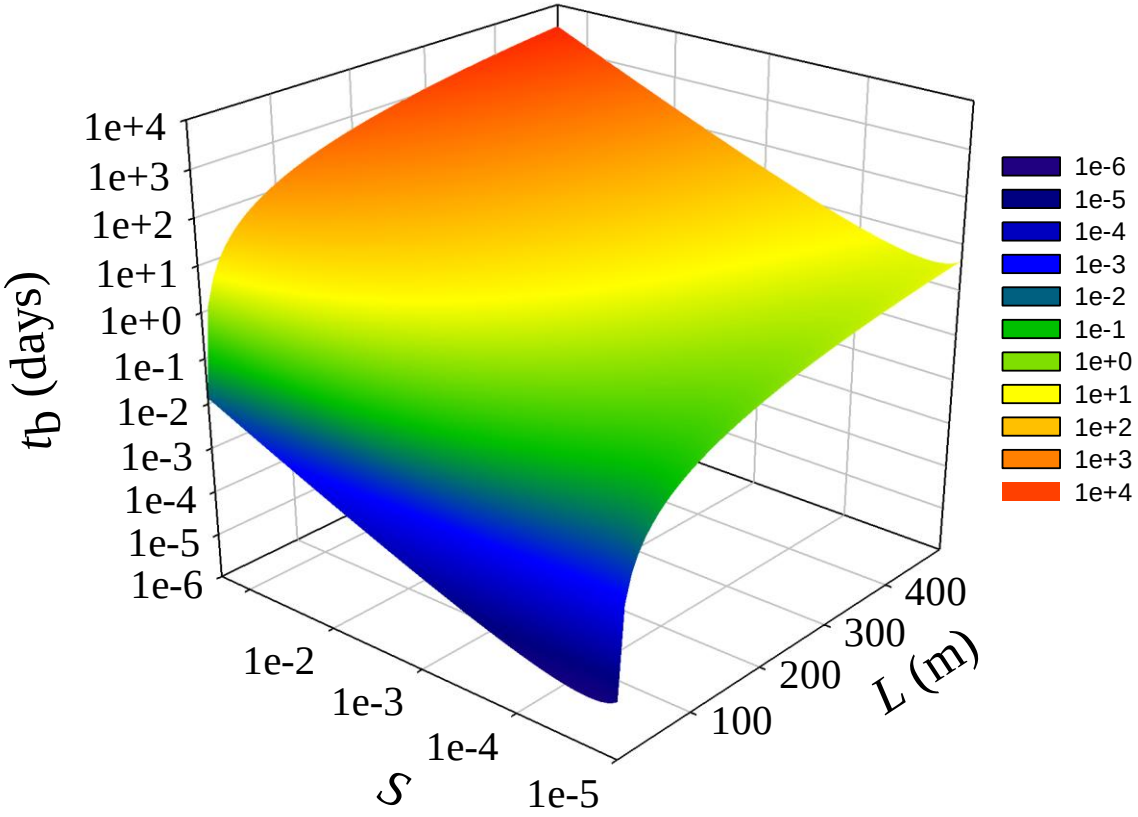

Figure 3.14 Surface plot of expected t_b times occuring as a function of S and L based on S_{sap} values.

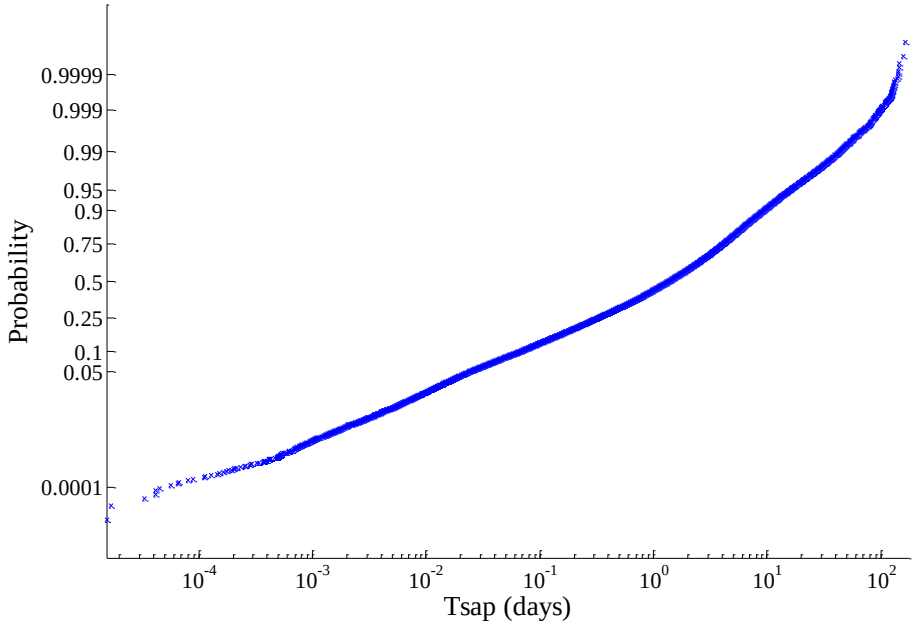

Figure 3.15. Probability of t_{sap} times based on random distribution of typical Piedmont values

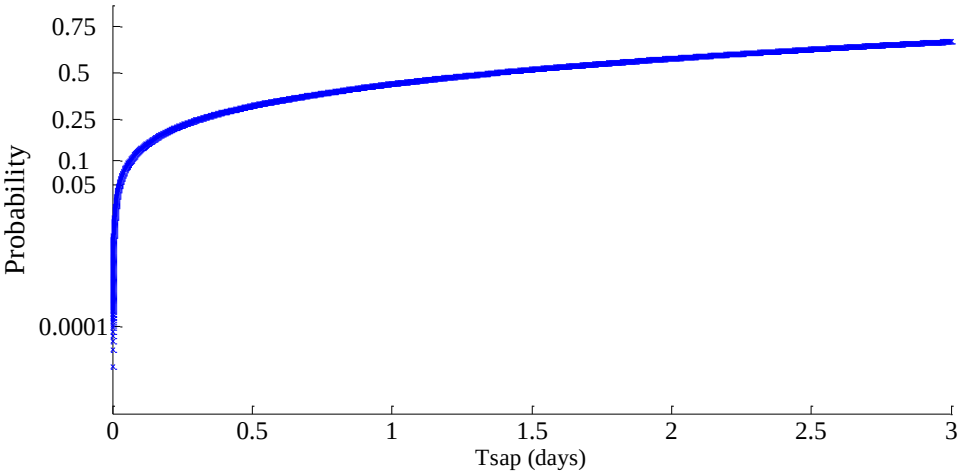

Figure 3.16. Probability of t_{sap} occurring within a typical 72 hour pumping test based on random distribution of typical Piedmont values.

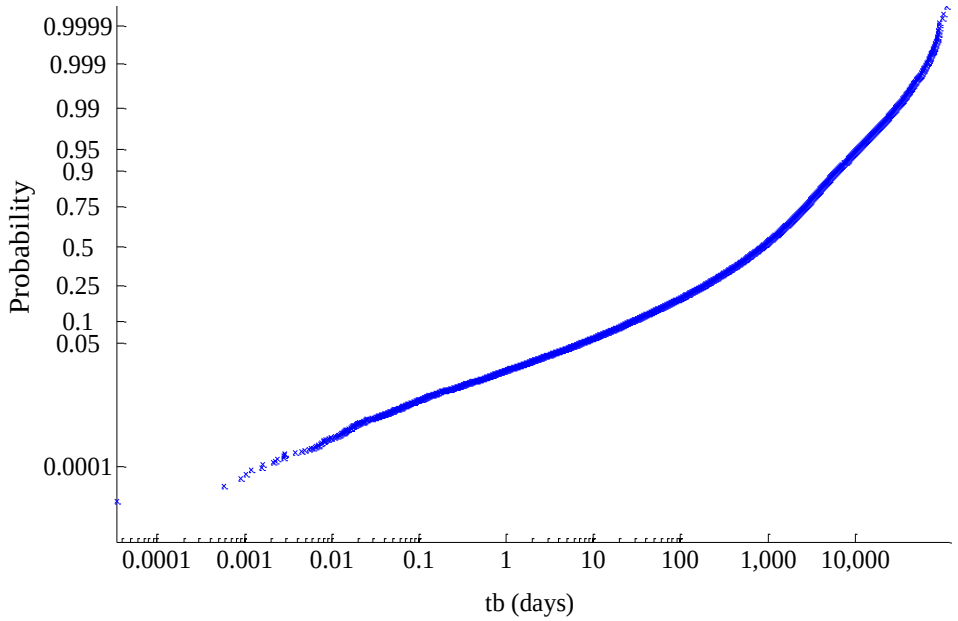

Figure 3.17. Probability of t_b times based on random distribution of typical Piedmont values.

GRAPHICAL ANAYLSIS

Times for t_{sap} and $t_{0.8}$ can be determined using eqs (3.2 and 3.3b) with known or estimated aquifer properties; although there may be instances during a pumping test when calculation of boundary times is not possible due to a lack of site information.

t_{sap} and $t_{0.8}$ appear to identify distinctive portions of drawdown curves from the numerical experiments (Figure 3.18), suggesting times for t_{sap} and $t_{0.8}$ may also be evaluated graphically in the field.

A graphical approach can be used to evaluate both the saprolite effect and stream interaction times using the derivative of drawdown with respect to the natural log of time. The semi-log slope of drawdown is commonly a semi-log straight line, so the derivative of drawdown will decrease when interaction with the saprolite occurs. (Figure 3.19)The longer early-time drawdown stabilizes as a result of the saprolite effect, over-estimation of S_{ssc} can occur. However, plotting the derivative of drawdown shows the slope approaching zero followed by an increase in slope as the saprolite effect ends (Figure 3.19)

Similarly, as the drawdown increases after the saprolite period ends, the interaction with a stream can be picked from this new semi-log slope (Figure 3.18). The new slope will begin to flatten prior to interaction with a stream boundary. When interaction with a stream begins, the slope will begin to decrease for a second time (Figure 3.18) and approach a slope of zero at steady state conditions

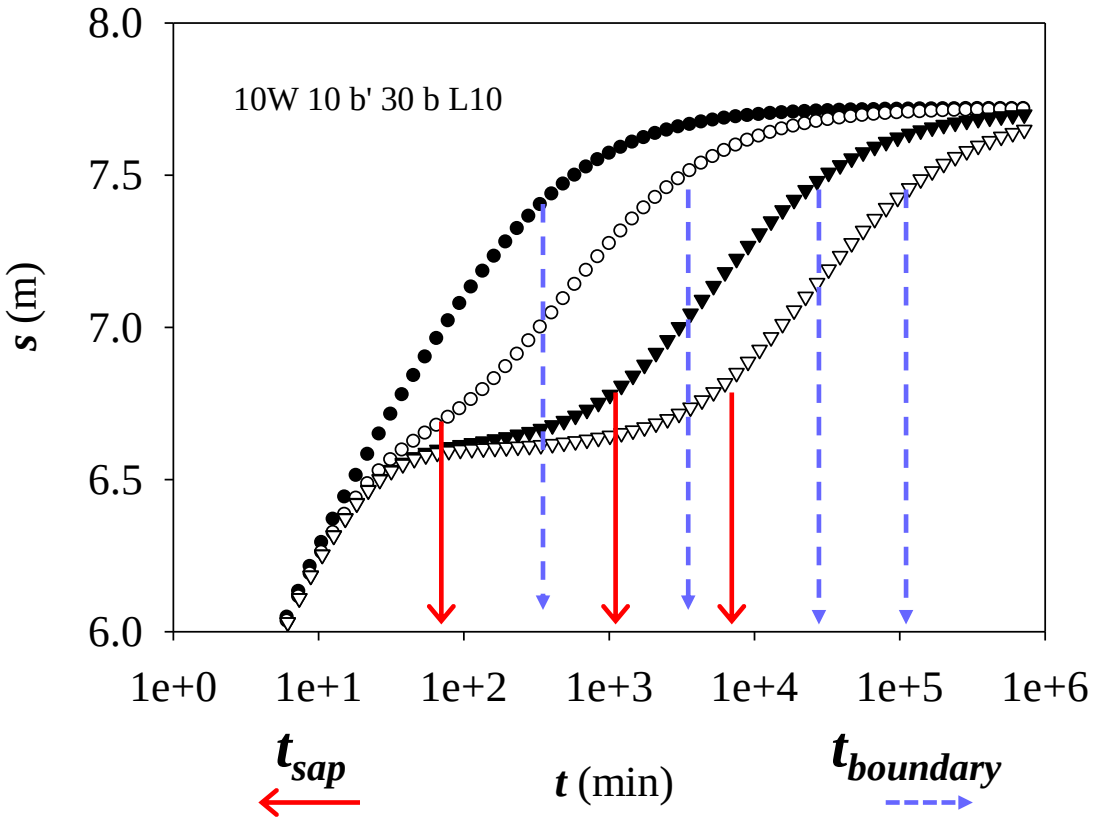

Figure 3.18. *s as a function of* t_d for t_{sap} (solid arrow) and t_b (dash arrow) using dual porosity approach.

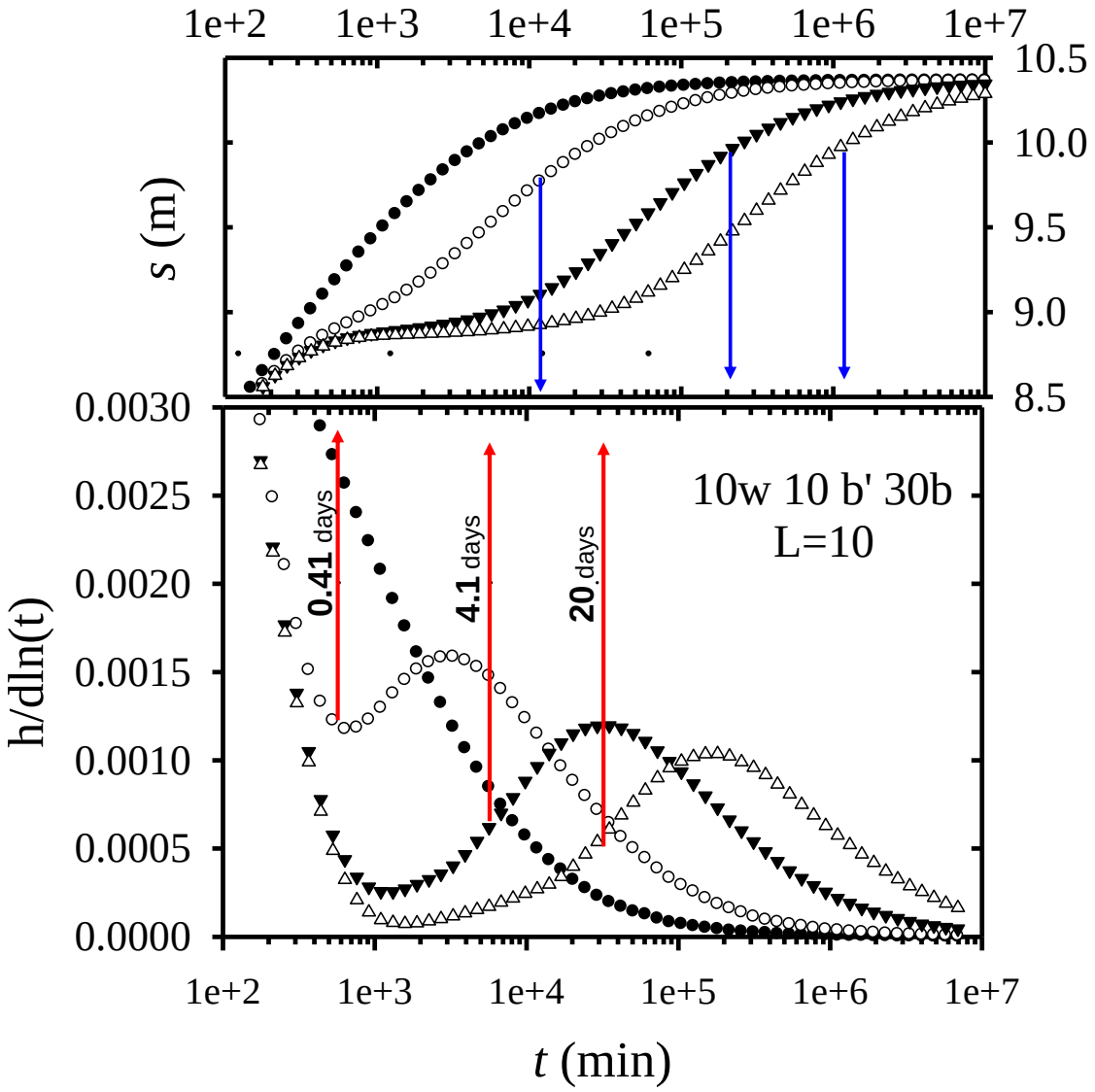

Figure 3.19. Top graph: drawdown showing calculated t_b times. Bottom graph: Derivative of drawdown with respect to the natural log of time showing calculated t_{sap} times.

DISCUSSION

The numerical evaluation is able to predict the analytical solution reasonable well for most cases.. The error from the analytical solution depends on the distance between the well and the stream (L/r_w) and the ratio of hydraulic conductivities between the aquifer and the saprolite (K_{sap} / K_{rx}). Generally the error is less then +/- 5%. The error increases to as much as 15% as the well approaches the stream due to a geometry effect.

Water released from storage in saprolite overlying the fracture rock aquifer is not included in the analytical solution. The saprolite and fractured rock behave similar to a dual porosity system. Saprolite storage effects can delay the time to stream interaction; however saprolite does not affect the long-term steady-state specific capacity. Water released from storage in saprolite only occurs temporarily, however this process may last many months or longer. This causes two important considerations. In one case, the saprolite effect can increase the well performance compared to an assessment that considers only the fractured rock aquifer. In this sense, the traditional conceptual model (LeGrand, 1988 and 2004; Heath, 1989; Daniel, 1992 and 2002; Rutledge, 1996; Swain et al 2004) indicating that saprolite releases water from storage during pumping is correct. However, the saprolite effect is only temporarily and in most cases it will end on time scales that are short compared to the life of a water supply well. This means that the performance of the well will diminish when $t > t_{sap}$, and an assessment of the well based on empirical short-term observations will certainly be overly optimistic.

CHAPTER 4

EXAMPLE APPLICATIONS

The chapter outlines several examples of the method to predict long-term well performance. The first examples use data from synthetic pumping tests simulated in Chapter Three, and they are followed by two examples from field tests conducted in the Piedmont Province.

SUGGESTED APPROACH FOR ESTIMATING WELL PERFORMANCE

The analysis outlined in Chapter Two and evaluated in Chapter Three is intended to be applied to the evaluation of drawdown data during pumping tests. The general approach is to determine S_{css} and then use the allowable drawdown to estimate a physically sustainable volumetric discharge. The procedure for applying the analysis is to try to use the full analysis first, and then apply one of the simplified methods as required based on available data (Figure 4.1).

A 5-step approach is outlined below to facilitate the application of the analyses described in Chapter Two:

Step 1. Determine basic properties of the aquifer and well

a.) Analyze drawdown data using conventional methods to determine T.

b.) Estimate S and s_k using data from a monitoring well.

c.) Determine r_w from drilling records or field measurements

Step 2. Determine dimensions and other properties.

a.) L, and w from surveying.

b.) b and b' from borings

c.) K_{sap}, S_{sap} by testing wells completed in saprolite

Step 3. Try full analysis Calculate β and S_{css} using the full analysis (eq. 2.15) and field data obtained from 1 and 2.

Step 4. If β cannot be determined from field data, use simplification. Is the semi-log slope constant? If Step 3 is infeasible because β cannot be determined then use one of the simplified methods. If the drawdown data follows a semi-log straight line with minimal slope change (change is less than 20%), then use Simplification Method 1: Measure L by surveying and apply eq. 2.16.

a.) It may be possible to refine the estimate from eq. 2.16 by either estimating missing data needed to calculate β, or using a typical value for β (Figure A-2), and then using eq. 2.15. Typical values for β in the Piedmont are $0.1 < \beta < 50$ (Figure A-1).

Step 5. Semi-log slope decreases If the semi-log slope is constant and then decreases, then you may be able to use this change to estimate performance. First decide whether the slope change is in response to interaction with a stream, with saprolite, or some other effect.

a.) calculate $t_{0.8}$ using eq. 2.22 to determine the expected time to interact with the stream (call this $t_{0.8calc}$), and t_{sap} using eq. 3.2 to determine the expected time for saprolite interaction to end. Determine $t_{0.8}$ from plot of data observed in the field (or from plot of semi-log derivative), call this observed value $t_{0.8obs}$.

b.) If $t_{0.8obs} \approx t_{0.8calc,}$ and $t_{0.8obs} > t_{sap}$, then the change in slope could be due to interaction with the boundary.

- If S is known then use Simplification Method 2: Substitute $t_{0.8obs}$ in eq. 2.24 to calculate S_{css}.
- If S is unknown then use Simplification Method 3: Determine the $S_{c0.8}$, the specific capacity at $t_{0.8}$, from the field data, and substitute into eq. 2.29

c.) If $t_{0.8obs} << t_{0.8calc}$ then the break in slope may be due to an effect other than interaction with a boundary. If $t_{0.8obs} < t_{sap}$ then the change in slope could be due to interaction with saprolite. Use Simplification Method 1: Measure L by surveying and apply eq. 2.16.

Well performance could be greater than expected from eq. 2.16 while $t < t_{sap}$. This occurs because the release of water from storage in the saprolite could significantly reduce drawdown while $t < t_{sap}$. It is possible that the duration of this period could be long enough to provide a meaningful increase in the overall productivity of the well. It is important to keep in mind, however, that S_c will decrease and approach S_{css} when $t > t_{sap}$.

d.) If $t_{0.8obs} >> t_{0.8calc}$, then the change in slope may be due to boundary interaction, but there is significant resistance to flow between the stream and the aquifer. Estimate values for β in eq. 2.9f and use the full method (eq. 2.15) to calculate S_{css}.

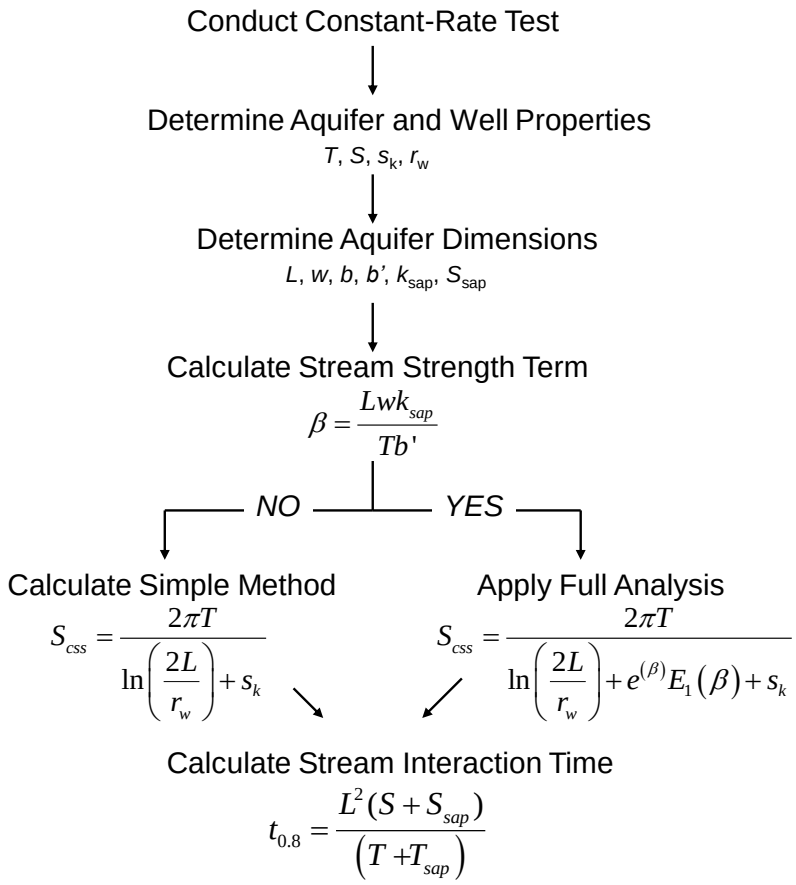

Figure 4.1. Flow chart of the Approach for Estimating Well Performance

APPLICATION TO AVERAGE WELL PERFORMANCE DATA

An initial evaluation of the proposed method can be derived from the range of discharge values and transmissivities summarized by Swain et al. 2004 for major rock types in the Piedmont (Table 4.1). Eqs 2.14 and 2.16 were rearranged to give $s = C_1Q/T$, where C_1 depends on r_w and L. Assuming r_w = 0.076m (6-inch diameter) and 50m < L < 500m gives 1.15 < C_1 < 1.52. The full range of C_1 and Q and the average T was used to estimate the range of drawdown for each rock type.

The analysis indicates that the minimum average drawdown spans a narrow range from 6m to 8m for the three rock types, whereas the maximum drawdown ranges from 22m to 55m.

Drawdown data are not given by Swain et al. 2004, and average drawdown is difficult to determine from operating wells. However, ambient water levels are 10 m to 15 m above the top of rock in many wells in the Piedmont, so the minimum drawdown in Table 4.1 is expected to be within the casing of most wells. This conforms to guidelines for well operation (Rosco Moss, 1990). Many wells in the Piedmont are 100m to 200m deep, so it seems reasonable that the high end of drawdown would be in the range of 50m. These wells would probably be completed in formations where one or two fractures occurred at significant depth. Daniels (1967) points out that wells with the greatest flow rates are 130m to 160m deep and are operated with significant drawdown. As a result, we conclude that the range of drawdown predicted by eq. 2.16 is consistent with available data on aquifer properties and well operation.

Table 4.1. Aquifer properties and well discharge from Swain et al 2004 and expect drawdown, *s*, determined using eqs. 2.14 and 2.16.

	T m^2/d	*Q* m^3/d	*s* m
Phyllite-Gabbro	3.7	27-55	8-22
Gneiss-Schist	10.2	55-327	6-48
Shale-Sandstone	32.5	190-1200	7-55

APPLICATION TO SYNTHETIC PUMPING TEST DATA

A drawdown curve from the numerical baseline evaluation will be used to illustrate the approach for predicting well performance from a short-term pumping test. The conditions of this problem are described in Table 3.2, and results shown in Figure 3.11. Each simulation was run long enough so the heads reached steady state. I will use data from the first 48 hours to represent a typical constant-rate test and apply the steps described above to calculate S_{css} (Figure 4.2). Drawdown curves from pumping wells were simulated for two data sets, A and B (Table 4.2), which are identical except for the saprolite storage values.

The actual steady state specific capacity from the simulations is $S_{css} = 2.69 \times 10^{-3}$ m^2/min. This value will be used to evaluate the effectiveness of the proposed method.

Analysis

1. Determine basic properties of the aquifer and well.

The semi-log straight portion of the curve was analyzed to determine the effective values of *T* using the Cooper-Jacob method (Cooper and Jacob, 1946). The semi-log straight line portion of the results for Datasets A and B were identical, giving $T = 2.92 \times 10^{-3}$

m^2/min (Figure 4.3). A monitoring well is unavailable for this case, so *S* cannot be determined from the simulated drawdown data. I will assume $10^{-4} < S < 10^{-3}$ based on typical properties of fractured rock in the Piedmont. . A well radius of 0.25m was assumed because the grid block containing the well was 0.5m (Table 4.2).

	L (m)	*w* (m)	*b* (m)	*b'* (m)	K_{sap} (m/min)	K_{rx} (m/min)	*T* (m^2/min)	S_{sap}	S_{rx}	β
Data A	50	10	30	10	5.9×10^{-5}	1.0×10^{-4}	2.9×10^{-3}	1.0×10^{-4}	1.0×10^{-4}	0.98
Date B	50	10	30	10	5.9×10^{-5}	1.0×10^{-4}	2.9×10^{-3}	0.3	1.0×10^{-4}	0.98

Table 4.2. Properties for numerical baseline evaluation for the well and the aquifer

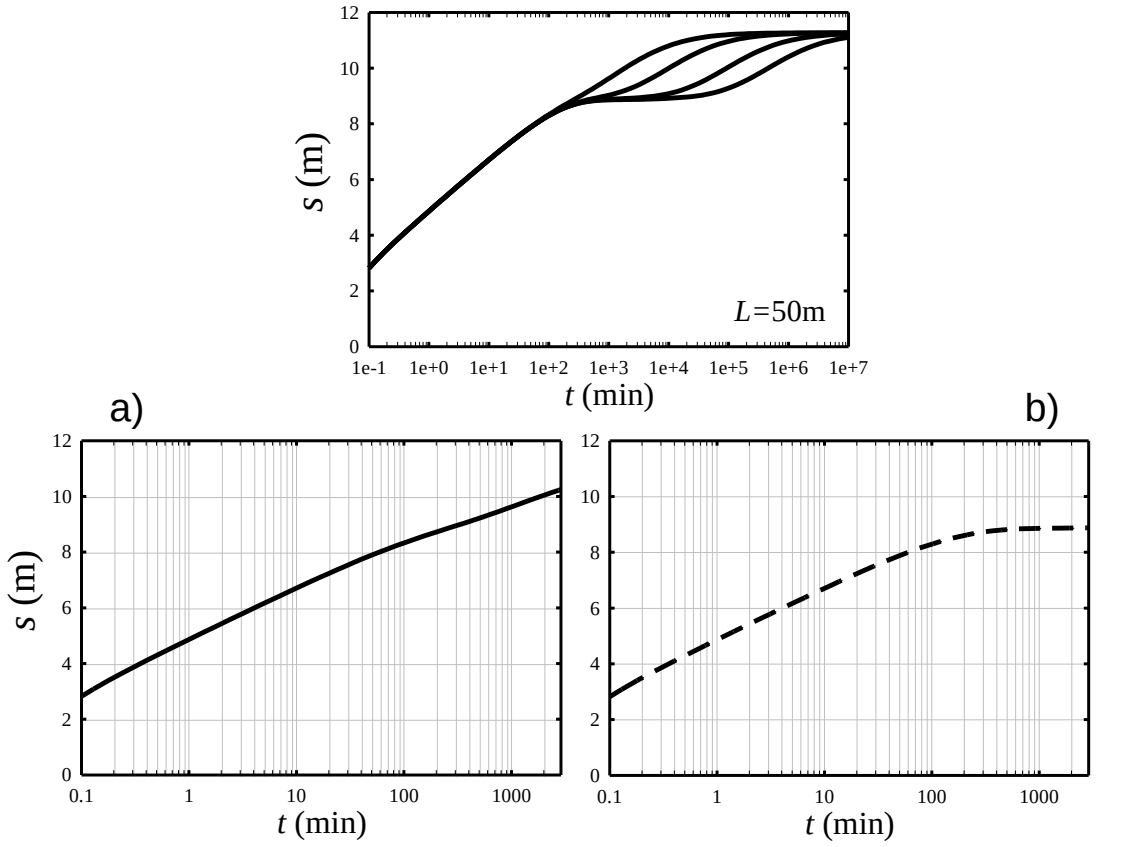

Figure 4.2. Drawdown in a well as functions of time from numerical baseline analysis, L =50 m. a) S_{sap} = 0.0001. b) S_{sap} = 0.3.

Step 2. Determine dimensions and other properties

The distance to the steam is L = 50 m and the stream w = 10m. These data are easily measured in the field, so it will be assumed that they are known. There is no well skin in either case, so $s_k = 0$.

Step 3. Full Analysis

The properties of the saprolite are unknown, preventing a definitive calculation of the stream strength term, β. In this case we will assume the full analysis (eq. 2.15) cannot be used.

Step 4. If β cannot be determined, use simplification. Semi-log slope constant

Both Datasets follow a semi-log straight line with a minimal slope change, so Simplification Method 1 (eq. 2.16) can be used for both of them

The parameters used for Simplification Method 1 are T, L, and r_w. Substituting into eq. 2.16 results in $S_{css} = 2.63 \times 10^{-3}$ m^2/ min. The actual S_{css} from simulations is $S_{css} = 2.69 \times 10^{-3}$ m^2/ min, which gives a relative error of less than one percent. This method seems to work well for both examples.

Step 5. Semi-log slope decreases

Both Datasets can be analyzed using Simplification Method 1 because L is assumed to be known. However, if we now assume that L is unknown, then Dataset A cannot be analyzed at all using the proposed method. The semi-log slope from Dataset B begins to flatten around t = 200 minutes, so we can used Step 5 to evaluate the S_{css}.

5a. Calculate $t_{0.8}$ and t_{sap}

Values needed are S, T. We know T and L. Calculating S from the pumping well may result in overestimating the S of the formation. .

We get the range 5 min < $t_{0.8}$ < 53 min using the assumed range for S_{sap} given above. The break in slope in Dataset B could occur at within the range of times,

according to a plot of the data (Fig. 4.3). Plotting the semi-log slope using eq. 2.18. allows $t_{0.8}$ to be identified more precisely as 42 min (Fig. 4.4). The result shows that the observed $t_{0.8}$ is within the range of expected values for $t_{0.8}$ based on an assumed range of S_{sap}.

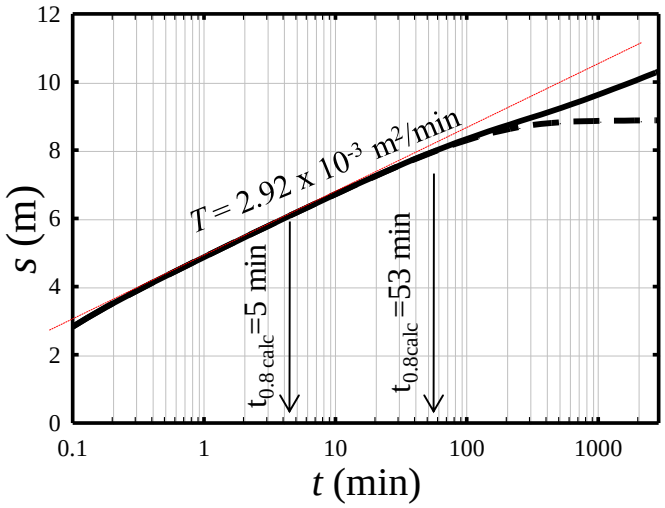

Figure 4.3. T and $t_{0.8}$calc times for data sets A (solid line) and B (dash line). $t_{0.8}$ calc = 5 mins uses S=0.001, $t_{0.8}$ calc = 53 mins uses S=0.0001.

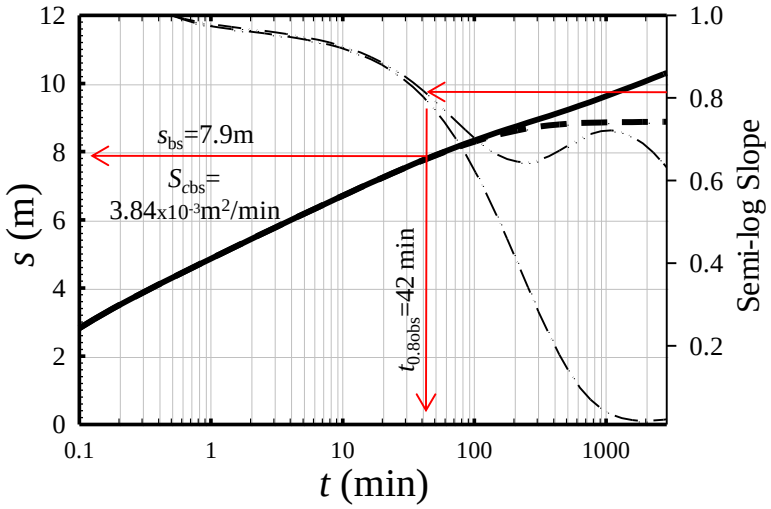

Figure 4.4. Drawdown and semi-log slope as function of time for both data sets. Break in slope $t_{0.8obs}$ = 42 min, the s_{bs}= 7.9 m, S_{cbs} = 3.84x10^{-3} m^2/min.

The saprolite time, $t_{sap,}$ depends on b',T', and S_{sap}. These values are unknown in this example, so the only course is to use typical values. I will assume 10m < b' < 20 m, $T' = T$, and S_{sap} =0.2. This gives a range of 3.5 days< S_{sap} 13.5 days.

The results indicate that $t_{0.8obs} \approx t_{0.8calc,}$ and $t_{0.8obs} < t_{sap}$. In this case, $t_{0.8obs}$ appears to be a result of release of water from storage in saprolite rather than interaction with a stream (because $t_{0.8obs} < t_{sap}$) (Fig. 4.5). This means that the break in slope is the temporary effect of saprolite and it cannot be used to estimate the long term performance using, for example, eq. 2.24 or 2.29. This means that only Simplification Method 1, eq. 2.16, can be used for this example. The results of this calculation are given above. .

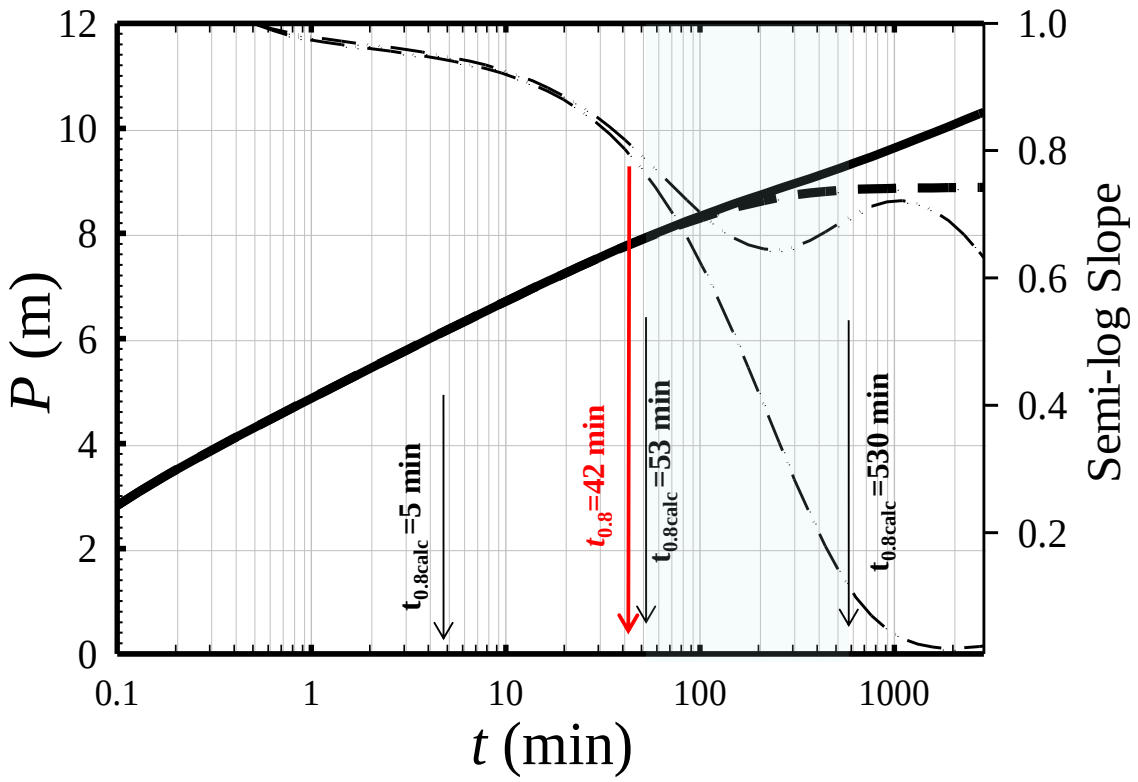

Figure 4.5. Drawdown and semi-log slope as function of time for both data sets. $t_{0.8calc}$ for S = 10 x 10^{-5}, 10 x 10^{-4}, and 10 x 10^{-3}.

Comparision to empirical estimate

Most state regulations involving well testing mandate that well performance be determined empirically as the discharge rate maintained after one to several days of pumping. The observed S_c at the end of pumping would have been 4.3 to 4.9 m2/d. The actual value of S_{css} in the simulations is 2.7 x 10^{-3}m^2/ min. This indicates that the empirical assessment would have over-estimated the actual value of S_{css} by 60 to 80 percent. The method proposed here predicted the actual value of S_{css} within 1 percent.

CLEMSON WELL FIELD EVALUATION

This evaluation was conducted by pumping a well for 5-days and using the results to calibrate a numerical model, which was used predict the drawdown at steady state. This drawdown was used to calculate the S_{css}, which was assumed to describe the true well performance. The field data were then truncated to 1 day of pumping, and these data were analyzed to determine aquifer parameters that were then used in the proposed method to estimate S_{css}. The results were compared to the value that was assumed to represent the true performance.

Setting of the Clemson Well Field

The test was conducted at the Clemson Well Field, which is located next to the Bob Campbell Geology Museum on the campus of Clemson University. The well field is within the Six-Mile thrust sheet (Nelson et al., 1990 and Horton and McCornnell, 1991), which consists of high-grade metamorphic rocks (Miller 1990).

The dominant rock type at the well field site is medium-grained biotite gneiss with moderate to well-developed foliation that strikes northeast and dips to the southeast (Svenson 2007; Nelson et al., 1990). The bedrock is overlain by approximately 20 m of saprolite.

The well field consists of four wells (designated LAR-1 through LAR-4) drilled to total depths of 60 to 120 m, and one well (LAS-1) drilled to 17 m and completed with a screen and gravel pack in saprolite (Figure 4.6). The rock wells are cased through saprolite to depths of approximately 20m, and continue as open holes, 15 cm in diameter,

in the rock. The screen on the well in the saprolite is 5 cm in diameter and between 6 and 7.6m depth. The water table at the site is at approximately 7.5 m depth.

The wells are spaced within a region approximately 10 m by 5 m on the edge of a paved parking lot. A first-order stream is located roughly 50 m to the south, so L = 50m.

The wells in rock were surveyed with a video camera, borehole flow meter, and characterized with pumping and slug tests between packers (Svenson 2007). This work identified fractures with significant transmissivity that connected the wells between depths of 25 m and 50 m.

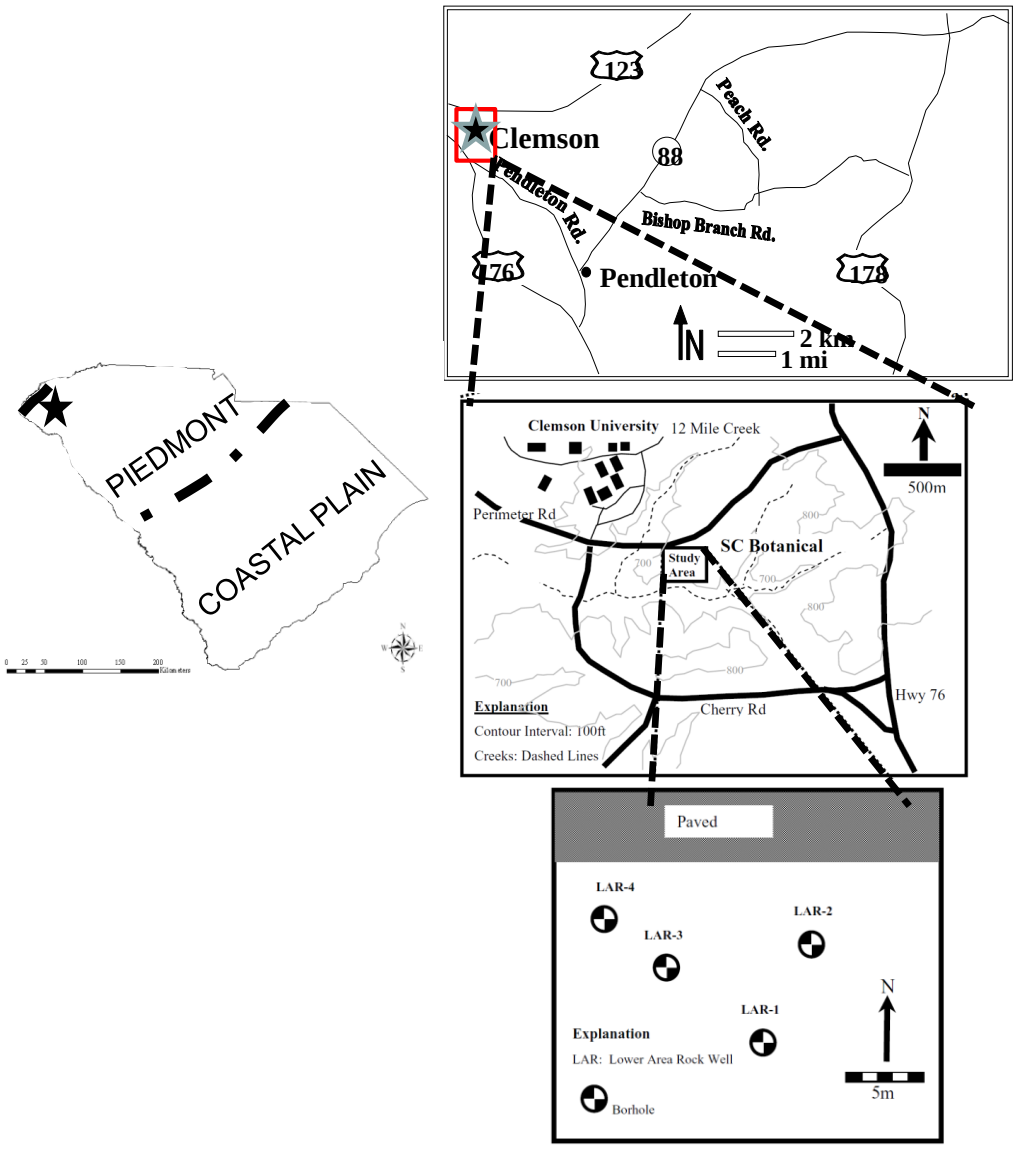

Figure 4.6. Schematic of Clemson well field site

Clemson Wellfield Constant-Rate Test

A 5-day-long well test was performed at the site using well LAR-1 as the pumping well and the other wells were used to monitor drawdown.

Flow Control System

The test was conducted using a submersible centrifugal pump attached to a device that controlled the flow rate. The submersible pump is a 4-inch diameter, ½ HP Sandhandler made by Franklin Pumps. The flow controlling device is a valve made by Plastomatic Valves, Inc., and designed to allow flow at 0.03 m^3/min when a minimum of 103 kPa inlet pressure is maintained. Installing the flow control valve allowed the pump to produce at a constant rate as long as the pressure produced by the pump exceeded 103 kPa.

Aquifer Test Data

LAR-1 was pumped for 124.1 hours at 0.03 m^3/min with a final drawdown of 9.4m. The specific capacity, S_c, decreased throughout the test. S_{cobs} = 2.7 m^2/day at the end of pumping, however, drawdown was increasing at the end of the tests so the system had not reached steady state. The largest drawdown in a monitoring well was 0.96 m observed in LAR-2, and the smallest response was 0.31 m in LAR-4 (Figure 4.7and Table 4.4).

During the test, the generator used to power the pump shut down unexpectedly a few times. The first time this happened was 2134 minutes into pumping and the pump stopped for 22 minutes before the generator was restarted. The pump stopped 2 other

times during pumping, but in those cases it was restarted within a few minutes. The effects temporary interruptions in pumping can be seen in the late time data as small intervals of rising and falling heads (Fig. 4.7).

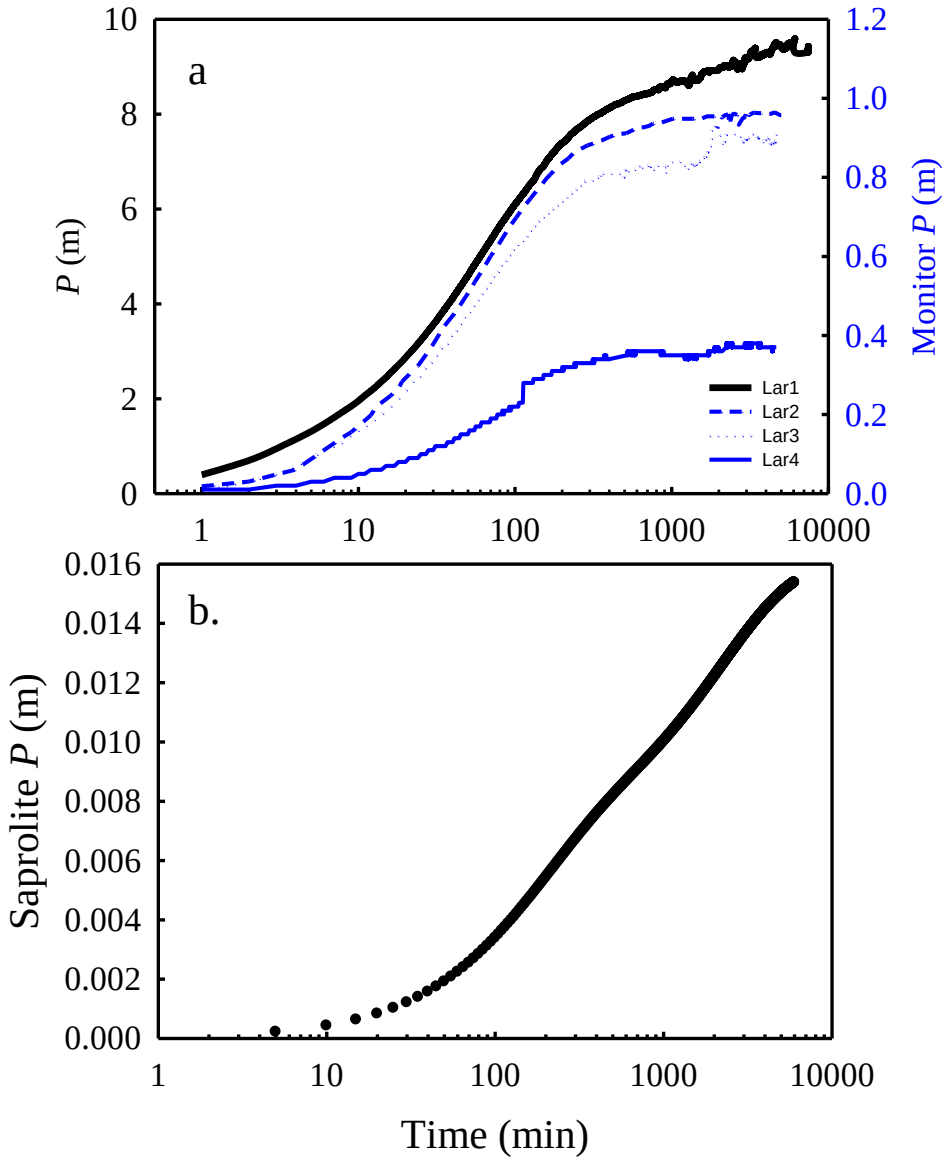

Figure 4.7. Drawdown response at the Clemson Well Field from constant-rate test. a.) data from wells completed in rock; b.) data from saprolite well

Estimating Steady State conditions

The well test was terminated before steady state conditions were reached, so the actual S_c is unknown. I set up a 3-D numerical model to the geometry of the site and calibrated it using the available pumping test data. This was done using MODFLOW by adjusting the baseline 10_50 model from Chapter 3 (Table 3.2) to fit the site conceptual model and aquifer dimensions (Figure 4.10). The initial model objective was to fit the response of LAR-1 during the early time drawdown to characterize the transmissivity of the aquifer from the pumping well response. The calibrated model was run forward in time until steady state conditions were reached. Steady state conditions, as defined by a criteria of 0.01 m of head change per 3 months, were reached after approximately 10.4 days of pumping in the simulation (Figure 4.11). The final drawdown is 9.83 m, which gives a final S_{css} of 0.0033 m^2/min. I will assume that this is the correct value for S_{css}.

Analysis of Well Performance

The full analysis (eq. 2.15) will be applied to the LAR-1 pumping test to estimate well performance. Site information is available to calculate a stream strength term, β. Aquifer properties and dimensions will first be determined and applied to eq. 2.15

1. Determine basic properties of the aquifer and the well

The drawdown at LAR-1fits a semi-log straight line from 20 to 120 minutes (Figure 4.9) and $T = 6.9 \times 10^{-4}$ m^2/min was calculated from this curve (Cooper and Jacob, 1946). Drawdown from the monitoring wells also formed a semi-log straight line and

using the same analysis as the pumping well gives a significantly larger value of T = 9.0 x10^{-3} m^2/min using data from LAR-2 and LAR-3, which are 5.8 m from the pumping well. Storativity calculated from the monitoring wells using the Cooper-Jacob method is S = 0.005.

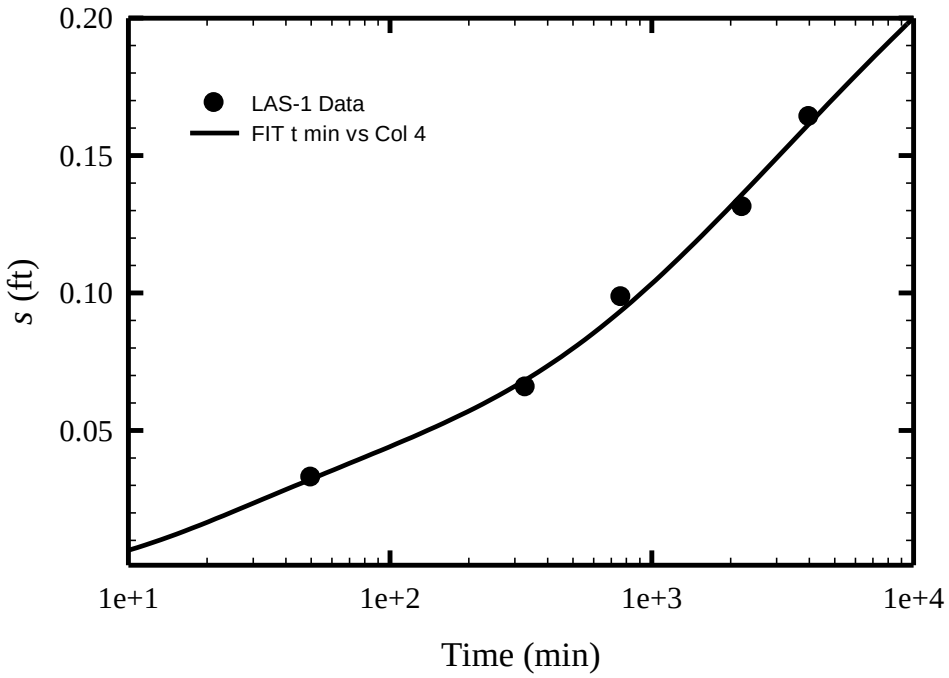

Figure 4.8. Drawdown at LAS-1during constant rate pumping test (points), and results from Neuman (1974) solution using S_y=0.28 (black line).

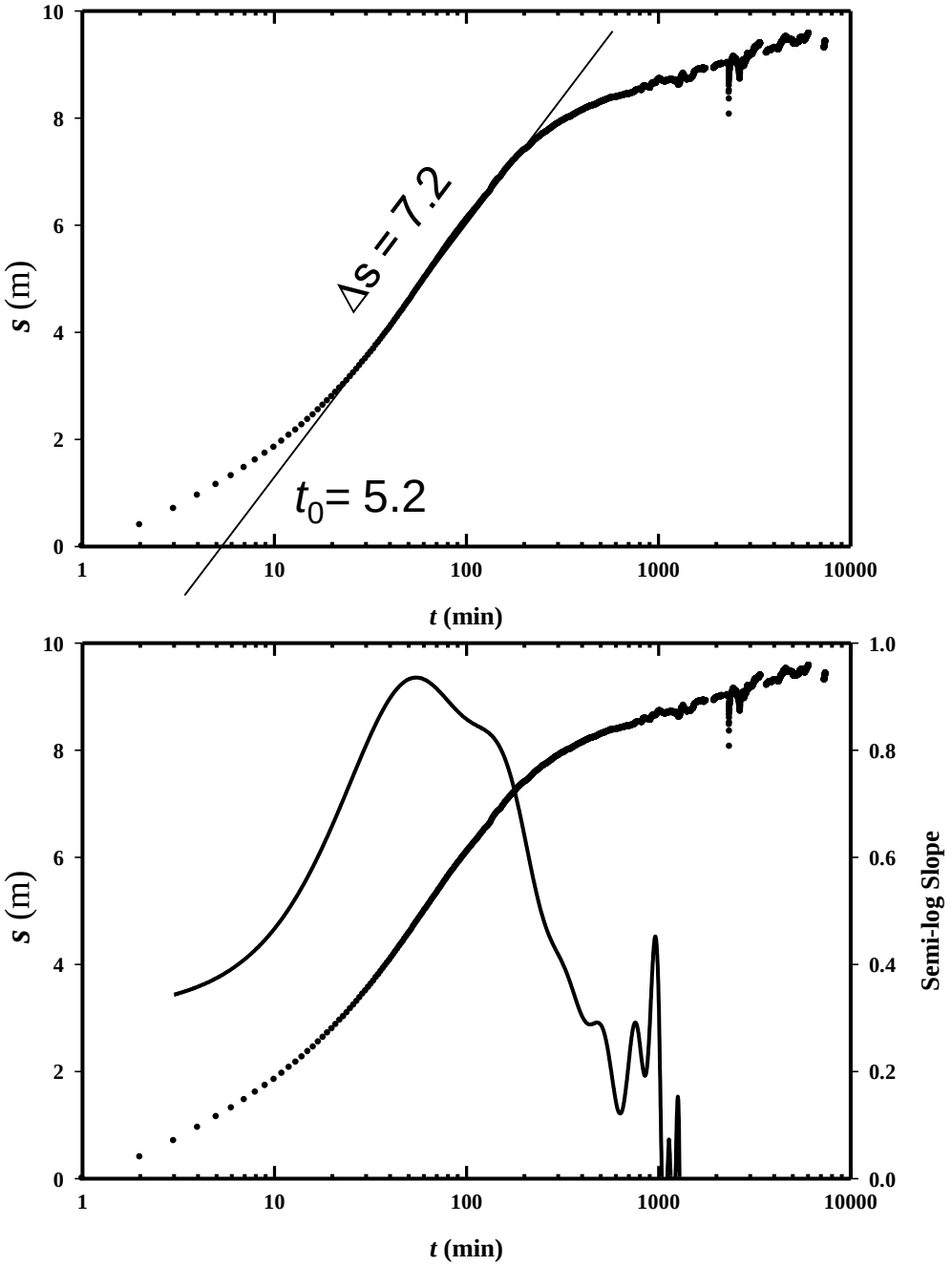

Figure 4.9. a.) Drawdown at LAR-1 as function of time showing best fit straight-line. b.) Semi-log slope as function of time (thin line) with the drawdown (thick line).

Step 2 Determine dimensions and other properties

The properties of the saprolite were determined by analyzing data from the monitoring well in the saprolite (LAS-1) using the Neuman (1974) analysis. This gives K_{sap} = 0.01 m/min, S_{sap} = 0.28 (Figure 4.8). The radius of LAR-1 is r_w = 0.076 m and the thickness of the aquifer is assumed to be b = 25 m based on the depths to and distances between fracture zones. The saturated thickness of the saprolite from drilling records is b' = 14 m.

A first order stream is located 50 m to the south of the Clemson well field, so L = 50 m. The width of the stream at the time of the aquifer test was approximately w = 1m. .

Determine s_K

The skin factors is (Earlougher, 1977)

$$s_k = \frac{2\pi T(s_a - s_e)}{Q} \tag{4.1a}$$

where s_a and s_e are the actual and expected drawdowns, respectively. The expected drawdown without skin was determined as (Cooper and Jacob,1946):

$$s_e = \frac{0.183Q}{T}\log\left(\frac{9.0Tt_w}{Sd_w^{\,2}}\right) \tag{4.1b}$$

where t_w is the time when the actual drawdown is observed, and d_w is the diameter of the well. This approach is only valid while the data follow a semi-log straight line, so using t_w=100 min with s_a = 6.2 m, the skin factor is determined as is s_k= 5.6.

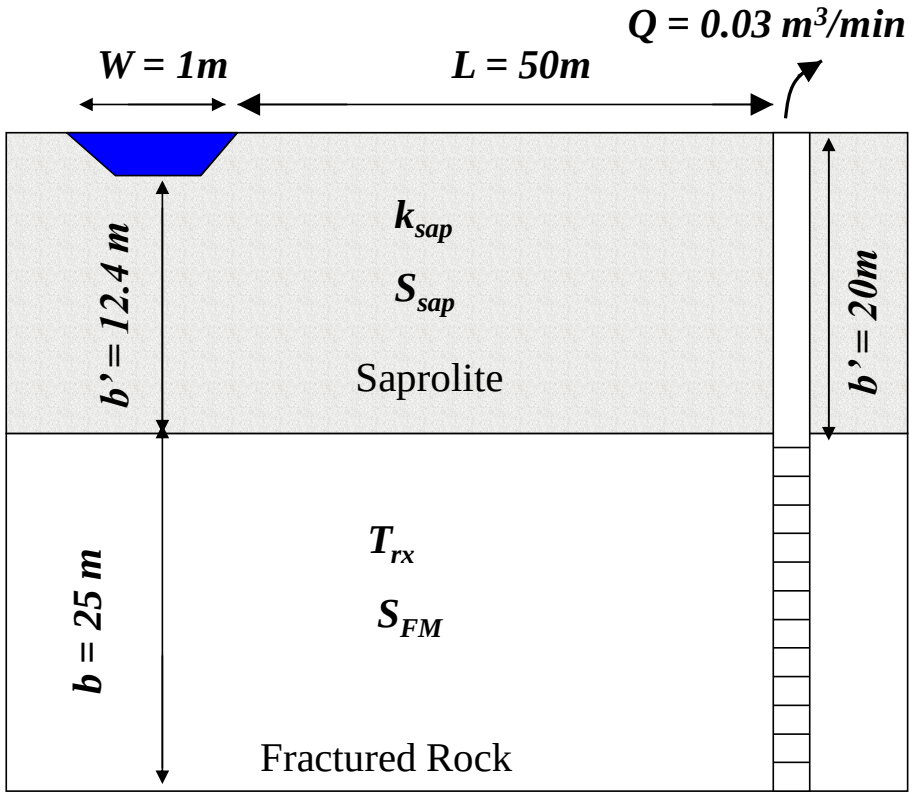

Figure 4.10. Conceptual model of the Clemson Well Field showing one well.

Well Name	R_w (m)	T (m2/day)	S (1/m)	b (m)	b' (m)	w (m)	L (m)
LAR-2	5.91	12.93	3.5E-03	35	-	-	-
LAR-3	5.70	12.93	4.4E-03	41	-	-	-
LAR-4	10.98	31.03	4.2E-03	41	-	-	-
LAR-1	0.08	1.09	-	25	-	1	50
LAS-1	5.7	291	0.28	-	20	-	-

Table 4.3. Aquifer properties and dimensions for analysis

Step 3 Full Analysis

The full analysis (eq. 2.15) requires estimates of β and s_k along with T, L, and r_w (Table 4.3) The estimates of parameters are T = 0.009 m^2/ min, s_k = 5.6, and β=6.5. These data give S_{css} = 4.42x10^{-3} m^2/min using eq. 2.15.

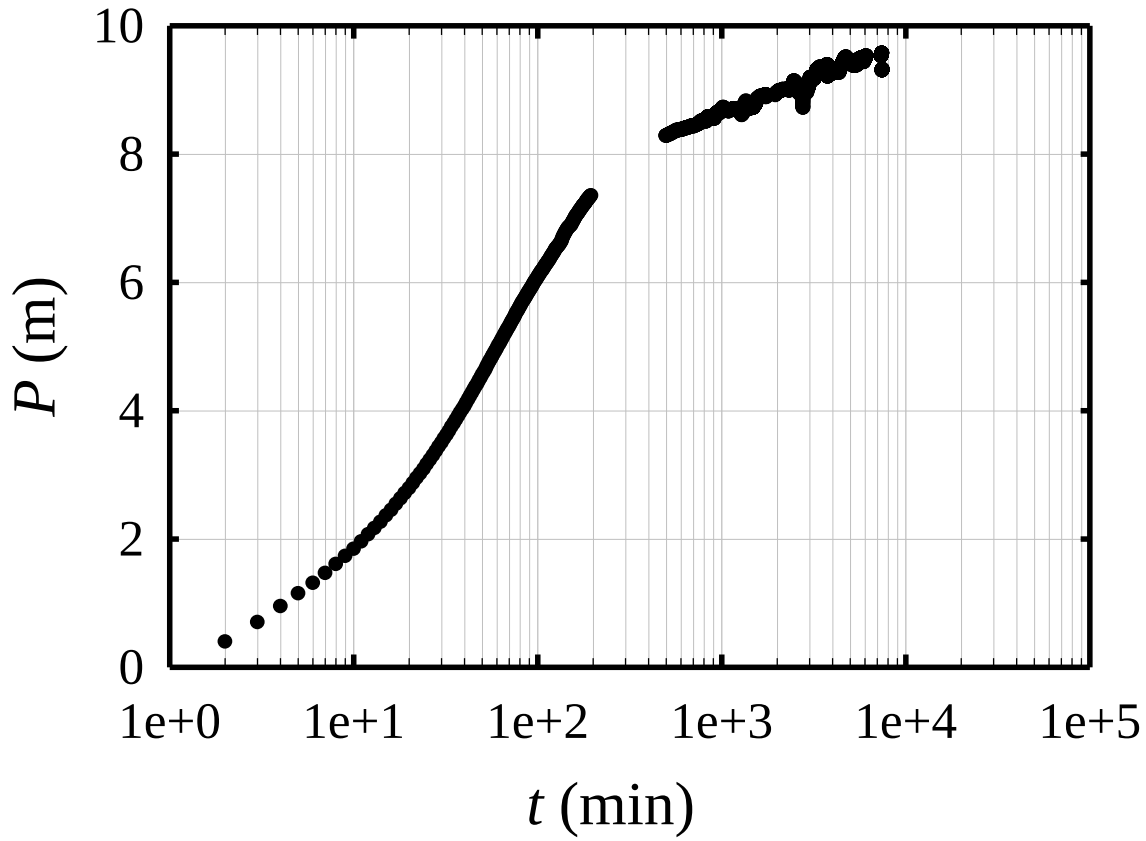

Figure 4.11. Numerical fit of LAR-1 drawdown as a function of time for LAR-1 field data (dots) and numerical fit (solid line).

Step 4. If β cannot be determined, use simplification. Semi-log slope constant

It is possible to estimate β from data available at the Clemson well field, but it is instructive to evaluate the analysis where β is omitted. In this case, we can omit data for *t* > 200min, leaving only the semi-log straight portion of the data. Using *T* = 0.009 m^2/

min, s_k = 5.6,, the approximate method 1 (eq. 2.16) gives S_{css} = 4.52x10^{-3} m^2/min, which is only slightly greater than the result from the full method. This occurs because s_k is much larger than the term in 2.15 that includes β.

Time to Stream Interaction, $t_{0.8calc}$

The time when the drawdown should interact with the stream can be estimated using 3.3a. The effective parameters are: T = 0.009 m^2/min based on the semi-log slopes of both the monitoring wells and the second slope of the pumping well; 0.005 < S < 0.28, with the low end derived from the analysis of the pumping test for 20 to 120 min, and the high end from the analysis of the monitoring well in the saprolite. This gives a range of $t_{0.8}$ using eq. 3.3a of 1 day < $t_{0.8}$ < 1 month.

The break in slope in the field data occurs at $t_{0.8obs}$ = 170 minutes. These results indicate that the observed break in slope occurs too early to be considered an interaction with the stream.

The drawdown curve at the well follows a semi-log straight line from 1 day < t < 6 days, suggesting that water was removed from storage and no interaction with the stream took place. It appears that more than 6 days of pumping is required for the well to interact with the stream.

Duration of Saprolite Effect

The time to the end of the saprolite effect (eq. 3.2) depends on b' = 14m, K_{sap} = 0.01 m/min, and S_{sap}=0.28, which gives t_{sap} = 286 min. This gives the time when heads in the saprolite equilibrate with the heads in the underlying rock aquifer.

The time calculated using eq. 3.2 is roughly 1.7x greater than the observed $t_{0.8}$ (Fig. 4.12). As a result, it seems likely that the break in slope is a result of interaction with the saprolite.

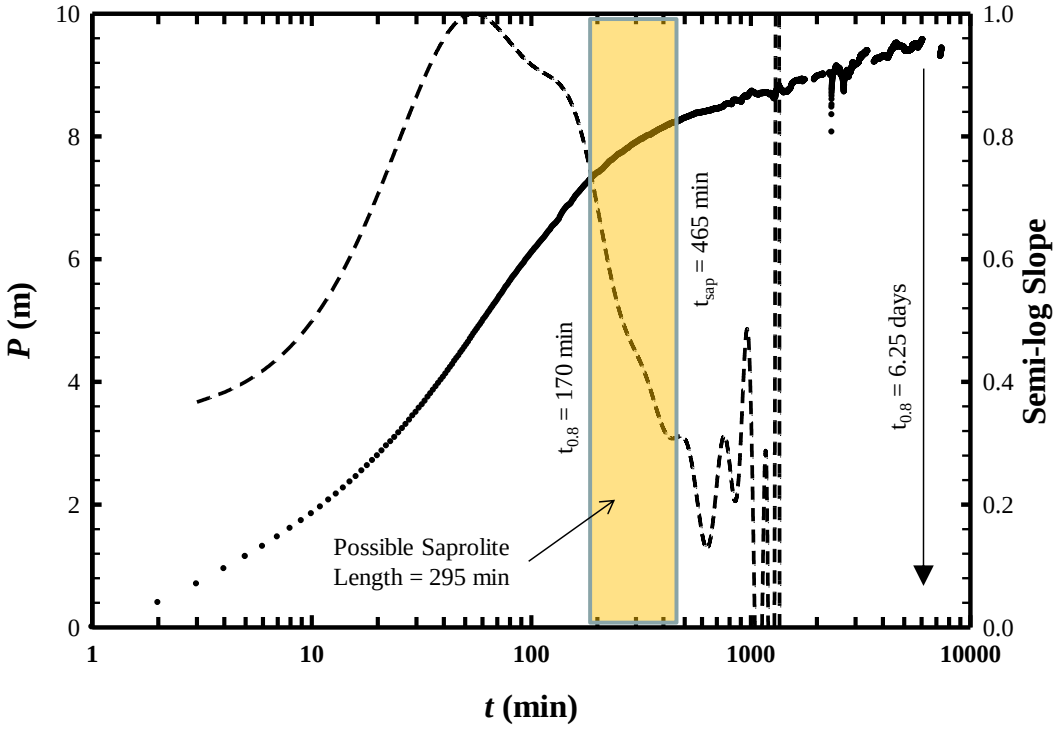

Figure 4.12. Drawdown and normalized slope as a function of time. $t_{0.8obs}$ = 170 min suggests beginning of saprolite effect; t_{sap} = 268 minutes, the end of the saprolite effect; 1500 min < $t_{0.8calc}$ < 47000 min, suggesting interaction with the stream would have occurred after the test was terminated.

GEGT Plant Aquifer Test Evaluation

The test from the Clemson well field was not long enough to identify the actual specific capacity, but another example is available where steady state was achieved. This example is from a site near Greenville, SC, where well performance data are available for six years. The operation of this well was preceded by a brief pumping test, lasting two hours where water levels were recorded with a hand tape. This example will use the results of that pumping test to estimate the performance of the well during the subsequent 6 years.

GEGT Site

The GEGT site near Greenville, Sc (Figure 4.14) has several contaminant plumes as product of past manufacturing practices and a well was installed in 1998 to capture one of the plumes. The conceptual model of the site is typical of the Piedmont (Fig. 1.9), with saprolite overlying a fractured bedrock aquifer located near a small stream approximately 100 m southwest of the pumping well (Figure 1.9). A 2-hour-long pumping test was conducted shortly after the well was installed. The well was brought online in 1999 and pumping rates and water levels have been measured every 3 months for 6 years.

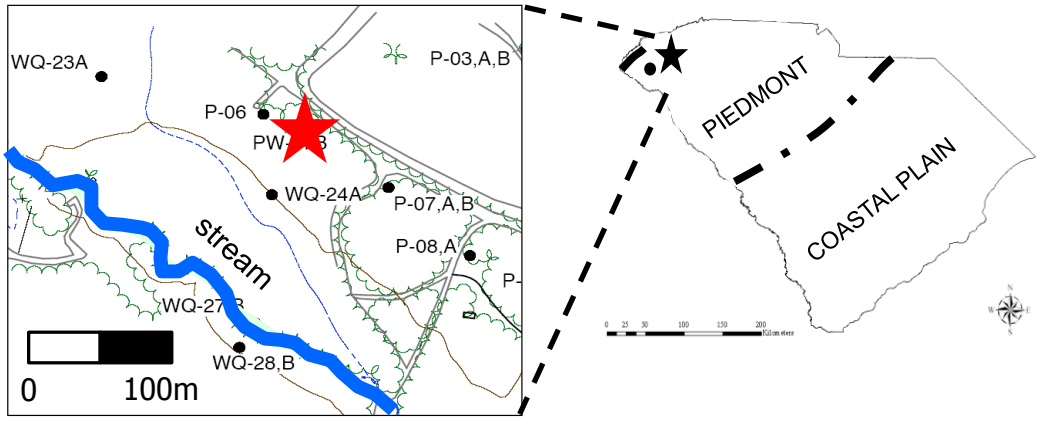

Figure 4.14. Location map of GEGT site (Red and black star).

AQUIFER TEST

The test well, P-07B, was pumped at 0.05m^3/min (13 gpm) for 2 hours. Hydraulic head was measured manually at the pumping well and 4 observation wells. The maximum drawdown in P-07 at the end of pumping was 2.74m (9.01 ft) (Figure 4.15).

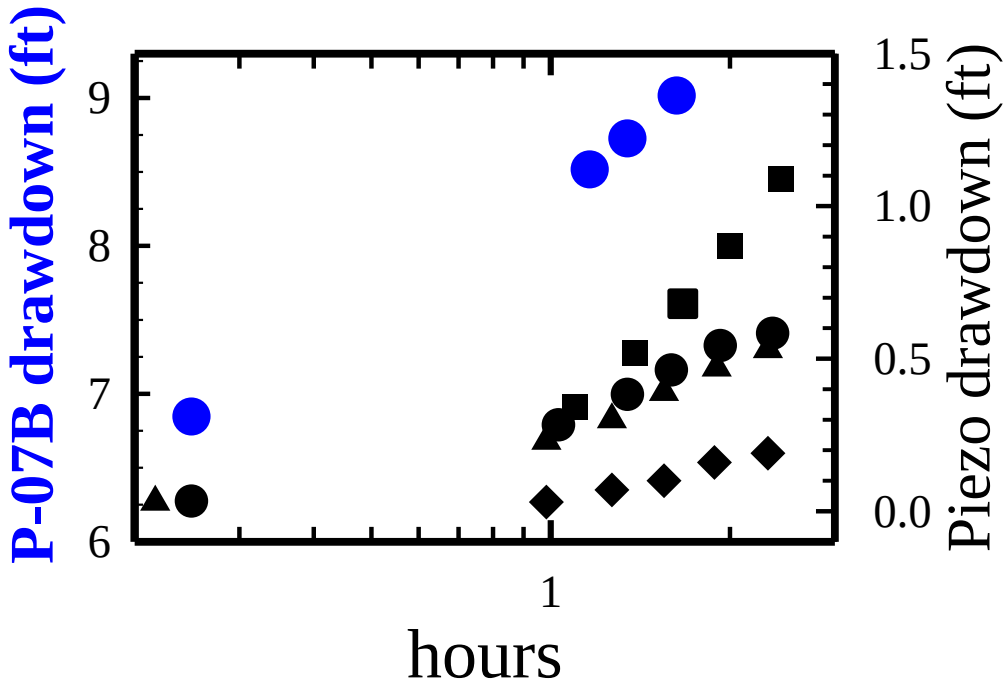

Figure 4.15. Drawdown as a function of time when well P-07B was pumped at constant-rate test.

Aquifer Parameters

T and *S* were calculated using the Jacob straight-line method. Data from P-07B give $T = 1.3 \times 10^{-3}$ m^2/day, whereas data from the monitoring wells give 1.5×10^{-3} m^2/min $< T < 6.1 \times 10^{-3}$ m^2/day. The mean value for $T = 3.0 \times 10^{-3}$ m^2/day, and the mean value of $S = 6 \times 10^{-4}$. Slug tests in wells in the vicinity give $K_{sap} = 3.85 \times 10^{-4}$ m/min (personal conversation with Greg Kinsman).

The distance to the stream, L, was determine from the site location map (Figure 4.14) as L = 100 m.

FULL ANALYSIS

To apply the Full Analysis, the real S_{ssc} has to be determined for comparison. Water levels and flow rates for a 6 year period are available to calculate the long-term specific capacity of P-07B (Figure 4.16). The average specific capacity over 6 years is S_c = 0.2 gpm/ft. This value will be considered as the long-term performance of P-07B for the analysis, S_{ssc}=0.2 gpm/ft.

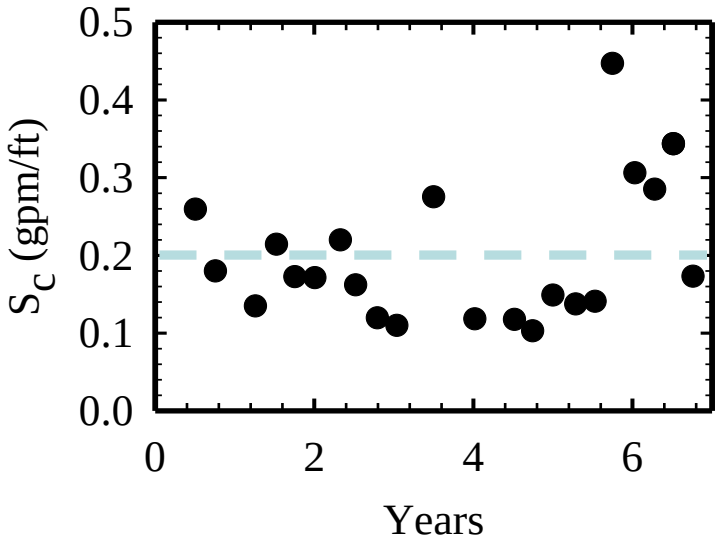

Figure 4.16. S_c values for well P-07B for a 6 year period. Dash line represents the average S_c for the monitoring period.

Before calculating S_{css}, the strength of the stream term, β, needs to be determined (eq 2.9f). Parameters used to determine β are K_{sap} = 3.85 x 10^{-4} m/min, T_{rx} = 3.0 x 10^{-3} m^2/min, b' = 7.6 m, L = 100 m, and w = 1 m. β was calculated as 1.6 with the previous parameters.

The predicted S_{css} from the Full analysis is 2.51 x 10^{-3} m^2/min. The assumed long-term S_c from the six year of data, S_{css}real = 2.49 x 10^{-3} m^2/min. The Full Analysis predicts the average Sc essentially exactly when using the mean values of T and S. This is an encouraging result, although some consideration should be given to the uncertainty in *T* and *S*.

Extrapolating out the 2 hour test data, the long-term S_{css} = 0.7 gpm/ft. This is almost a factor 2.5 greater than the observed operational S_c at late time. Appling the Jacob analysis to the short-term test extrapolated to six year results in a S_{css} = 0.27 gpm/ft (Figure 4.18). The Jacob prediction results fall within one standard deviation of the operational data over the last six years, an acceptable result. Extrapolating the test data overestimated the long-term well performance by a factor of 2.5, this suggests care must be taken when apply this method into the long-term operational span of a well. The Jacob analysis prediction was closer than the field data extrapolation by almost a factor of 2. The Full Analysis S_{css} was able to represent the long-term well performance with a Es_c < 7% with estimated stream strength, β, values.

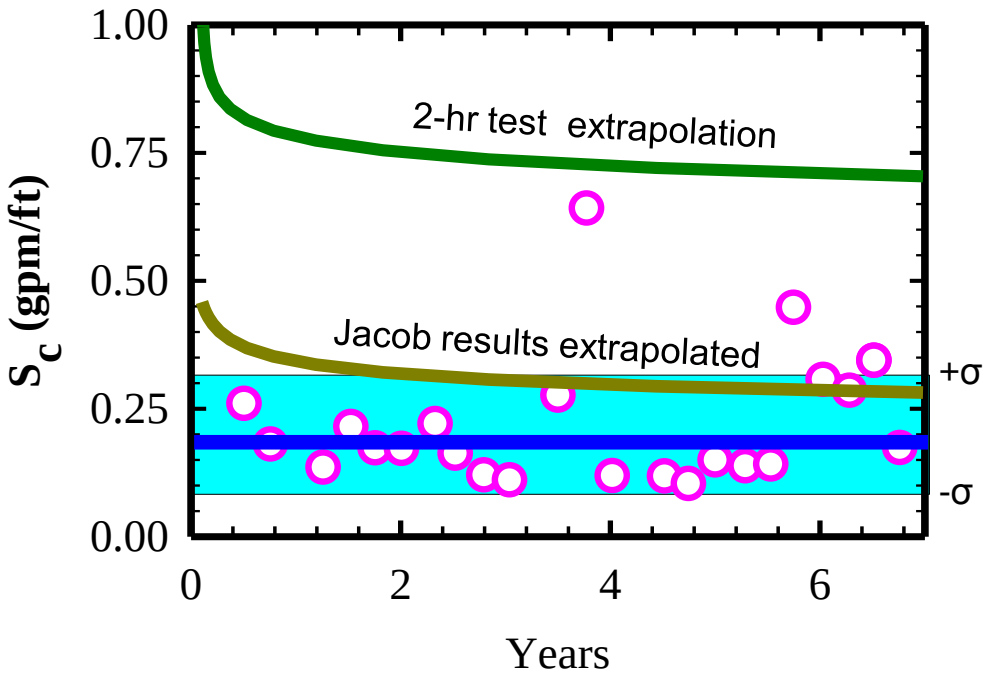

Figure 4.18. S_c as a function of time for well P-07B showing 2-hr test and Jacob result extrapolations from the short-term well test.

Duration of Saprolite Effect

t_{sap} was calculated to predict the length of time for saprolite to equilibrate with the underlying aquifer. No data is available for saprolite storativity on site. I will assume the storativity ranges from a low of S =0.1 to a high value of S = 0.28 because these value occur in a similar setting near Clemson.

Parameters used for t_{sap} (3.2) are K_{sap} = 3.85 x 10^{-4} m/min, b' = 7.6 m, and S ranges of 0.1, 0.2, and 0.28. The results indicate that t_{sap} = 1 day when considering the lower end of S and t_{sap} = 2.81 days using an S = 0.28. The duration of the saprolite effect would have been short compared to the operation of the well.

Boundary Interaction

t_b was calculated using L = 100 m, S_{FRM} = 5.96 x 10^{-4}, T_{rx} = 3.02 x 10^{-3} m^2/min, and S_{sap} ranging from 0.1 to 0.28. Using the high range of S_{sap} =0.28, t_b = 1.6 years, and t_b = 0.57 years when S_{sap} = 0.1.These results suggest that P-07B has been interacting with the stream for most of the 6-year-long data set.

DISCUSSION

A method to estimate the long-term performance of a well was presented in Chapter 2, numerically evaluated in Chapter 3, and applied to field tests in the current chapter. A suggested approach to calculate well performance was outlined (Figure 4.1*) based on available site and aquifer data and confirmed using a synthetic data set.

Basic assumptions made for unavailable aquifer properties using an sythentic example resulted in a Es_c = -0.89 % between the known numerical results and predicted well performance. This suggests the approach for predicting well performance may be applied to pumping test data when some of the aquifer properties and dimensions are unknown. The minimum requirement to calculate S_{css} requires a T value from a pumping test, along with the distance to a stream, L. If the distance to the stream is unknown, an effective distance can be determined using eq. (2.23) and substituted for L.

Clemson Site

The approach was then applied to a well test performed on LAR-1 from the Clemson Well Field. The site information available allowed the full analysis to be applied to the field data. During pumping, LAR-1 had not reached steady state conditions, so numerical evaluations were used to fit field data to calculate steady state conditions under steady state conditions. The S_{css} determined from the numerical model may differ based on geometries and aquifer properties used. The predicted value of S_{css} over estimated the anticipated true value by approximately 35%. This is a significant error, and one that is larger than expected. Indeed, the empirical method of estimating well performance as the

observed performance at the end of pumping would have given approximately $3.3x10^{-3}$ m^2/min, which is much closer to the expected actual value.

A suggestion to the reason for this large error is given in the shape of the drawdown curve (Fig. 4.12). The drawdown increases and approaches a semi-log straight line at relatively early time, and then the slope flattens and once again becomes a semi-log straight line. This curve differs from the idealized behavior, where the curve continuously flattens until it reaches a slope of zero (Fig. 2.2). That is, the second, semi-log straight line portion of the plot in (Fig. 4.12) is absent from the idealized plot. Drawdown curves with two segments that form straight lines on semi-log plots were described by Passinos (2001). She recognized that this behavior can be caused by a well completed in a region composed of two domains separated by a vertical boundary. The slope of the first segment is inversely proportional to the transmissivity of the domain in which the well is completed, whereas the slope of the second segment is inversely proportional to the arithmetic mean of *T* of the two domains.

I suspect that well LAR-1 is completed in a domain with a smaller *T* than the adjacent material. This is why the apparent *T* calculated using the drawdown in the well is one tenth that of *T* calculated using data from the monitoring wells.

The proposed analysis does not consider an aquifer consisting of two domains separated by a steep boundary. This effect is currently lumped into the skin factor, and indeed, the analysis indicated there was a significant skin around LAR-1 (s_k = 5.6). However, a skin factor will offset a drawdown curve, but it will not change the slope on a semi-log plot. Clearly, the slope in Figure 4.12 changes at roughly 170 minutes, so it appears that this

effect may to due to two domains. It is worth noting that the semi-log slope of the second segment in Figure 4.12 is only slightly steeper than the semi-log slopes of the monitoring wells, which further suggests that LAR-1 is embedded in a low *T* region.

I suspect that the relatively large error given by eq. 2.15 is because of the effect of two domains, which are not considered in the analysis. Additional work will be required to further evaluate this issue.

GEGT Site

The analysis performed well at the GEGT data set, essentially predicting the average long-term specific capacity to within a few percent. The long-term data exhibit considerable variability, likely because short-term variations in pumping rate could have caused short term variations in drawdown, which were recorded as 3-month averages. Another factor that could have caused variability is seasonal fluctuations in recharge. The analysis assumes that recharge is constant, but clearly fluctuations in recharge will alter drawdowns and change the specific capacity. It is possible to include effects of rainfall in the analysis, and this is recommended for future investigations.

CHAPTER FIVE

CONCLUSION

A new method was developed to predict the long-term performance of a well from short-term pumping tests in an idealized hydrogeologic setting resembling the Piedmont province in the eastern U.S. (Fig. 1.9). The method is based on a theoretical analysis of a well and a stream represented as a Cauchy-type boundary of variable conductance (Hunt, 1999; Butler, 2001). Interaction between the well and the stream is the key to understanding steady state conditions. The stream-aquifer interaction is characterized using a dimensionless term β (eq. 2.9f), which includes the conductance of material between the stream and the aquifer, and other geometries and properties that can be determined with straightforward field measurements. When $\beta > 10$, the stream behaves like a constant head boundary and the well begins to approach steady conditions (Fig. 2.2 and 2.3) when $t > 0.62\frac{SL^2}{T}$ (eq. 2.22). In this ideal case, the steady state specific capacity is given by $S_{css} = 2\pi T / \ln\left(2L / r_w\right)$ (eq. 2.16). The effect of the stream on the performance of the well diminishes as β is reduced (Fig. 2.2). The effect of a variable interaction between stream and well is included by adjusting β and using eq. 2.15 to calculate S_{css}.

The analysis for estimating S_{css} includes the effect of interaction between a well and a stream, which seems to be of fundamental importance, but the analysis omits many other hydrogeologic factors that occur in the Piedmont. Numerical simulations of wells in various configurations that included some of these factors were conducted and then the proposed analysis was used to predict well performance in the simulations. Aquifers in the Piedmont consist of fractured rock overlain by saprolite (Fig. 1.9), and the numerical configurations included aquifers and saprolite of different thicknesses and hydraulic conductivities (Table 3.1). The results indicate that contrasts in the hydraulic conductivities of these two units caused errors ranging from -11% to 6% (Fig. 3.7).

The saprolite is unconfined and highly porous, and release of water from storage in saprolite is recognized as an important factor affecting performance of wells in the Piedmont (LeGrand, 1967; Swain *et* al., 2004, Daniels, 2002, Williams, 2001). Increasing the storativity of the saprolite in the simulations had a significant effect on the drawdown curve, causing it to flatten at lower levels and sooner than predicted by the proposed method (Fig. 3.9), which assumes a homogeneous aquifer. The flattening of the drawdown curve in the simulations was only temporary, and eventually the drawdown increased and approached a much larger value (Fig. 3.10). This is a potential concern because the premature flattening of the drawdown curve caused by release of water from saprolite can occur after a few hours and could be interpreted as the well approaching steady state. This temporary effect would lead to overestimation of the true steady state performance of the well.

The proposed method was capable of predicting the ultimate steady state specific capacity with errors of -11 to 6%. The effect of saprolite will increase the well performance compared to that predicted by the proposed method (eq. 2.15), and the duration of this increased performance can be anticipated (eq.3.11).

Changing the separation distance between the well and the stream also affected errors, and in general, the proposed method (eq. 21.5) over-predicted well performance as the separation decreased. This effect results from the convergence of flow paths on the stream, which occurs in the numerical model, and in the field, but is omitted from the 2-D analysis. This geometric effect is only important when the ratio of the separation distance to the thickness of the aquifer is less than approximately 10. In most of the configurations, the maximum error caused by this effect is 5% to 10%, but it was 10% to 15% for configurations where the saprolite was particularly thin (Fig. 3.8).

The general finding of the numerical simulations is that a variety of hydrogeologic effects that are common in the Piedmont but omitted from the proposed analysis will result in errors in S_{css} of less than roughly 15%. This is probably an acceptable uncertainty for most applications. Some effects, like the influence of saprolite on the drawdown curve, can be recognized and taken into consideration in the analysis. These findings are encouraging because they suggest that the proposed method (eq. 2.15) could be robust in field applications. This assertion was tested by using the proposed method to evaluate both synthetic type curves and the results from field tests at two sites in the Piedmont. An approach for implementing the proposed analysis was developed with suggested steps to guide a user through several options for determining S_{css} from a

well test. The parameters required by the full analysis may be unknown in some cases, so simplifications are given to account for these situations. This results in a.) a full analysis to use when all parameters are available; b.) a simplification to use when the drawdown curve is semi-log straight and parameters in the vicinity of the stream are unknown; c.) two simplications to use when the semi-log slope of the drawdown curve decreases with time.

Application of the implementation approach to synthetic pumping tests shows that with as little information as T, L, and r_w, from the pumping well, the Simplification Method 1 is able to predict the long-term well performance quite well, with errors of a few percent. The full analysis was also successful estimating S_{css} even when the parameters for were estimated β. Using typical Piedmont values for S_{sap}, K_{sap}, and w appears to be a satisfactory starting point when parameters are unavailable because β is generally large enough to have only a minor effect.

The evaluation of the Clemson Well Test provided a field example with a saprolite transmissivity 10 times greater compared to fracture rock aquifer. The K_{sap}/K_{rx} - >> 1. The analysis over-predicts the expected actual specific capacity by approximately 30%. THis appears to occur because there appear to be two domains with different T values. The pumping well is embedded in the lower T domain, whereas the monitoring wells are in a domain with a higher T. This effect is crudely approximated by a well skin, but a revised analysis appears to be needed to fully explain this test.

The GEGT example included an data set of well performance over a 6 year period. A 2-hour-long pumping test conducted prior to the well going into service was

used to test the approach. The analysis was used with average values for T from the well test, along with L, and r_w from the site. The results predict Scss within a few percent of the long-term average Scss observed at the site. This estimate appears to be considerably better than those derived from alternative methods.

APPENDICES

Appendix A

Typical Piedmont Values

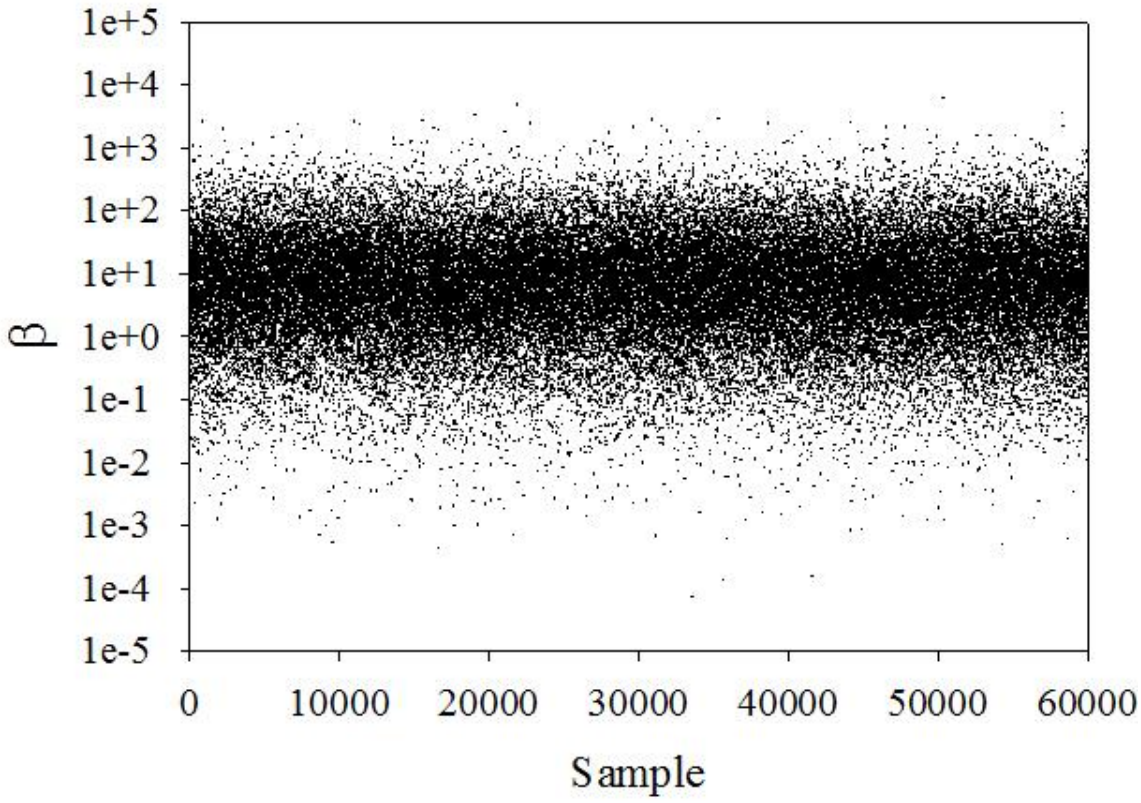

Figure A-1: Distribution of b based on random sampling of typical Piedmont parameter ranges. .

	L (m)	w (m)	b' (m)	T (m^2/d)	S_{sap}	S_{rx}	β
Minimum	1	1	1	1	1.E-04	1.E-06	1
Maximum	500	30	30	30	0.3	1.E-03	50

Figure A-2: Typical Piedmont parameter ranges.

REFERENCES

Alley, W.M., Reilly, T.E., and O.L. Franke (1999). Sustainability of ground-water resources. U.S. Geological Survey Circular 1186. 79 pp.

Anderson, M. P., and W.W. Woessner (1992). Applied Groundwater Modeling: Simulation of Flow and Advective Transport. San Diego, Academic Press.

Bear, J. (1972). Dynamics of Fluids in Porous Media. New York, Dover.

Bennett, G.D. and E.P. Patten Jr. (1960). Borehole geophysical methods for analyzing specific capcacity of multiaquifer wells. U.S.G.S. Water-supply Paper 1536-A.

Boulton, N. S. (1954). "Unsteady radial flow to a pumped well allowing for delayed yield from storage." International Association of Scientific Hydrology(Publication 37): 472-477.

Bouwer, H. (1978). Groundwater Hydrology. New York, McGraw-Hill.

Bredehoeft, J. D., Papadopulos, S.S., Cooper H.H. Jr. (1982). The water budget myth. In Scientific Basis of Water Resources Management. Studies in Geophysics Washington DC, National Academy Press: 51-57.

Bredehoeft, J. D. (1997). Safe yield and the water budget myth. Ground Water 35(6): 929.

Bredehoeft, J. D. (2002). "The water budget myth revisited: why hydrogeologists model." Ground Water 40(4): 340-345.

Brown, R.H., Ferris, J.G. Jacob, C.E., Knowles, D.B., Skibitzke, H.E., and C.V. Theis (1963). Methods of determining permeability, transmissibility and drawdown. U.S. Geological Survey Water-Supply Paper 1536-I. 98 pp.

Bott, T. L., Newbold, J.D., and David Arscott (2006). "Ecosystem Metabolism in Piedmont Streams: Reach Geomorphology Modulates the Influence of Riparian Vegetation." Ecosystems **9**: 398-421.

Cimen, M. (2001). "A simple solution for drawdown calculation in a large-diameter well." Ground Water 39(1): 144-147.

Rosco Moss Company. (1990). Handbook of ground water development. New York, Wiley.

Conkling, H. (1945). "Utilization of Ground-Water Storage in Stream System Development." American Society of Civil Engineers Transactions: 275-303.

Cooper, H.H. and C.E. Jacob, 1946. A generalized graphical method for evaluating formation constants and summarizing well field history, Am. Geophys. Union Trans., vol. 27, pp. 526-534.

Daniel, C.C., III, 1992**,** Correlation of well yield to well depth and diameter in fractured crystalline rocks, North Carolina, in Daniel, C.C., III, White, R.K., and Stone, P.A., eds., Ground water in the Piedmont: Clemson, South Carolina, Clemson University, Conference on Ground Water in the Piedmont of the Eastern United States, Proceedings, p. 638-653.

Daniel, C.C., III, 2002, Preliminary Hydrogeologic Assessment and Study Plan for a Regional Ground-Water Resource Investigation of the Blue Ridge and Piedmont Provinces of North Carolina, U.S. Geological Survey Water Resources Investigations Report 02-4105, Raleigh, North Carolina.

Darama, Y. (2001). "An analytical solution for stream depletion by cyclic pumping of wells near streams with semipervious beds." Ground Water 39(1): 79-86.

GDNR. (1990). Permit Application. Amended. 391-3-2.04: 6.

Driscoll, F. G. (1986). Groundwater and Wells. St. Paul, U.S. Filter/Johnson Screens.

Hantush, M. S. (1965). "Wells near streams with semipervious beds." Jnl. Geophysical Research 70(12): 2829-2838.

Harman, H. D. J. (1989). The unique performance of an electrical resistivity technique in designing an effective fractured bedrock monitoring system. Ground Water in the Piedmont: Proceedings of a Conference on Ground Water in the Piedmont of the Eastern United States, Clemson, SC.

Heath, R.C. 1989, The Piedmont Ground Water System. pp. 1- 12. In: Daniels and others, Ground Water in the Piedmont; Proceedings of a Conference on Ground Water in the Piedmont of the Eastern United States, Clemson University, Clemson, South Carolina.

Hunt, B. (1999). Unsteady stream depletion from ground water pumping. Ground Water 37(1): 98-102.

Horton and McCornnell, 1991, Western Piedmont, In: Horton and Zullo, The Geology of the Carolinas, The University of Tennessee Press, Knoxville, TN, p. 127-141.

Kalf, F. R. P. a. D. R. W. (2005). Applicability and methodology of determining sustainable yield in groundwater systems. Hydrogeology Journal 13: 295-312.

Kasper, J. G. (1989). Ground water monitoring and recovery system design in a low-yield crystalline rock aquifer in wester south carolina. Ground Water in the Piedmont: Proceedings of a Conference on Ground Water in the Piedmont of the Eastern United States, Clemson, SC.

Kruseman, G. P., de Ridder, N.A. (1991). Analysis and Evaluation of Pumping Test Data. Nertherlands, ILRI.

Lee, C. H. (1915). "The determination of safe yield of underground reservoirs of the closed basin type." Transactions of American Society of Civil Engineers(paper no. 1315): 148-251.

LeGrand, H. E. (1967). Ground water of the piedmont and blue ridge provinces in the southeastern states.

LeGrand, H.E., Region 21, Piedmont and Blue Ridge. 1988, Geol. Soc. Am. : Boulder, CO, United States: United States. p. 201.

LeGrand, H.E., A Master Conceptual Model for Hydrogeological Site Characterization in the Piedmont and Mountain region of North Carolina. 2004, North Carolina Department of Environment and Natural Resources. : North Carolina. pp.40.

Meinzer, O.E., 1920. Quantitative methods of estimating ground-water supplies, *Bull. Geological Soc. Am.* 31 (1920) (2), pp. 329–338.

Meinzer, O.E., 1923. The occurrence of groundwater in the United States with a discussion of principles. US Geol. Surv., Water-Supply Paper 489, 321 pp.

Miller, J. (1990). "Ground water atlas of the united states segment 6." 22-23.

Muskat, M. (1937). The Flow of Homogeneous Fuilds Through Porous Media. New York, McGraw-Hill.

Muskat, M. (1949). Physical Principles of Oil Production. New York, McGraw-Hill.

Neuman, S.P., 1974. Effect of partial penetration on flow in unconfined aquifers considering delayed gravity response, Water Resources Research, vol. 10, no. 2, pp. 303-312.

Osborne, P. S. (1993). Suggested Operating Procedures for Aquifer Pumping Tests. O. o. R. a. Development, EPA: 23.

Passinos, P.A. 2001. Well tests to characterize idealized lateral heterogeneities. *Master's Thesis, Clemson University*.

Rorabaugh, M.I. (1953). Graphical and theoretical analysis of step-drawdown test of artesian well; ASCE, v.79, Separate 362, 23 pp.

Rutledge, A.T., Estimated hydrologic characteristics of shallow aquifer systems in the Valley and Ridge, the Blue Ridge, and the Piedmont physiographic provinces based on analysis of streamflow recession and base flow, in U. S. Geological Survey Professional Paper,. 1996, U. S. Geological Survey : Reston, VA, United States: United States. p. B1.

Rutledge, A.T., and Mesko, T.O., 1996, Estimated hydrologic characteristics of shallowaquifer systems in the Valley and Ridge, the Blue Ridge, and the Piedmont physiographic provinces based on analysis of streamflow recession and base flow: U.S. Geological Survey Professional Paper 1422-B, 58 p.

Ritter, D. F., Kochel, R.C., Miller, J.R. (1995). Process Geomorphology. Boston, WM C. Brown.

Rosenshein, J., Bennett, G.D. (1984). Groundwater Hydraulics. Washington, D.C., American Geophysical Union.

Sakr, S. A. (2001). Type curves for pumping test analysis in coastal aquifers. Ground Water 39(1): 5-9.

Seaton, W. J., and T.J. Burbey (2000). "Aquifer characterization in the Blue Ridge physiographic province using resistivity profiling and borehole geophysics: Geologic analysis." Journal of Environmental and Engineering Geophysics **5**(3): 45-58.

SCDHEC (2006). R.61-58 State Primary Drinking Water Regulation. S. C. D. o. H. a. E. Control, Bureau of Water: 438.

Sophocleous, M. (2000). "From safe yield to sustainable development of water resources-the kanas experience." Journal of Hydrology 235: 27-43.

Sophocleous, M., M. A. Townsend, et al. (1988). "Experimental studies in stream-aquifer interaction along the Arkansas River in Central Kansas -- Field testing and analysis. Journal of Hydrology 98(3-4): 249-273.

Stern, C. W., Carroll, R.L., Clark, T.H. (1979). Geologic Evolution of North America. New York, J Wiley & Sons.

Summers, W. K. (1972). Specific capacity of wells in crystalline rocks. Ground Water 10(6): 11pp.

Svenson, E. 2006. Methods for measuring and analyzing transient head and aperture changes during air-slug tests in fractured bedrock. *Master's Thesis*, *Clemson University*.

Swain, L.A, Mesko, T.O., Este Hollyday, 2004. Summary of the Hydrogeology of the Valley and Ridge, Blue Ridge, and Piedmont Physiographic Provinces in the Eastern United States: Regional Aquifer-System Analysis: Professional Paper 1422-A, pp. 23

Theis, C.V., 1935. The relation between the lowering of the piezometric surface and the rate and duration of discharge of a well using groundwater storage, Am. Geophys. Union Trans., vol. 16, pp. 519-524.

Theis, C. (1940). The source of water derived from wells: essential factors controlling the response of an aquifer to development. Civil Eng 10(5): 277-280.

Todd, D. K. (1959). Groundwater Hydrology. New York, Wiley.

van Tonder, G. J., J.F. Botha, W.-H. Chiang, H. Kunstmann, Y. Xu (2001). Estimation of the sustainable yields of boreholes in fractured rock formations. Journal of Hydrology 241: 70-90.

van Tonder, G. J., and J. F. Botha. (2001). "A generalised solution for step-drawdown tests including flow dimension and elasticity." Water Sa 27(3): 345-354.

VDEQ, 2007. Technical advisory for preparing an aquifer test plan as part of a Virigina ground water withdrawal permit application. DEQ Aquifer Test plan. 13 pp.

Walton, W. C. (1968). Selected Analyitical Methods for Well and Aquifer Evaluation, State of Illinois.

Walton, W. C. (1970). Groundwater Resource Evaluation. New York, McGraw-HIll.

Wang, H. F., Anderson, M.P. (1982). Intoduction to Groundwater Modeling. San Francisco, Academic Press.